Applied Surface Science Advances 6 (2021) 100141

Contents lists available at ScienceDirect

Applied Surface Science Advances

journal homepage: www.sciencedirect.com/journal/applied-surface-science-advances

Development of electrodeposited multilayer coatings: A review of fabrication, microstructure, properties and applications

M. Aliofkhazraei [a,*], Frank C. Walsh [b], Giovanni Zangari [c], Hakan Köçkar [d], Mürsel Alper [e], Conrad Rizal [f], Luca Magagnin [g], Vyacheslav Protsenko [h], Ramanathan Arunachalam [i], Amirreza Rezvanian [j], Arian Moein [k], Sahar Assareh [j], Mohammad Hossein Allahyarzadeh [j]

[a] Department of Civil and Environmental Engineering, University of South Florida, Tampa, FL 33620, USA
[b] Electrochemical Engineering Laboratory, Energy Technology Research Group, Department of Mechanical Engineering, University of Southampton, Highfield, Southampton SO17 1BJ, United Kingdom
[c] Materials Science and Engineering, University of Virginia, 351 McCormick Rd., Charlottesville, VA, 22904, USA
[d] Physics Department, Science and Literature Faculty, Balikesir University, Cagis, Balikesir TR-10145, Turkey
[e] Department of Physics, Science and Literature Faculty, Uludag University, TR-16059 Gorukle, Bursa, Turkey
[f] Seed NanoTech International Inc., Brampton, ON L6Y 3J6 Canada
[g] Dipartimento di Chimica, Materiali e Ingegneria Chimica "Giulio Natta", Politecnico di Milano, Via Mancinelli 7, Milan 20131, Italy
[h] Ukrainian State University of Chemical Technology, Gagarin Ave., 8, Dnipro 49005, Ukraine
[i] Mechanical & Industrial Engineering Department, College of Engineering Sultan Qaboos University Al Khod, Muscat 123 Oman
[j] Department of Materials Engineering, Faculty of Engineering, Tarbiat Modares University, Tehran, P.O. Box: 14115-143, Iran
[k] School of Metallurgy and Materials Engineering, Iran University of Science and Technology, Tehran, Iran

ARTICLE INFO

Keywords:
Compositionally modulated layer
Corrosion
Electrodeposition
Microstructure
Multilayer coatings
Nanocomposite

ABSTRACT

The demand for robust engineering materials demonstrating good tribological performance under arduous service conditions has forged the development of novel coating materials and techniques. In the field of surface engineering, multilayer structures have attracted great interest. Electrodeposition offers a versatile and controlled route to engineering coatings in tribology. Electrodeposited coatings can provide tailored electronic, magnetic, mechanical, wear-resistant and corrosion-resistant characteristics as well as an improved load-bearing capability. The performance of multilayered electrodeposits can significantly exceed that of single layers. This paper critically reviews the fabrication, microstructure, engineering properties and potential applications of electrodeposited multilayer coatings. Such coatings can provide powerful, complementary additions to the toolkit for engineering electrodeposition, enabling future advances. Critical aspects requiring further R & D endeavors are identified.

1. Introduction

The ever-increasing demand for materials with superior engineering properties has encouraged materials scientists to develop novel materials having higher efficiency and lower costs. To achieve this, both engineering ingenuity and cost effectiveness are needed. It is often necessary to improve the resilience of engineering components in aggressive environments or enhance the magnetic features of an alloy while preserving its strength; on some occasions, both the wear

Abbreviation: AAO, anodic aluminum oxide; AFM, atomic force microscopy; AMR, anisotropic magnetic resistance; ANSI, American National Standards Institute; ASTM, American Society for Testing and Materials; BCC, body centered cubic; BEM, boundary element method; CE, counter electrode; CG, coarse-grained; CMA, composition modulated alloy; CVD, chemical vapour deposition; DC, direct current; DMF, dimethylformamide; DNC, dynamic nanostructure control; DPSA, dimethyl-dithiocarbamic acid; EDS, energy dispersive X-ray spectroscopy; EIS, electrochemical impedance spectroscopy; EMF, electromotive force; EPMA, electron probe microanalyzer; FCC, face centered cubic; FG, fine-grained; GMR, giant magnetoresistance; HCP, hexagonal closed pack; LMR, longitudinal magnetoresistance; MBE, molecular beam epitaxial; MJED, multiple electrolyte jet electrodeposition; ML, multilayer; MNW, metallic nanowire; MR, magnetoresistance; MWCNT, multi-walled carbon nanotubes; NC, nanocrystalline; PCB, printed circuit board; PEG, polyethylene glycol; PR, pulsed reverse; PVD, physical vapour deposition; RE, reference electrode; SCE, saturated calomel electrode; SEM, scanning electron microscopy; SHE, standard hydrogen electrode; TEM, transmission electron microscopy; TMR, transverse magnetoresistance; WE, working electrode; XRD, X-ray diffraction; XTEM, cross-sectional transmission electron microscopy.

* Corresponding author.
E-mail address: maliofkhazraei@gmail.com (M. Aliofkhazraei).

https://doi.org/10.1016/j.apsadv.2021.100141
Received 14 February 2021; Received in revised form 25 July 2021; Accepted 12 August 2021

Nomenclature

Symbol

Bs	magnetic flux density T
E	electrode potential V
E^o	standard electrode potential V
f	frequency Hz
F	faraday constant (96 485) $C{\cdot}mol^{-1}$
H_c	coercivity Oe = $A{\cdot}m^{-1}$
I	current A
I_M	current used to deposit metal A
j	current density $A{\cdot}cm^{-1}$
j_{rms}	mean (root mean squared) current density during pulsed current $A{\cdot}cm^{-2}$
M	molar mass of metal $g{\cdot}mol^{-1}$
M_r	magnetic remanence T
M_s	saturation magnetization Dimensionless
N	number of electrodeposit pairs Dimensionless
q	electrical charge C = A·s
S	area under the pulsed current vs. time curve C
t	time s
t_{on}	on time during current pulse ms
t_{off}	off time during current pulse ms
t_{on}	pulse on time ms
t_{off}	pulse off time ms
$t_{reverse}$	current reverse time s
T	temperature K
T_m	melting point K
x	thickness of deposit cm
x_A	thickness of deposit A cm
x_B	thickness of deposit B cm
z	electron stoichiometry Dimensionless

Greek

l	wavelength during pulse nm
y	current efficiency for metal deposition Dimensionless
μ	permeability $N{\cdot}A^{-2}$
r	density of metal $g{\cdot}cm^{-3}$

resistance and corrosiono resistance of tools and engineering components must be improved. Control of the microstructure of materials in a cost-effective manner enables the development of novel high-performance materials. Such a goal can be achieved using simple, low-cost methods suited to industrial processing, such as electrodeposition. Although electroplating is a traditional process, it is still possible to develop novel materials with unique characteristics continue to be developed by controlling the deposition parameters. Nowadays, this technique is frequently employed as a successful industrial procedure for materials having an ultrafine structure [1–6].

Among the novel materials which have attracted a great deal of interest recently, are multilayer or chemically modulated structures. The primary concept behind multilayers, presented by Koehler for the first time in a 1970 review concerning strategies to build a strong solid [7], was the enhancement of physical properties of a component by sequentially depositing layers of materials, A and B (having different elastic constants and similar thermal expansion). When stress is applied to such a structure, the dislocations originating from the material with a lower modulus (A) move towards the A/B interface. These dislocations would be hindered at the interface of material with the higher modulus (B) due to the repulsive forces, consequently resulting in increased tensile strength and Young's modulus of the multilayer. In addition to this mechanism, numerous studies have been undertaken on the subject of the multilayers with nanocrystalline, amorphous/nanocrystalline, as well as amorphous structures, and various other mechanisms have been introduced for improving the mechanical properties of the multilayers [8]. It is possible to deposit multilayers using the dual-bath technique; the limitations of this technique and the simplicity of a single-bath have resulted in the emergence of improved single-bath techniques in the majority of recent studies [1].

Research is still being undertaken on tailored multilayers in different industries [9,10]. For example, magnetic properties of alloys, such as copper and cobalt, have been successfully improved for applications as biosensors, magnetic field sensors, or utilization in miniature devices [11,12]. In several other studies, toughness, wear resistance, mechanical properties, and load-bearing capability as well their corrosion resistance have been enhanced through developing specific multilayers [13–16]; such multilayers have found applications in all moving parts in a drilling machine and rock-drilling tools, as well as in oil/gas drilling in hostile environments [8].

Potentiostatic control of the cathode working electrode is common practice in R & D laboratories, but it is rarely applied in industry due to unfamiliarity. The traditional laboratory use of costly feedback controlled, high current power supplies, the need for a reference electrode in the cell and lack of familiarity severely limit the use of potentostatic growth in industrial processing. Controlled current operation is common in modern power supplies and can expand the range of multilayer materials having applications in diverse industries, as illustrated in Fig. 1.

2. Multilayer production techniques based on electrodeposition

Considering the broad variety of deposition processes and types of coating, such as nanograined, superlattice, multilayer, thin-film and nanocomposite coatings, it is important to carefully select the deposition technique and coating type tailored to match properties to the application. The most commonly used deposition techniques are physical vapour deposition (PVD) and chemical vapour deposition (CVD), chemical and electrochemical techniques, physical coating spraying and roll-to-roll coating methods [17]. Electrodeposition and vapour phase deposition have been widely employed in the manufacturing of multilayer films. However, electrodeposition has always been facile for the production of alloyed multilayer coatings of various metals.

PVD and CVD of nitride or carbide coatings have attracted attention, both in the laboratory and at industrial scale, due to the excellent adhesive and strength properties of the deposits as well as high resistance against heat and abrasion. The production of multilayer and gradient coatings, however, is much simpler and cheaper using electrodeposition [18,19].

As shown in Fig. 2, there are many parameters affecting conditions and the obtained properties of electrodeposited layers such as the conditions of electrolyte, type of anode and cathode, etc. One may achieve the desired coatings by gradually, stepwise or alternatively altering any of these parameters. Applying different current densities or potentials has been the most widely used technique so far in the manufacturing of multilayer and gradient coatings. In fact, these two (current density and potential) are often used since they are easy to control, easy to apply changes, repeatability and high accuracy of the equipment used to implement changes. Other parameters that may affect the properties of multilayer coatings (including thickness and morphology) are pH, nanoparticle concentration, solution agitation, anode to cathode gap, electrolyte temperature, bath composition (including additives), deposition using more than a single bath and the duration of deposition.

More complex equipment is required to successfully control and change the above parameters while their effects would not be even close to the effects of changing the current density or potential [20]. All

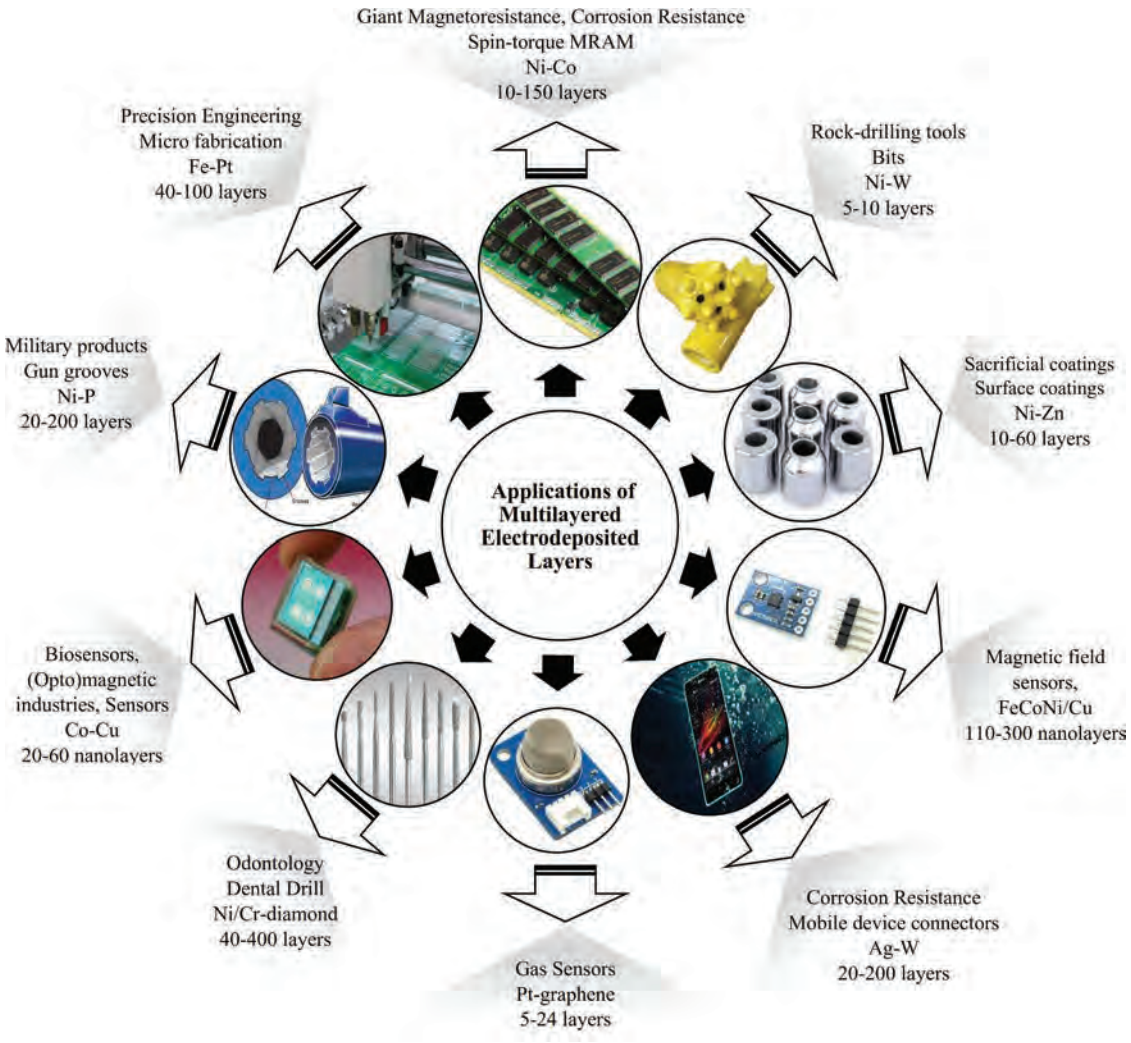

Fig. 1. A schematic of the variable applications of multilayered electrodeposited coatings.

parameters which may be more conceivably altered to achieve the desired coatings are given in Fig. 2. It should also be mentioned that some of these parameters are affected by other factors. Direct (continuous) or pulsed current can be used. Direct current is only influenced by the amplitude of the current whereas pulsed current is influenced by frequency, duty cycle, average current density and reverse pulse current. The switching of the current density between two/multiple values is suitable for technological purposes where the thickness of each layer may be controlled by adjusting the deposition time and current density.

Altering the applied potential is another process for the manufacturing of multilayer coatings which requires a three-electrode cell as its control is more complicated. Changing the electrode potential (pulse width and amplitude) leads to the variations in the composition of the deposits. This method provides the following advantages when used in the production of multilayer coatings: 1) low deposit temperature which reduces internal diffusion rate between layers, 2) a thickness that may be controlled by monitoring the electrical charge and 3) the layer composition may be tailored by controlling the electrode potential.

3. The importance of current control in the production of multilayer and gradient coatings

Electrodeposition is one of the most widely applied techniques to produce metal/alloy multilayer coatings. Many interrelsated parameters are involved in the plating process effective control is needed to achieve tailored multilayer coatings. The current is a key parameter in direct and pulse current techniques [21]. In addition to the chemical composition of the bath, the use of different modes of current control also affects the morphology and microstructural properties of deposits. For example, pulsed current influences mass and charge transfer during plating whilst reverse anodic current can improve mechanical and structural properties [22–24]. In direct current electrodeposition, multilayer coatings are produced by changing the current density and deposition time; in pulsed current, several parameters, other than current density, (such as frequency, duty cycle and reverse pulsed current) are also involved, as addressed in later sections.

3.1. Direct current

As previously mentioned, the direct current is a well-known method for the production of multilayer and gradient coatings. The main difference observed in coatings produced by direct and pulse techniques, is related to the process duration. Generally, changing the current density between two or more specific levels, each representing a metal or alloy, leads to the formation of multilayer coatings. Usually, the deposition time for each layer via the direct current varies between 1 s to 5 min or more. The other impact of current density is attributed to the growth kinetics and grain size. When direct current is used for the production of multilayer coatings, each layer may show different characteristics in

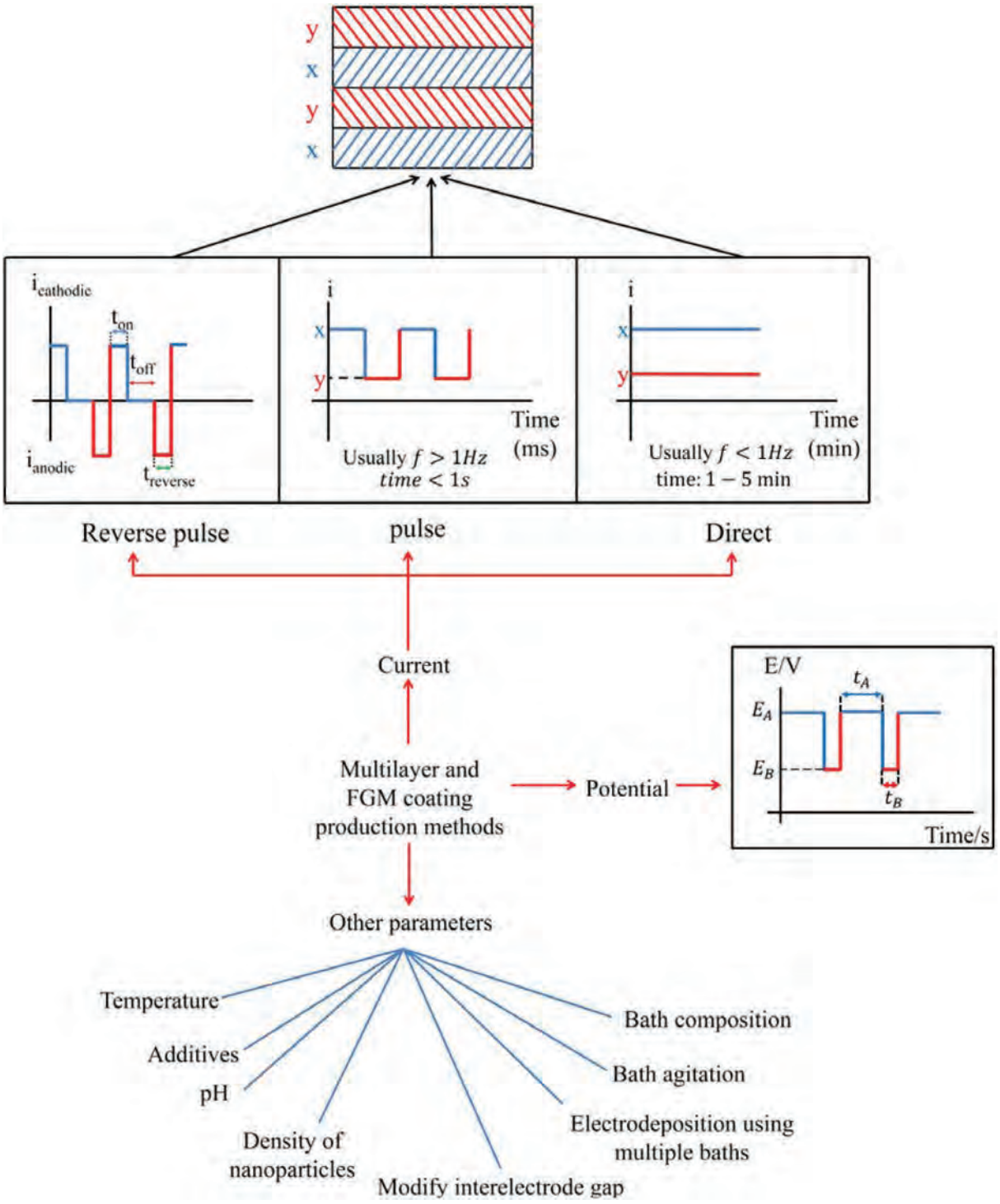

Fig. 2. Techniques used to produce multilayer and gradient coatings.

terms of the chemical composition, structure, grain size, growth kinetics and consequently the deposition rate of metals. Direct current can be used to deposit multilayer coatings by varying the current (with respect to each metal or alloy) in 2, 3 or more steps. Each step can last from several seconds to several minutes and leads to the formation of a layer with unique properties.

While direct current is generally applied using single metal baths, additives or nanoparticles may also be introduced to the bath. In Ni/SiC functional gradient coating, for instance, SiC content is increased from the substrate towards the surface by gradually increasing the current density. In this coating, SiC content increases with an increase in current density reaching a maximum value of 30 vol.% at 1200 rpm [25].

The electrosynthesis of advanced materials requires selection of suitable catalytic coatings and adequate control of the reaction environment, including mass transport and fluid flow. This has been significantly effective in the development of a new series of coatings called as composite modulated multilayer films. As seen in Fig. 3, Ni-W alloy coatings have been produced in single-layer (a) and multilayer (b) forms within the current density of 10-40 mA.cm^{-2} [26]. In addition to increasing the W content by increasing of current density, corrosion

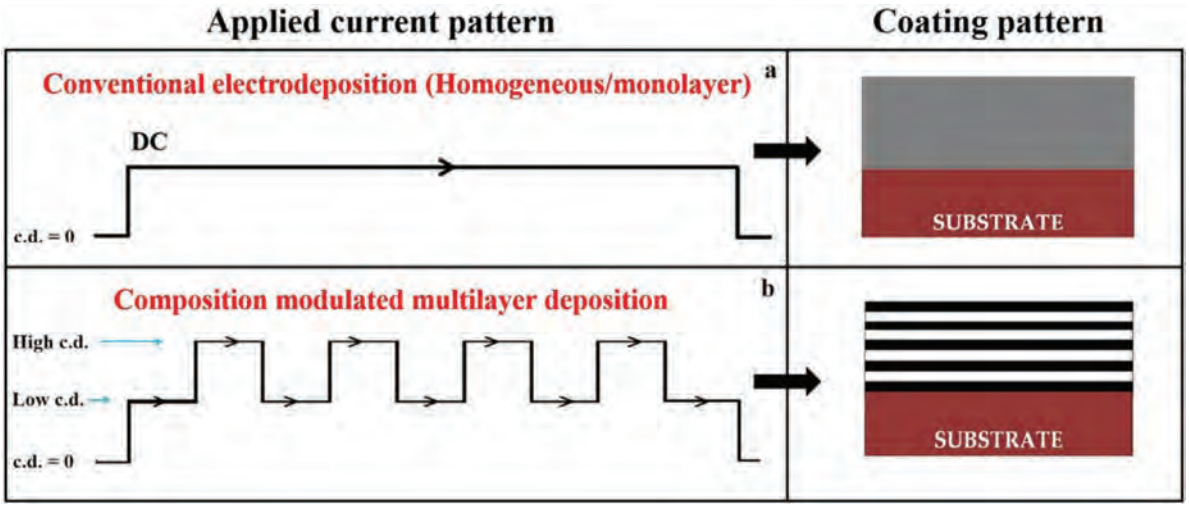

Fig. 3. The current waveform used to electrodeposit single-layer and multilayer coatings using (a) constant current and (b) pulsed direct current [26].

resistance of multilayer coatings was also noted to be higher than that of single-layered ones.

Another group of researchers managed to produce multilayer nickel-tungsten (Ni-W) coatings using a similar approach. Nickel-tungsten (alternate W-rich/W-poor) multilayers were produced through a variation of direct current density over given time intervals. An increase in hardness had been seen to adversely affect the single-layer Ni-W coatings as it caused an increase in internal stress and cracking, while W-rich/W-poor multilayer coatings provided an improvement in hardness at a minimum level of internal stress and even provided crack-free surfaces [27]. In order to compare direct currents with the pulse and reverse pulse currents, researchers produced alloyed Cu/Co coatings via direct currents and Co-Cu/Cu multilayer coatings using pulse and reverse pulse currents. The number of layers varied between 700 and 1500 [28]. Controlling the current density results in the fabrication of a $Co_{95}Cu_5$ alloy with the direct current method and a $Co_{95}Cu_5$/Cu multilayer using pulse and reverse pulsed current. The lower current was always employed for deposition of copper, while, the higher current was applied for deposition of cobalt/copper. The use of a constant/direct current made layer thickness control easier but the copper distribution was less uniform in direct current deposition [28].

FeCoNiCu/Cu multilayer coatings were produced by the current density variation, using low values for deposition of copper layers and high values for deposition of cobalt-rich alloys. Applying different currents over given time intervals led to the formation of multilayer FeCoNiCu coatings with Co-rich and Cu-rich layers [29]. Apart from magnetic properties, current density also affected the grain orientation and grain size within 20-80 nm in each layer of coating. In alloy plating systems, it is possible to produce multilayer coatings through the variation of direct currents among certain levels. In this case, each layer bears a unique alloying composition. In addition to conventional multilayer and gradient coatings, alloyed or composite multilayer nanowires may be deposited on anodic aluminium oxide (AAO) substrates. For instance, an increase in current density from the edge towards the centre of the template improved deposition rate in CoPt/Pt multilayer nanowires. Examination of the crystalline structure (at the nanoscale) revealed that each CoPt/Pt multilayer nanowire had a bamboo-like, periodic and regular structure [30]. Other types of coatings produced by direct current control in electroplating are shown in Table 1.

3.2. Pulsed current

Another method that provides effective control of composition and structure of electrodeposited coatings is by the use of pulse current which is known as pulse plating. Pulse currents have different shapes such as unipolar (on and off) and bipolar (reverse current) in Fig. 4. In the case of bipolar pulsed current, metal deposition occurs during the cathodic pulse while partial dissolution of metal occurs during the anodic pulse [31]. This method, also known as reverse pulsed deposition, leads to grain refinement through increasing the nucleation rate due to the application of higher current densities in comparison to the direct current method. In addition, mechanical properties of coatings such as toughness, tensile strength and yield stress were improved due to better hydrogen evolution conditions which, in turn, hindered the formation of metallic hydrides and rough depositions and also prevented pH variations. Using pulse plating, a homogenous film is produced which depends on frequency, peak current density, duty cycle and, partially, anodic current (reverse pulse) [32]. The plating process may be affected by variation in any of the parameters mentioned above.

In pulsed current plating, the duty cycle is defined as the ratio of the current on time (t_{on}) to the sum of the t_{on} and t_{off} :

$$\text{Duty cycle} = \frac{t_{on}}{t_{on} + t_{off}} = t_{on} f \tag{1}$$

where the frequency, f is obtained as:

$$\text{Frequency} = \frac{1}{t_{on} + t_{off}} = \frac{1}{t} \tag{2}$$

Different plating conditions may be obtained through the application of various frequencies and duty cycles or changing t_{on} and t_{off}. Peak current density is another pulse current parameter that is directly related to the average current density so that peak current multiplied by duty cycle is the average current density. If frequency and duty cycle are kept constant in plating, the properties of multilayer coatings can be changed by changing current density [21]. Fig. 4 (b) illustrates potential and current behaviours in specific duty cycle and frequency values applied for pulse electrodeposition of multilayers consisting of copper (frequency: 0.2 kHz, duty cycle: 60%) and cobalt (frequency: 0.4 kHz, duty cycle: 80%) [33].

3.2.1. Frequency

Pulse current creates a monolithic coating which usually becomes fine-grained with an increase in frequency. It can be seen in Fig. 5 that changing the frequency leads to the formation of a multilayer coating in which the crystalline structure and grain size of its layers are different. The pulse current frequency has been shown to be effective in controlling grain size. It is also possible to produce layers having different properties by gradual or incremental alteration of frequency. Assuming

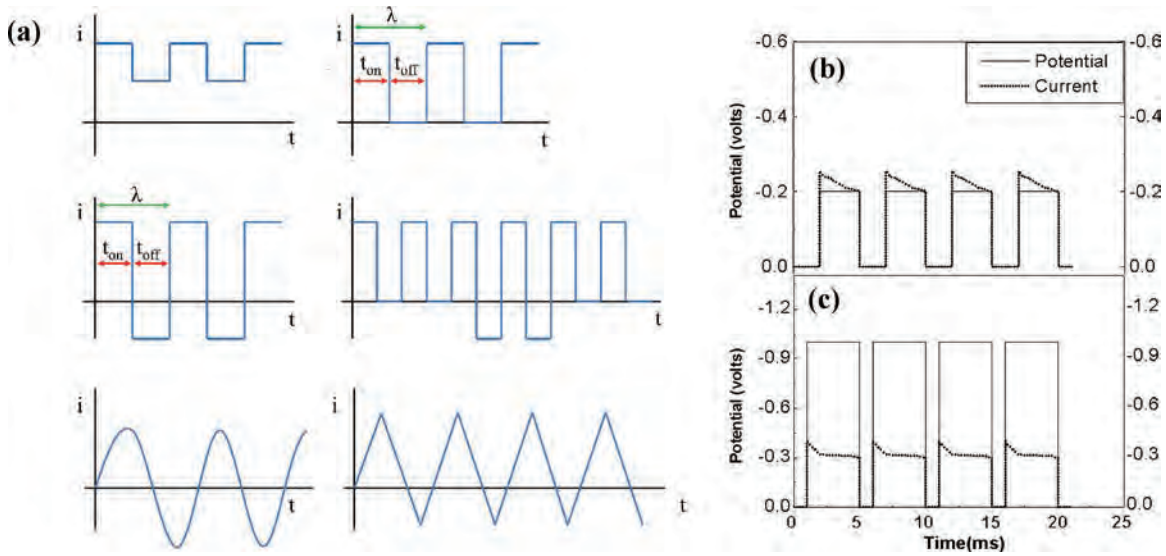

Fig. 4. (a) Different forms of pulsed current together with typical potential and corresponding current waveforms for (b) copper and (c) cobalt deposition (j is pulsed current density, t_{on} and t_{off} are on and off pulse durations) [33].

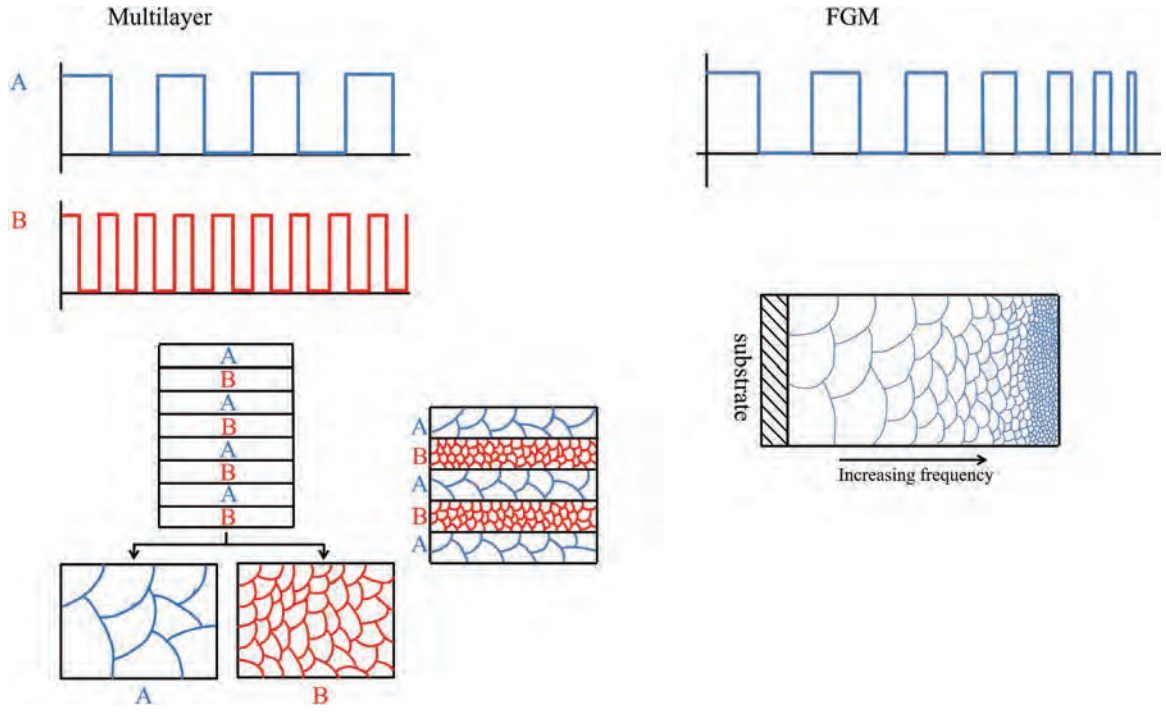

Fig. 5. The role of frequency in electrodeposition of multilayer coatings.

that other parameters are constant, the chemical composition of plated coatings can be simply controlled by alterating the frequency [32,34]. Since pulse frequency change, can influence directly on the doable layer thickness, it will change the value of limiting current density; in this way, pulse frequency can lead to alter the chemical composition of plated coatings, specially when one and/or all of the electroactive species are under convective-diffusion mass transport control.

Apart from chemical composition control, metal deposition and nanoparticles concentration, mechanical properties like hardness or internal stress may be influenced by frequency alteration. For instance, it was observed that an increase in frequency from 0.2 to 20 kHz in a Ni-W coating with incorporated multi-walled carbon nanotubes (MWCNTs), in addition to the slight change in tungsten content, hardness of coatings with 12 wt.% MWCNT was raised from 522 to 798 Hv [35]. Allahyarzadeh et al. [34] reported that alumina nanoparticles and tungsten contents were increased from 0.5 to 1.5 wt.% and 2 to 5 wt. %, respectively, in gradient Ni-W coatings containing alumina nanoparticles, at a constant duty cycle and average current density of 30 $mA{\cdot}cm^{-2}$, simply by increasing frequency from 0.1 to 1.5 kHz from the substrate towards the top surface of the coating as time progressed [34]. On the other hand, Torabinejad et al. [36] produced Ni-Fe-Al_2O_3 multilayer coatings at the duty cycle equal to 88% by varying the frequency between 0.1 to 6.4 kHz. According to energy dispersive spectroscopy (EDS) experiments, frequency fluctuations had no effect on alumina nanoparticle deposition or even the Ni and Fe content. The role of frequency in the improvement of corrosion and wear resistance has

been reported to be much more significant than other effective parameters. Considering the essential role of frequency alteration in influencing crystalline structure and other properties, various alloys that have been produced by the same process, together with operating conditions, are shown in Tables 1 and 2 [36].

3.2.2. Peak and average current densities

Current density may be manipulated to produce alloy multilayer coatings. In pulsed current electrodeposition, the average current density (j_{rms}) provides a reference state. Fig. 6 (a) shows that the same amount of deposited metal can be achieved using a direct current density equal to the average value (j_{rms}). The area under the j_{rms} curve is equal to the area under the pulsed current curve.

For instance, arrays of multilayer Cu/Co nanowires were produced on an anodized alumina oxide template using the pulse direct current at particular times and current densities for cobalt and copper. Due to the continuous metal exchange, the thickness of the cobalt layer partially decreases as long as the copper deposition period is extended. Hence, the desired thickness may be obtained by accurately controlling the current density and deposition time [37]. Cobalt/copper multilayer coatings may be produced through electrodeposition by changing average current density; however, due to the different cobalt and copper deposition rates, it is necessary to first obtain the deposition current range to reach the maximum deposition rate and process control [38].

The relationship between current density and the concentration of Co and Cu in multilayer coatings is shown in Fig. 6 (b) it can be observed that Co content in the electrodeposited film increases as a function of current density so that little amount of copper is deposited under 0.4 $mA.cm^{-2}$ in a coating containing 93 at.% cobalt [39]. $Co_{86}Cu_{14}$ multilayer coatings were obtained using current densities above 10 $mA.cm^{-2}$. Neurohr et al. [40] produced Co/Cu multilayer coatings on wafer/metallic Si substrates with a (100) plane orientation, using a combined technique (galvanostatic= constant current and potentiostatic = constant potential) to study the effect of gold as a surfactant in the electrodeposition process. The magnetic cobalt layer was plated at a constant current density of 19.2 $mA{\cdot}cm^{-2}$. The deposition was fragmented at low current densities; while, the bright metallic surface became opaque filled with dark non-metallic dots at high current densities. An increase in concentration of gold ions in the electrolyte led to an increase and decrease in cobalt and copper deposition concentrations, respectively [40]. The same multilayer coatings were also produced via two-pulse plating (a combination of galvanostatic and potentiostatic methods) where the magnetic layer (rich in cobalt) was formed via constant current deposition and the non-magnetic layer (rich in copper) was formed under potentiostatic control [41].

Moreover, cobalt-copper multilayer coatings may be produced in the form of Co-Cu/Cu multilayer films where growth is laterally continuous at high current densities; a 75% reduction in current density will lead to columnar grain growth containing bits of the multilayer stack [42].

A complexing agent is required for simultaneous deposition of copper and nickel by means of the pulse deposition technique. Current density has to be adjusted in the range 50-250 $mA.cm^{-2}$ in order to achieve uniform deposition and a smooth surface. In addition, deposition time decreases with an increase in current density while the nickel content is increased in the coating [43]. Rotary cylindrical electrodes were used elsewhere for deposition of Ag/Co multilayer coatings in a pulse current deposition bath considering the positive effect of temperature on current efficiency. It was reported that these multilayer coatings could be produced through alternating current density values (a low value for silver and a higher one for cobalt). It should be mentioned that an increase in current density at low temperatures leads to a considerable decrease in the silver deposition rate. The deposition rate was reported to be insignificant at high temperatures [44]. Ni-P-W multilayer coatings were produced on copper substrates by electrodeposition through changing the current density. It was reported that pulse current variation was directly related to tungsten content. For instance, increasing the cathodic pulse current density by ten times led to formation of a W-rich layer [45].

3.2.3. Duty cycle

The influence of different aspects of the duty cycle on pulse electrodeposition has been investigated, and the findings have shown to be very significant. There have also been various multilayer coatings produced on different metallic substrates with/without micro- and nanoparticles. It can be seen in Fig. 7 that the duty cycle is very important for the alloy and nanoparticle deposition rates. A large value of t_{on} implies

Table 1
The effect of current and other parameters on electrodeposition of multilayer and gradient coatings produced using direct current.

Coating	Type of coating	% Embedded particles / Chemical composition	Current density (mA. cm^{-2})	Wave length (length of two continious alternating layers - nm)	Number of layers	Approx. layer thickness (nm)	substrate	Ref.
Ni/SiC	gradient	SiC (5-30 vol%)	10-50	-	-	19000-262000	stainless steel	[25]
Ni-W	multilayer	%W: 0.95-12.5	10-40	-	10-600	8300-16000	-	[26]
Ni-W	multilayer	%W: 11.5-40 at. %	10,40	80	32	Total: 360	-	[27]
Cu-Co	multilayer	$Co_{95}Cu_5$	-32.5-1.25– 0.4	-	700-1500	8500-18000	polycrystalline titanium sheet	[29]
Co-Cu	multilayer	-	0.1-20	-	-	300	copper	[39]
Co-Ag	multilayer	-	0.1 & 40	10	50 (1.5 μm)	Total: 1500 Co:5 Ag:5	copper foil	[44]
CoCu/ Cu	multilayer		0.3-20	-	50	CoCu: 1.5 Cu: 1.5	copper	[51]
Co-Ag	multilayer	$Co_{32}Ag_{68}$	Co:10 Ag: 0.1	-		300	copper foil	[52]
Ni/Cu	multilayer	-	Ni/Cu: 10 Ni: 50	-	-	-	polycrystalline nickel silicon	[53]
Al-Mn	multilayer	Mn: 1-3 %	4,10	-	-	50 - 200	copper	[54]
Cr/Ni	multilayer	Ni: 95-5 %	50- 350	40-120	-	Total: 5000 Cr: 20 Ni: 50	low carbon steel	[55]
NiCo/ Cu	multilayer	-	35,53	7	-	Total: 300 NiCo:2 Cu: 5	silicon wafer covered with Cr and Cu	[56]

Table 2
The effect of current and other parameters on electrodeposition of multilayer and gradient coatings produced by pulsed current.

Coating	Type of coating	% Embedded particle / Chemical composition	Current density (mA. cm^{-2})	Wave length (nm)	Duty cycle	Frequency (Hz)	Number of layers	Approx. layer thickness (nm)	substrate	Ref.
Co-Cu/Cu	multilayer	$Co_{95}Cu_5$/Cu	Co:32.5 Cu: 0.6	3	60-92% for Cu	0.12-0.61 Hz	700-1500	8500-18000	titanium	[28]
CoPt/Pt	multilayer	$Co_{72}Pt_{28}$ /Pt	60	236	25%	25 mHz	≈42	CoPt: 167 Pt: 69	AAO template	[30]
Cu/Co	multilayer	Cu:4.37 % Co:95.63%	Cu: 0 - (-0.3) Co: 0 - (-0.4)	6.2	Cu: 60% Co: 80%	Cu: 200 Co: 400	40	-	copper foil	[33]
Ni-W-Al_2O_3	gradient	~2.6 wt.% Al_2O_3 ~0.3 wt.% W	I average: 30	-	10-90%	100-1500 Hz	8	Each layer: 15000	carbon steel	[34]
Ni-Fe-Al_2O_3	multilayer	15 wt.% Fe ~ 1.3 Al_2O_3 wt.% 37 wt.% Fe ~ 0.75 Al_2O_3 wt.%	I average: 30	30000	11% 88%	100, 6400 Hz	8	Each layer: 15000	low carbon steel	[36]
Co/Cu	multilayer	-	Co: 40 Cu: 0.5	225	30-60% fo Cu	-	-	Co: 145 Cu: 80	AAO template	[37]
Co/Cu	multilayer	-	0.53 for Cu and 5 for Co	-	0.95% for Cu and 5% for Co	≈0.05 -10 Hz	100	1.0-1.5	Copper foil	[38]
Co/Cu(Ag)	multilayer	1-8 at.% Ag	Co: 19.2	10.3-10.5	-	-	-	Total: 800	Si/Cr/Cu wafer	[40]
Co/Cu	multilayer	-	50	2.5-8	-	-	Not constant	Total: 300 Cu: 0.5-6 Co: 2	Si/Cr/Cu	[41]
Co-Cu/Cu	multilayer	-	84, 20.7, and 9.6 for Co	6.9-7.7	-	1-8.3 Hz	91	Co-Cu: 3.3 Cu: 4.0	Si/Cr/Cu wafer	[42]
Ni-Cu	multilayer	$Cu_{87}Ni_{13}$ $Ni_{77.5}Cu_{22.5}$	50 250	-	-	-	-	75000 35000	mild steel & copper	[43]
Ni–P–W	multilayer	Ni-%8P-15%W Ni-%5P-45%W	20 200	8-6000	q_c/q_a =3.6 q_c/q_a = 3.2	-	2-1000	25000	copper	[45]
Ni–Fe–Mn/Al_2O_3	gradient	Mn: 0.3-1.5 wt.% Fe: 22-47 wt.%	I peak: 40 I average: 4.4-35.2	-	11-88%	50-400 Hz	8	Total: 70000 Each layer: 9000	mild steel	[48]
Ni–Fe–Cr	multilayer	18%Fe-11.2%Cr 38%Fe-3.6%Cr	I peak: 80	1500 1000 300	20 & 90%	50 Hz	16 32 64	1000 500 200	mild steel	[49]
Co/Ag	multilayer	$Co_{92}Ag_8$	0.1-25	5.5	-	-	100	Co:0.5-2 Au:0.5-2	copper	[57]
Co/Au	multilayer	$Co_{95}Au_5$		3.3-4.5	-	-	100	Co:0.3-1.5 Ag:0.5-3.0		
FeCoNiCu/Cu	multilayer	Cu rich Co rich	0-80	170	94%	~2mHz	FeCoNiCu/Cu: 200/20 FeCoNiCu/Cu: 20/10	46 for Cu-rich and 124 for Co-rich	AAO & polycarbonate template	[58]
Ni-W	multilayer	$Ni_{91.3}W_{8.7}$	Forward (20 ms): 200 Reverse (3 ms): 150	100-1000	~87%	~43Hz	~ 600	Total: 30000 Each layer: 50	stainless steel	[59]
Ni-W	gradient	W: 1.5-5 wt.%	I average: 30	-	11-88%	100-1500 Hz	8	50000	carbon steel	[60]
Ni– Fe – Mn-Al_2O_3	multilayer	Mn: 0.15-1.40 wt. % Fe:24-51 wt.% Al_2O_3:0.9-1.2 wt.%	I peak: 40 I average: 8-36	5000	20, 50, 90%	50, 200, 400 Hz	32	Each layer: 2500	mild steel	[61]

that deposition periods are sufficiently long to affect the alloy content depending on the alloy or nanoparticle type. In most cases, the role of the duty cycle on the variation of metal or nanoparticle contents was investigated. This is due to the variety of metals and alloys in nature, as well as their different deposition rates and diffusion models. For instance, induced or anomalous electrodeposition is known as the reason for the differences observed in alloy deposition processes. Researchers produced high-content Ni-W/carbon nanotube nanocomposite layers with a uniform distribution by means of pulsed current with 20, 50 and 80% duty cycles [46,47]. In similar studies, Ni-Fe-Al_2O_3 nanocomposite multilayers were produced through variation of the duty cycle at constant frequency and current density values [36]. According to EDS results, the influence of the duty cycle variation on the metal content, particularly iron, was very significant; so, increasing the duty

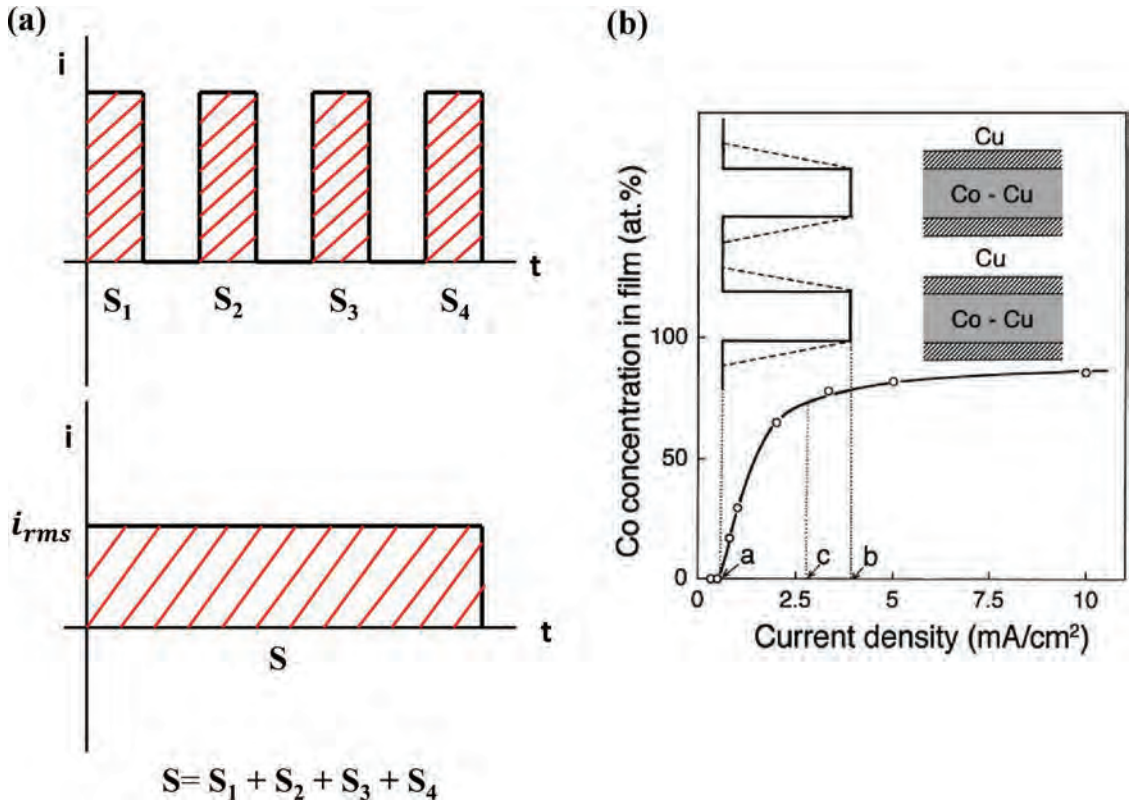

Fig. 6. (a) Average current density and its equivalent current density (j_{rms}) (S = the area under the curve) and (b) current density versus cobalt content in a multilayer coating [39].

cycle from 11 to 88% led to an increase in iron content from 15 to 37 wt. %. In Ni-Fe-Mn/Al_2O_3 gradient coatings electrodeposited using pulsed current, increasing the duty cycle from 11 to 88% produced a maximum manganese content (1.35wt%) with minimum alumina nanoparticles and iron content [48]. Consequently, the highest corrosion resistance was obtained with the maximum manganese content. In all cases, the duty cycle variation had an effect on microstructure and other properties such as corrosion and wear resistance, which will be discussed in future sections [34,36,48,49]. Tables 1 and 2 present a summary of the studies conducted in this field.

When pulse plating parameters like duty cycle, frequency, peak current density changes and the factors controlling kinetic and thermodynamic aspects of deposition can alter. When the deposition kinetics change the chemical composition of the developed layers can change which directly can influence on microstructure/properties of the multilayer coatings. For example, when one of the constituents in a binary system was under mass transport control, any changes, e.g. an increased frequency, which leads to thinning of the diffusion layer, can alter the chemical composition, microstructure and properties of electrodeposits. Other deposition parameters, sauch as electrolyte pH and temperature remain important.

3.2.4. Reverse pulsed current

The reverse pulse current technique may be used for the production of coatings with uniform and defect-free surfaces. However, due to the different properties and behaviour of alloys, the determination of optimum pulse parameters for each alloy requires many experiments. This section provides some information on multilayer coatings produced by the pulse electrodeposition technique. Note that the current efficiency of reversed pulsed current is always less than that of pulsed current [50].

For Ni-TiO_2/TiO_2 multilayer electrodeposits on copper substrates, it has been reported that an increase in titania deposition during the reverse pulse is caused by partial dissolution of nickel [28]. Increasing the reverse pulse duration contributes to a drop in pH. Co-Cu/Cu multilayer coatings deposited using the reverse pulse technique; the spontaneous reduction of cupric ions by reaction with Co during the reverse pulse led to the formation of a pure copper layer within the coating structure [28]. Other techniques for the production of multilayer coatings through variation of reverse pulse currents are presented in Table 1.

4. The effect of electrode potential

In addition to the current density, the electrode potential can be used for the production of multilayer coatings depending on the metal type and electrodeposition conditions. This technique is mostly used for electrodeposition of multilayer coatings which have significant potential differences. Multilayers produced under potential control in a single bath were introduced in similar studies [62–65]. The system consists of a computer controlled potentiostat and three electrodes in the electrochemical cell (electrolyte). The desktop computer controls the process and integrates the current to record the charge passed between the counter electrode (anode), the working electrode, W.E. (cathode). The cathode potential is monitored with respect to a reference electrode, R. E. in the cell. The working electrode is the substrate (sample) on which deposition occurs while the counter electrode, C.E. is often a high area platinum gauze (in the laboratory) or platinized titanium mesh (in industry). The shape and position of the counter electrode determine the current distribution over the working electrode surface. The distance between the working electrode and reference electrode leads to a potential drop but this is much smaller than between the counter electrode and the working electrode. According to the table of electrode potentials in Fig. 8, metals in groups A and B are mostly used to produce multilayer coatings by potential control. Co/Cu and Ni/Cu or composite multilayer coatings are the major types produced by means of this technique. In principle, the noble metals (A) in the potential series deposit at positive

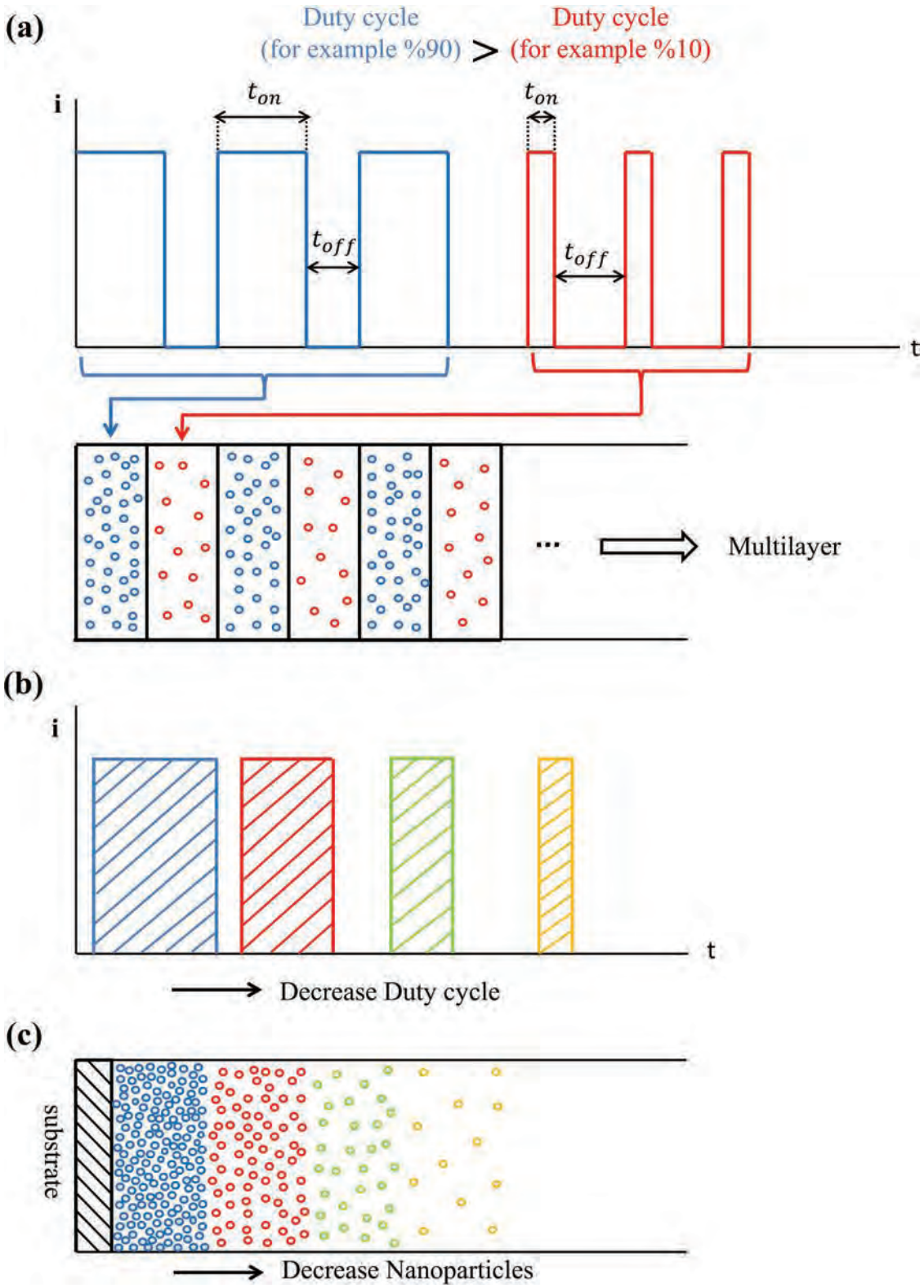

Fig. 7. Schematic figure illustrating (a) changing duty cycle of pulsed current (versus passing time) in each step and resulted multilayered structure with alternating alloying element, (b) decreasing duty cycle of pulsed current versus deposition time, (c) resulted gradient structure and its nanoparticle content.

potentials. In order to deposit metals, according to the potential series, one has to apply a potential more negative than the deposition potential of the intended metal. Since group (B) of metals deposit at potentials more negative than noble metals, it is not possible to deposit a single metal using a deposition potential less than that of noble metals. In other words, a slight content of the noble metal (A) always deposits with the less noble metal (B). The multilayer coatings produced are often made of alloying layers having different metal compositions. The presence of the nobler metal in alloy layers depends on pH, metallic ion concentration, potential and other parameters. Formation of the alloy layer occurs

Metal	Reduction Reactions	E° (V)	
Zinc	$Zn^{2+} + 2e^- \rightarrow Zn$	-0.763	
Chromium	$Cr^{3+} + 3e^- \rightarrow Cr$	-0.744	
Iron	$Fe^{2+} + 2e^- \rightarrow Fe$	-0.440	B
Cobalt	$Co^{2+} + 2e^- \rightarrow Co$	-0.277	
Nickel	$Ni^{2+} + 2e^- \rightarrow Ni$	-0.250	
Tin	$Sn^{2+} + 2e^- \rightarrow Sn$	-0.136	
Lead	$Pb^{2+} + 2e^- \rightarrow Pb$	-0.126	
Hydrogen	$2H^+ + 2e^- \rightarrow H_2$	0.000	
Copper	$Cu^{2+} + 2e^- \rightarrow Cu$	+0.340	A
Silver	$Ag^+ + e^- \rightarrow Ag$	+0.800	
Platinum	$Pt^{2+} + 2e^- \rightarrow Pt$	+1.199	
Gold	$Au^{3+} + 3e^- \rightarrow Au$	+1.420	

Fig. 8. The metals commonly used in multilayer coatings electrodeposited by controlling electrode potential and the standard potential of the metal/metal ion redox couple, E^{o} (V).

when a single bath is used for the electrodeposition process. Two different baths give a multilayer coating made of two different types of pure metallic layers. It may be concluded that if noble ions are present in the bath; the noble metal would also deposit at the potential applied for deposition of the less noble metal. It is also clear that a more negative potential needs to be applied for deposition of the less noble metal.

Co/Cu multilayer coatings are commonly produced through pulse plating on various types of substrates using a single bath. Copper is more noble than cobalt; thermodynamically, it is more likely to deposit at a more positive potential. During deposition of cobalt, however, copper always co-deposits leading to formation of a cobalt-rich copper alloy. Unless coatings are produced using two separate baths, the cobalt layer in the Co/Cu multilayer coatings is often impure and contains some copper. Fig. 9 (a) and (b) show schematics of a Co/Cu multilayer coating electrodeposited in a single bath where the thickness of each layer was 100 nm and the total thickness reached 1000 nm [66–70].

Application of a magnetic field changes copper deposition potential due to magnetohydrodynamic effect while cobalt deposition decreases due to preferred hydrogen discharging. In the absence of a magnetic field, the cobalt deposition rate increases with increasing cathodic potential [72]. The chemical composition of multilayer coatings can be controlled by altering the deposition duration at potentials suitable for copper and cobalt deposition [73]. Cobalt can be alloyed with iron and nickel to form CoFe/Cu and CoNi/Cu multilayer coatings [74,75]. An increase in pH within the range of 2.7–3.7 led to the improvement in the copper content of CoFe/Cu multilayer coatings [76]. When the copper concentration increases, cobalt content decreases and iron remains constant. Hence, the copper layer thickness increases with increase in deposition duration [75]. CoPt/Pt and CoAg/Ag multilayer coatings are amongst other types of coatings where, due to the more negative deposition potential of cobalt, both platinum and silver always exist in the Co-rich layers [77–79].

Ni-Cu multilayer coatings are also very commonly used for practical purposes. The nickel deposition potential is higher than the copper deposition potential and the thickness of layers may be changed through variation of the potential pulse. It was reported that in the case of nickel deposition at -1.2V, the formation of nickel hydroxide and nickel hydride is prevented [80]. An increase in temperature and annealing time leads to the decrease in nickel content and an increase in copper content [81,82]. It was found that the formation of pure substrates requires low potential for the copper deposition and high potential for the nickel deposition as, the deposition rate is slow at low potentials on the one hand, and, coarse grains form at high potentials, on the other hand. The optimum potential values for nickel and copper were found to be between 1.8 and 2.8 [83]. It is also possible to produce nickel alloys using other metals in multilayer coatings such as Ni-Co-Cu/Cu, Fe-Co-Ni/Cu, Cr-Fe-Co-Ni/Cu, Fe-Ni-Cu/Cu and Cu/Ni-P. For instance, a Ni-Co-Cu/Cu multilayer coating was electrodeposited from a sulfate/sulfamate bath through potential control for magnetic layer (alloying layer) and non-magnetic layer (copper layer). The magnetic layer and copper layer are produced under galvanostatic (constant current) and potentiostatic conditions, respectively. The use of a pulsed current led to an increase in the nickel and decrease in the cobalt deposition rates. Table 3 presents other approaches to the production of multilayer coatings by controlling

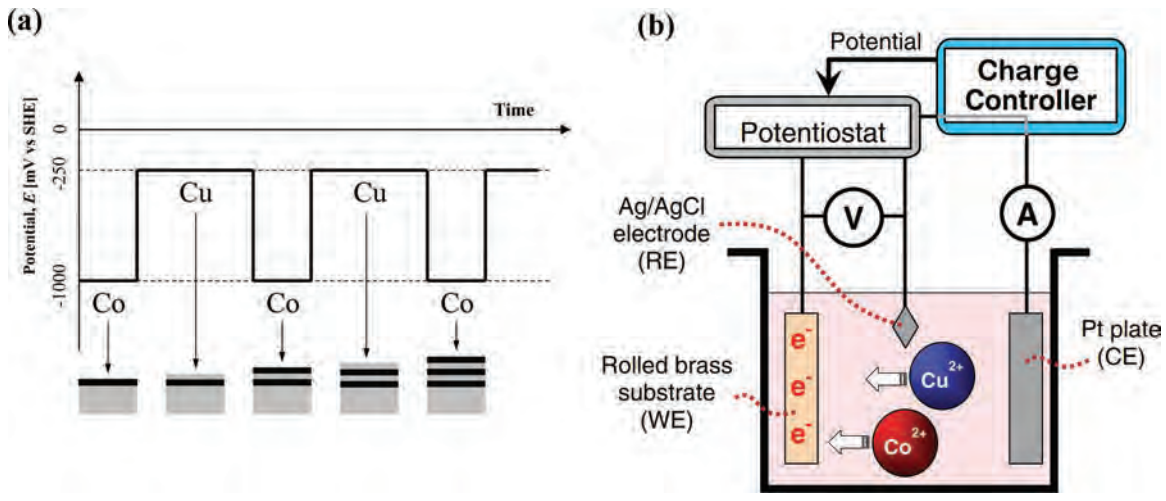

Fig. 9. (a) Potential pulse form for production of Co/Cu multilayer coating, (b) Electrodeposition of Co/Cu multilayer coatings [71].

the deposition potential.

5. Other parameters and methods

In this section, electrodeposition bath conditions are explained. The bath parameters are: pH, nanoparticle concentration, bath agitation, [100], distance between anode and cathode, temperature, bath composition, additives in the bath [101] electrodeposition in more than one bath [18,102] and plating time [103]. A variation in the electrolyte pH leads to a change in the evolved hydrogen level on the cathode surface. A more basic electrolyte may lead to less evolved hydrogen and the porosity of the coating may decrease. However, deposition of each metallic ion occurs at a certain pH which needs to be controlled. Increase in nanoparticle concentration in the bath, according to Fig. 10, usually leads to a higher nanoparticle content in the deposit, which improves mechanical properties. It shows how nanoparticles concentration can be changed in electrolyte with alternative addition from two container (A and B).

Agitation reduces the polarization at the anode surface, increasing the feasibility of ions being released from the surface. In addition, fewer hydrogen bubbles are formed on the cathode. The common methods to agitate the solution are magnetic stirring, mechanical stirring, ultrasonication and pumped electrolyte circulation. According to Fig. 11, increasing the anode to cathode distance reduces the throwing power on the cathode surface.

Temperature is an important parameter; higher values improve the electrical conductivity of the bath and diffusion rate of ions, providing an increased rate of metal dissolution at the anode and deposition at the cathode. An increase in temperature also prevents formation of a roughened deposit due to enhanced mass transport. It is often recommended that the temperature of plating baths should be greater than 50 °C. As seen in Fig. 12, the temperature during plating can also affect the optical reflectivity of coatings.

Electrodeposition of a metal may be performed using one or more bath compositions Two or more baths can be used to deposit two or more metal ions; each metal can be deposited in a separate bath. In addition, additives may be introduced to the solution for e.g. surface polishing, crack reduction and removal of surface stress. The parameters mentioned above are less effective than current density in influencing the thickness of multilayer coatings and achieving the desired mechanical properties. In practice, current density is often the simplest parameter to change and the most effective in controlling the properties of multilayer coatings.

Ni/Cu multilayer coatings were produced from two types of baths through the galvanostatic approach. Sulfamate and sulfate baths were used for the deposition of nickel and copper, respectively [104]. Electroplating of Ni/Cu multilayer coatings by the multiple electrolyte jet electrodeposition (MJED) approach is illustrated in Fig. 13. Nickel and copper were sprayed separately from two different baths using two nozzles on a rotary cathode (after spraying, electrolyte came back to its main container). According to the results obtained, an increase in copper spray time led to the formation of a thicker copper content (for a constant nickel spray time). Under constant spray times, increasing the copper current density also increased the thickness of the copper layer [18].

Ni/NiP_x, NiP_x/NiP_y ($0 < x, y < 25$at. %), Cu/Ni, Co/NiP_x multilayer coatings were produced through electroplating using two separate baths. The substrates were alternately placed in the two baths. Electroplating is performed on rolled copper and silicon substrates on a rotating disk. Where two nozzles are attached to the baths from the underlying plate. Electroplating is performed through rotation of the disk during its contact to the substrate. The substrate is prepared for the next spray stage using a cold/warm distilled water jet, nitrogen jet and sweeping by a slight pressure from a rubber. Sulfamate and Watts solutions are used for deposition of nickel whilst sulfate and phosphorous containing nickel baths were used for deposition of copper-cobalt and nickel-phosphorous alloys, respectively. Variation of the rotation rate and current density affects deposition efficiency. The phosphorous content in the deposited film increased with an increase in phosphoric acid concentration in electrolyte as well as a decrease in current density. Thus, coatings with minimum phosphorous contents were obtained at high current densities [102]. Cu/Ni multilayer nanowires were obtained through potentiostatic electroplating in separate baths (in order to prevent co-deposition). The thickness of each layer was readily controlled through variation of deposition period. It was observed that under a constant deposition period for each pair of layers; thickness of the nickel layer was greater than the copper layer [105]. Co-Cu/Cu multilayer coatings were produced in sulfate baths with/without NaCl through current control. EPMA tests revealed that an increase in NaCl concentration reduced the deposition efficiency of copper content and deposition current of multilayer coatings [101]. Co/Zn multilayer coatings were produced using a dual bath system (both sulfamate) through the potentiostatic approach. The thickness of layers may be controlled by means of the electrical charge passing throughout the electrolyte [106]. Cu/Sn/Zn multilayer coatings were produced by using the galvanostatic approach on Mo-coated glass substrates. Copper deposition is performed through different compositions of the plating electrolyte. Considering the molybdenum nature and its surface oxidation, it not only improves corrosion resistance but also enhances adhesion of copper. However, an important issue is oxide formation since Mo oxidizes in both acidic and basic electrolytes; adhesion and surface quality (homogeneity and smoothness) of a copper deposit on molybdenum are significantly better in alkaline solutions. In case of using acidic environments, one may improve quality and adhesion of Cu by addition of various compounds such as thiourea [107]. $BiTe_3/Sb_2Te_3$ multilayer coatings were deposited using an acidic bath through the pulse potentiostatic approach. The absence of complexing agents caused a competition for dissolution between Bi, Te and Sb which require low pH values. The presence of complexing agents, therefore, improves the deposition process. However, an increase in their concentration alters the metal deposition potential. Deposition of metal compounds is possible. Finally, formation of a ternary alloy structured multilayer coating requires long process durations, controlling the concentration near the electrode and controlling the deposition rate [108].

Copper exists in present in many multilayer coatings produced using the dual bath technique due to the fact that copper appropriately adheres to the underlying layer so that the coated sample may be easily removed from one bath to another one or exposed to spray of electrolyte. This is commonly not applicable for other metals with weak adhesion properties. However, the method for electrodeposition of a three-layer zinc-iron-chromium electroplated coating was developed in which an intermediate iron layer ensured adhesion of chromium to zinc [109]. The iron layer was deposited from a weak-acid citrate Fe(III) plating bath that exhibited no strong etching effect on various materials (such as zinc) Other procedures proposed for manufacturing of multilayer coatings and their effects on coating properties are indicated in Table 4.

6. Microstructural aspects of multilayer coatings produced by electrodeposition

In this section, various microstructural parameters of the electrodeposited multilayer coatings, including morphology and grain size, topography, crystallographic characteristics and compositions, are investigated. Modifying these parameters has a direct effect on the deposit properties.

6.1. Grain size & morphology

The effects of deposition conditions on the grain size are considered in this section.

The chemical composition of alloy deposits can significantly influence the grain size. For example, in the Ni-W system, higher levels of

Table 3
Effect of deposition potential on the electrodeposition of multilayer and gradient coatings.

Ref.	pH	Temperature	Electrode potential	Total deposit thickness	Thickness of each layer	Substrate	Coating
[71]	2.3	35-40	Co: -950 mV vs. (Ag/AgCl) Cu: -550 mV vs. (Ag/AgCl)	1 μm	4 nm	brass	Co/Cu
[81]			Co: -1000 mV vs. SHE Cu: -250 mV vs. SHE	1 μm	100 nm	copper	Co/Cu
[66]	5-7	25	Co: -1100 mV to -1800 mV vs. SCE Cu: -550 mV vs. SCE		Co: 0.5- 3 nm Cu: 1 nm	copper disc	Cu/Co
[84]			Cu: -190 mV vs. SCE Co: -1080 mV vs. SCE Cu: -170 mV vs. SCE Ni: -1190 mV vs. SCE		Cu: 0.5-8 nm Co: 3.2 nm Cu: 0.5-8 nm Ni: 3.2 nm	—	Cu/Co Cu/Ni
[68]			Cu: -600 mV vs. SCE Co: -1000 mV vs. SCE		Cu = Co = 150 nm Cu = Co = 50 nm	Ion track-etched polycarbonate membrane filters	Co/Cu
[69]	3.25		Cu: -585 mV vs. SCE Co: 35.1 mA.cm^{-2} (current density)	7 nm to 70 nm	Co: 2 nm Cu: 5 nm Co: 2 nm Cu: 2.5nm	Si wafer	Co/Cu
[70]	4	25	Cu: -300 mV vs. SCE Co: -1050 mV vs. SCE			Mild steel	Co/Cu
[85]			Co: -900 mV vs. SCE Cu: -400 mV vs. SCE			track-etched polycarbonate templates	Co/Cu
[72]	5.4	25 and 50	Cu: -450 to -550 mV vs. Ag/AgCl Co: -950 to -1050 mV vs. Ag/AgCl		Co-Cu: 2.5 nm Cu: 1.9 nm	Si wafer	Cu/Co-Cu
[73]		25	Cu: -650 mV vs. SCE CoCu: -1200 mV vs. SCE	30 μm	CoCu: 124 nm Cu: 14.2 nm	AAO templates	CoCu/Cu
[74]	2.2	25	Cu: -200 mV vs. Ag/AgCl CoNi: -1000 mV vs. Ag/AgCl		CoNi: 2-510 nm Cu: 4.2-42 nm	Anodized alumina template	CoNi/Cu
[76]	2.7-3.7	40	Cu: -300 mV vs. SCE CoFe: -1600 mV vs. SCE		6 nm	Ti	CoFe/Cu
[75]	2.1	40	Cu: -300 mV vs. SCE CoFe: -1600 mV vs. SCE		CoFe: 6 nm Cu: 0-6 nm	Ti	CoFe/Cu
[78]			Pt: -650 mV vs. Ag/AgCl Co: -850 mV and -1500 mV vs. Ag/AgCl			Cu	Co/Pt
[79]		25	Co: -850 mV vs. Ag/AgCl Pt: -300 mV or -650 mV vs. Ag/AgCl		Co: 1 nm Pt: 0.5 or 2 nm CoNi: 1 nm Pt: 0.5 nm	Pt or Cu	Co/Pt CoNi/Pt
[86]	2-3	30	CoPt: -1000 mV vs. SCE Pt: -300 mV vs. SCE	5μm	Pt: 20 nm CoPt: 10 nm	AAO template	CoPt/Pt
[30]		25	Pt: -400 mV vs. Ag/AgCl CoPt: -1000 mV vs. Ag/AgCl	1-25 μm	Pt: 71-163 nm CoPt: 60-282 nm	AAO template	CoPt/Pt
[77]	2.7	25	CoAg: -1000 mV Ag: -650 mV		CoAg: 5 nm Ag: 20 nm	Polycarbonate membranes	Co-Ag/Ag
[87, 88]	3.5-4	40	Cu: -140 mV vs. SCE Ni: -700 mV vs. SCE	8 μm	8-300 nm	beryllium bronze	Cu/Ni
[89]			Cu: -160 V vs. Ag/AgCl Ni: -1000 mV vs. Ag/AgCl		5-125 nm	Polycarbonates membranes	NiCu/Cu
[90]				3 μm	5 nm and 100 nm	Cu	Ni/Cu
			NiCo< -500 mV vs. SHE Cu> -500 mV vs. SHE	1 μm	100 nm		CoNi/Cu
[80]			Ni: -1200 -1250 mV vs. SCE Cu: -400 -800 mV vs. SCE			alumina template	Ni/Cu
[91]	4	25	Ni: -1200 mV vs. SCE Cu: -700 mV vs. SCE				Ni/Cu
[82]		200-1000	Co: -1000 mV vs. SHE Cu: -250 mV vs. SHE		100 nm	polycrystalline copper substrate	CoCu/Cu
[92]		25	1400 - 4000 mV	20 μm	80 nm	carbon steel	Cu/Ni
[93]	3.6 -3.9	30	Cu: -30 mV vs. SHE Ni: -650 mV vs. SHE	1-10 μm	3-500 nm	polycrystalline copper substrate	NiCu/Cu
[83]	7.2-7.5	25	Ni: < 2000 mV Cu: > 1000 mV	20 μm		ANSI 1045 steel	Cu/Ni
[94]		25	Cu: -500 mV vs. SCE NiCo: -1500 mV vs. SCE		Cu: 10 nm NiCo: 200 nm	alumina templates	NiCo/Cu MNW
[95]	3	25	CoNiCu: -15 to -45 mA·cm^{-2} Cu: -585 mV vs. SCE	1.5 μm	CoNiCu: 1.2-12 nm Cu: 1.1-2.3 nm	titanium	CoNiCu/Cu

(*continued on next page*)

Table 3 (*continued*)

Ref.	pH	Temperature	Electrode potential	Total deposit thickness	Thickness of each layer	Substrate	Coating
[96]	2.3 and 2.9	25	Cu: -250 to -400 mV vs. SCE (Cr)FeCoNi: -1800 to -2400 mV vs. SCE			AAO	FeCoNi/Cu and CrFeCoNi/Cu
[97]	3	25	Cu: -600 mV vs. SCE NiFe: -1200 and -1400 mV vs. SCE		Cu:10 nm NiFe: 20 nm	Anodized alumina membranes	NiFe/Cu
[98]		25	Fe-Ni-Cu: -1500 mV vs. SCE Ni-Cu: -1450 mV vs. SCE Cu: -200 mV vs. SCE		5 nm/3 nm and 5 nm/2 nm and 4 nm/2 nm	Au/Cr/glass substrate	Ni-Cu/Cu and Fe-Ni-Cu/Cu
[99]		25	NiFe: -1400 mV vs. Ag/AgCl Pt: -400 mV vs. Ag/AgCl	5-10 μm	NiFe: 300 nm Pt: 60 nm	AAO	NiFe/Pt

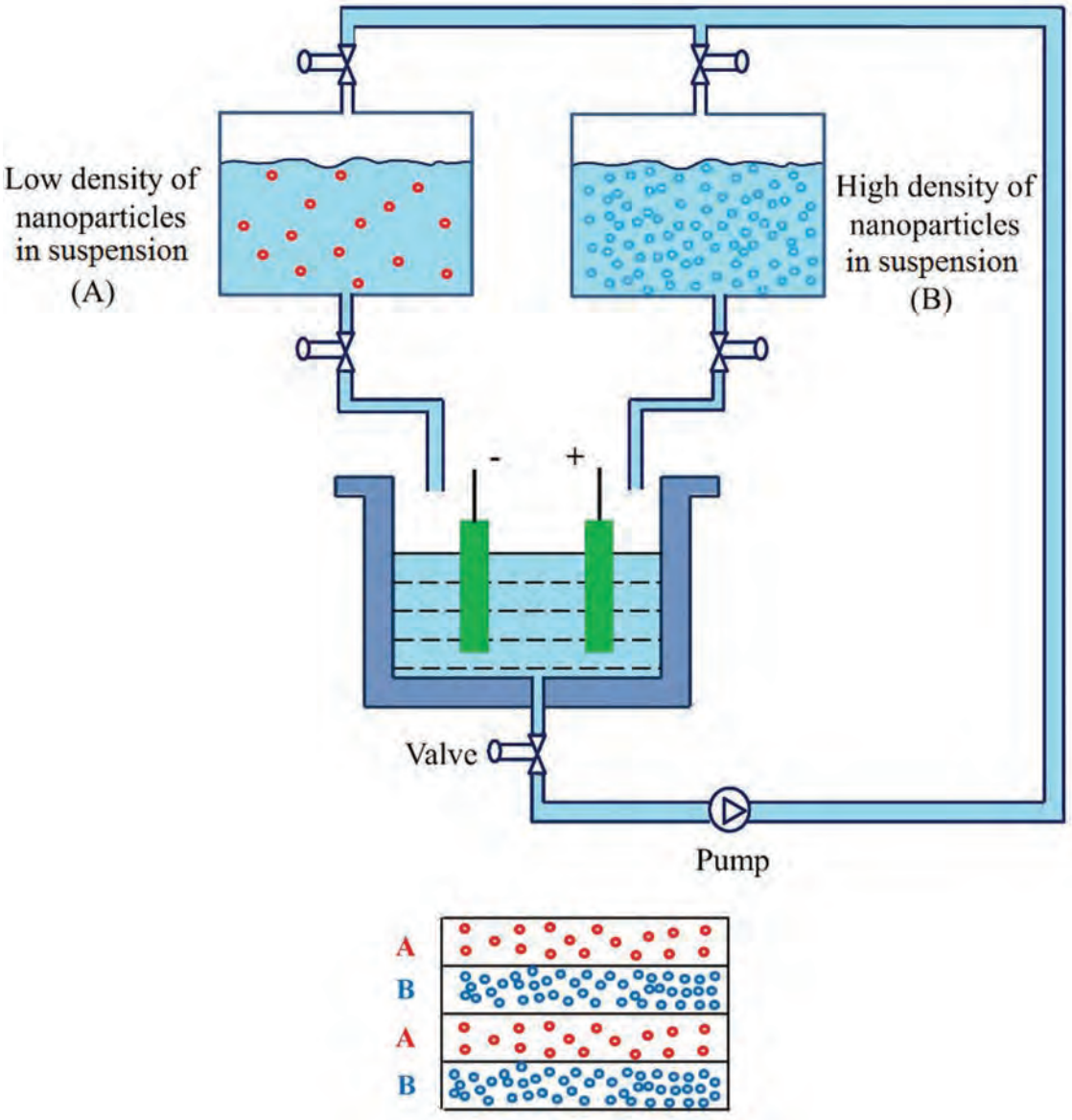

Fig. 10. Achieving alternate layers having different nanoparticle contents in a multilayer coating.

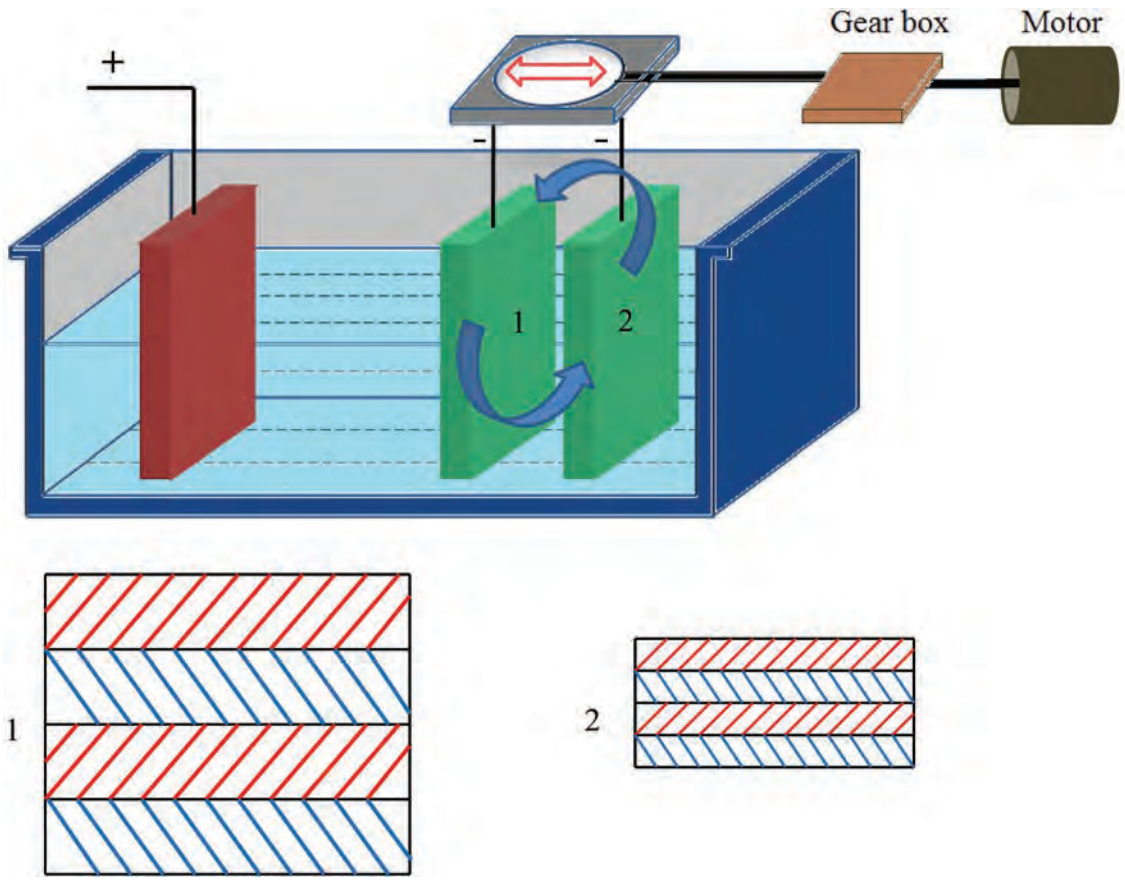

Fig. 11. The effect of altering the anode to cathode distance on the thickness of a multilayer coating.

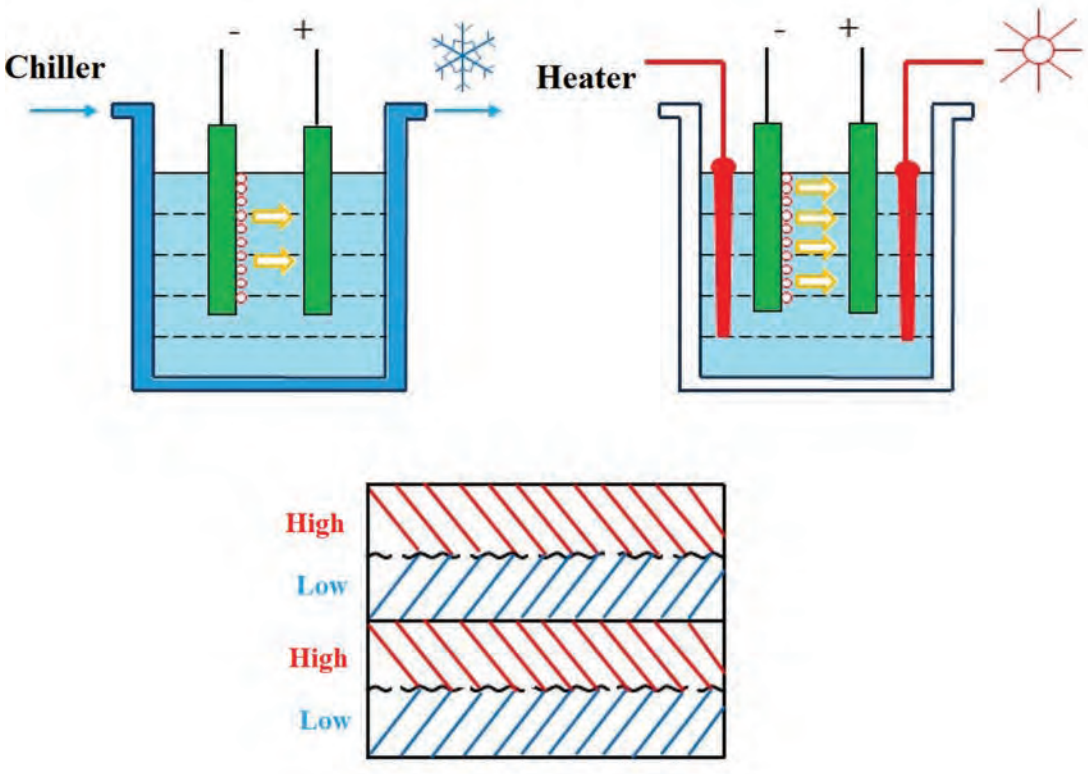

Fig. 12. The effect of temperature on the surface finish of multilayer coatings.

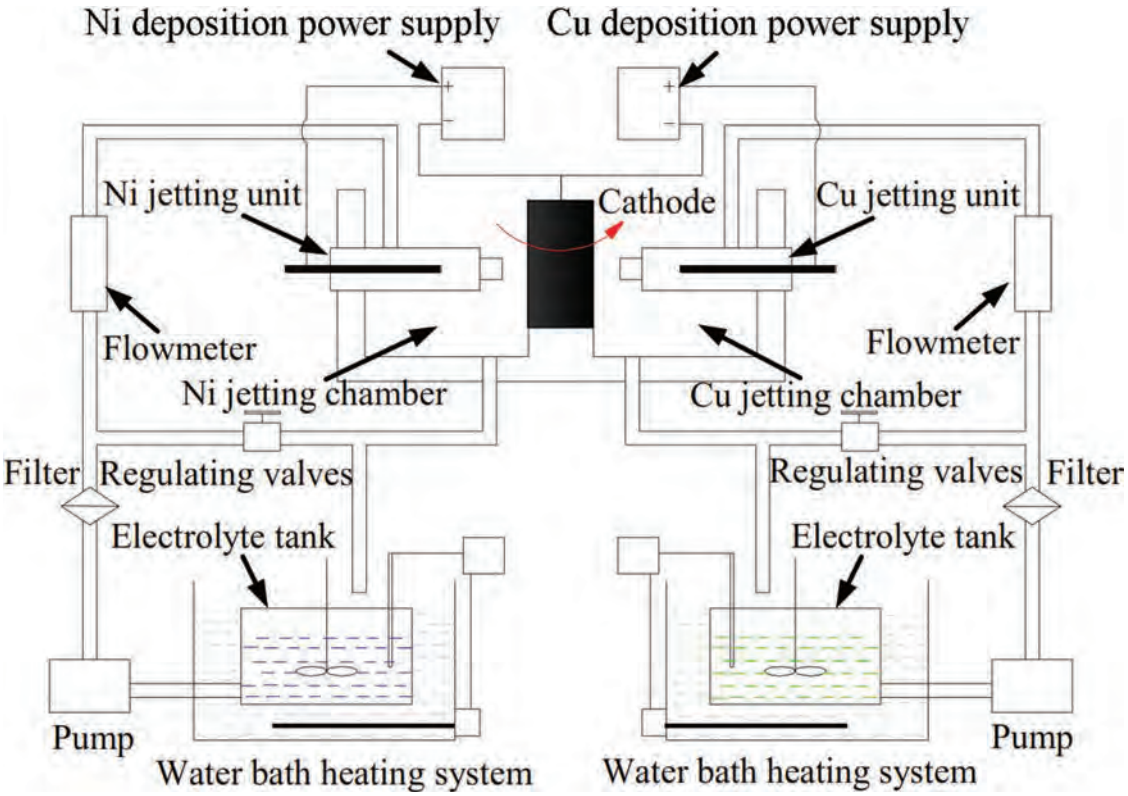

Fig. 13. The use of the dual plating bath electrodeposition technique [18].

tungsten in the alloy result in a reduction in grain size, which is beneficial for the synthesis of nanocrystalline nickel based coatings [27]. Udompanit et al. [59] attributed this to the separation of tungsten atoms at the grain boundaries of nickel, resulting in thermodynamic stability of the grain structure [59]. A further increase in the tungsten level causes amorphization of the alloy. This effect can be used to control the microstructure of multilayer films by alternating the chemical composition between concentrated and dilute tungsten layers. For instance, the tungsten rich (≈ 40 at.%) layer is amorphous while the layer containing less tungsten (≈ 11 at.%) is nanocrystalline [27]. The alloy composition can be controlled by tailoring the electrolyte composition. By altering the concentration of nickel and iron ions in the electrolyte, the chemical composition and grain size of the Ni-Fe deposits can be altered. When the concentration of nickel in the electrolyte, and the deposit, is high, smaller grains form. When the concentration of iron in the electrolyte is high, twinning and formation of larger grains are promoted [111]. The type of current control (pulsed or direct) can effectively alter the grain size and morphology. Under pulsed current conditions, a smaller crystallite size is generally seen in alloys, leading to more smoother surface, compared to direct current conditions. Often, a small crystallite size leads to a smoother surface topography and a smooth interface between multilayers. In a study of Cu-Co alloy deposition, it was observed that under direct current, the microstructure was fully dense and consisted of fine grains which covered the entire surface of the substrate. By applying pulsed deposition, the grain size of the deposit decreased [70]. The grain size of the electrodeposits can be dependent on the thickness [112]. For instance, it has been reported that in Fe-Co-Ni-Cu/Cu multilayer with a copper layer thickness of 20 nm and thickness layer of Fe-Co-Ni-Cu 200 and 40 nm, the grain size depended on the thickness of the cobalt-rich alloy layer, so that the increase in the thickness of the Fe-Co-Ni-Cu layer with a constant thickness of the copper layer leads to an increase in the grain size of the multilayer structure [29]. A comparison of copper multilayers produced by ultrasonic-electrodeposition with a monolithic deposit showed that the grain size in the multilayer is much smaller than in single-layers [113].

The influence of electrodeposition conditions on the grain morphology of multilayers has been reported in several studies. In a Fe/Pt multilayer, due to the presence of the iron layer a nanocrystalline disordered film forms which results in unusual features in the diffraction pattern. The Fe/Pt multilayer have granular, polycrystalline structure formed by Wollmer-Weber growth mechanism, which is a deposition mechanism that occurs when atoms in the deposit are more strongly bound to each other than to the substrate. The shape and crystalline size are dependent on the first layer deposited on the substrate (Pt or Fe) [114,115]. Another study reported that TEM analysis of multilayered Co-Cu/Cu showed the simultaneous deposition of copper and cobalt resulted in a large separation near the boundaries, creating columnar grains. The adjacent areas of the grain boundaries have higher copper and lower cobalt than the center parts of the columnar grains (i.e. the formed columnar grains are separated by the copper domains) which results in the fluctuations in the two-layer thickness [42].

In a Cu/Sn/Zn multilayer, shown in Fig. 14, coarse-grained deposition of Sn on Cu resulted in island like nucleation and growth which did not cover the entire surface of copper, while deposition of Zn on Cu was more compact and more homogeneous than Sn [107].

6.2. *Surface & interface topography*

Surface topography is an important parameter both for functionality and aesthetic appearance of the coatings. Various deposition conditions, directly change the surface topography. For instance, when a current density of 0.8 mA/cm^2 is applied in the Cu/Ni multilayer, a nodular structure with deep valleys is obtained between the individual nodules. Under these conditions, due to the presence of these large nodules, the surface shows a significant roughness and the copper layers are straight and parallel. When the current density is 0.4 mA.cm^{-2}, the growth of copper layers was more irregular and wave like; the surface became smooth with small bumps having a diameter of approx. 200 to 400 nm

Table 4
Other methods for electrodeposition of multilayer and gradient coatings.

Coating	Type	Potential	Current density	Bath constituent	Time	% Embedded particle	Variable parameters	Number of layers	Bath condition	Thickness	Substrate	Description	Ref.
Ni/Cu	Multilayer	-	10 mA.cm^{-2}	Ni(sulfamate) Cu(sulfate)	deposition time-determined from deposit thickness	-	type of electrolyte bath, current density, pH value and temperature	-	-	total thickness of 5 μm, with different layer thickness (from 30 nm to 1 μm)	Rectangle cold-rolled polycrystalline	decreasing the layer thickness (and increasing the number of interfaces) from 1 μm to 30 nm, the composite hardness of the systems (film and substrate) increases	[104]
Ni-Cu	multilayer	-	Ni(600–1400 mA·cm^{-2}) Cu(800–4000 mA·cm^{-2})	Ni (nickel sulfate, nickel chloride, boric acid) Cu (copper sulfate, sulphuric acid)	-	-	time and current density	-	-	1.2 mm	stainless steel	Ni & Cu were sprayed on rotary cathode from 2 separate bath under controlling (electrolyte was entered into tank after spraying on cathode)	[18]
Ni-P and other alloys	multilayer	-	above 25 mA·cm^{-2}	Ni (sulfate, sulfamate) Cu,Co (sulfate) Ni alloys (nickel bath with P)	-	-	Current density, substrate revolution, efficiency	-	In the dual-bath technique, a substrate is moved between each bath and a layer is plated from each electrolyte in turn	The thickness of each layer of the deposit is proportional to the time per substrate revolution, the current density, and the efficiency	substrate was rotated on orbital disk which was contained 2 section of silicone & Cu rolling.	-	[102]
Cu/Ni	multilayer	Cu(−0.08 V vs. SCE) Ni(–0.9 V vs. SCE)	-	Ni (nickel sulfate, boric acid) Cu (copper sulfate, sodium sulfate)	150 s/150 s 150 s/300 s	-	time	-	potentiostatic deposition using double bath	Control with time deposition of each layer	Alumina that 200 nm gold film on it.	-	[105]
Co-Cu/Cu	multilayer	-	Cu (-0.6 mA·cm^{-2}) Co (-32.5 mA·cm^{-2})	sulfate	listed in table of paper	-	Current density, presence and absence of NaCl, time	Between 880 and 1500	-	total multilayer thickness ≈. 10 μm	Ti	Density of Cu & deposition rate of multilayer were reduced with increasing the amount of NaCl.	[101]
Co/Zn	multilayer	-	-	Dual sulfate bath	-	-	Layer thickness	50	Potentiostatic	Coulostatic	copper	-	[106]
Sn/Zn/Cu	multilayer	-	Cu,Zn(1.5 mA·cm^{-2}) Sn(2 mA·cm^{-2}	Cu deposited from various baths	-	-	Potential-Time	-	Galvanostatic	-	Mo- coated glass	Metallic stacked layers of Cu, Zn and Sn were sequentially electrodeposited	[107]
Bi_2Te_3/Sb_2Te_3	multilayer	-	-	Acidic aqueous	-	-	Current density-potential	2 and 3	Potentiostatic	Thickness of layers: 17 nm	Si, Au coated by Ti deposition	-	[108]
Cu/Ni/Cr	multilayer	-	-	Stannate	5 - 180 s	-	Time	-	-	-	Sn used as underlayer for the deposition multilayers on e.g.,Al	-	[103]
Ni/Cu , Co/Cu	multilayer	alternating the potential between -0.2 and -1.6 V vs. (state R.E.)	-	Acid sulfate	-	-	Current-Time	-	Potentiostatic	1.5 nm for each layer of Cu & 3 nm for each Layla of Co in Co/Cu	Silicon	-	[110]
Cr/Fe/Zn	multilayer	-	Zn (10–20 mA·cm^{-2}), Fe (5–25 mA·cm^{-2}), Cr (50–200 mA·cm^{-2})	Zn – alkaline zincate, Fe - weak-acid (pH 5) citrate-chloride Fe (III) plating bath, Cr – sulfate-formate trivalent bath	-	-	Electrodeposition in three different baths	3	-	Zn – 9 μm, Fe – 1; 3 or 5 μm, Cr – 0.5 μm	steel	The metallic layers were sequentially electrodeposited from individual baths.	[109]

[116]. SEM analysis of the Co-Fe/Cu multilayer showed that, on decreasing the pH, level homogenization of the surface decreases, and the time of the deposition of the copper layer increases. At a pH of 2.7, a large number of grains with the same size accumulated; on increasing the pH to 3.7, a regular grain structure was achieved [76].

The deposition potential also affects the surface topography. In a study on the effect of the applied potential on the surface roughness of the Ni-Co/Cu multilayer, it is reported that at deposition potential of -800 mV, the Ni-Co deposition alloy has a rough surface, but at the potential of -1600 mV, a smooth surface is achieved. The cobalt-rich alloy has hcp structure and the Ni-rich alloy has fcc structure. The lattice parameter can affect the surface roughness; if the Co-Ni layer has an FCC structure, epitaxial growth in the same orientation occurs in grains on the polycrystalline copper substrate [90].

Another factor that can affect the structure of the deposition layers and the surface roughness of the layers is the addition of additives to the electrolyte. For example, when a brightener is added to the electrodeposition electrolyte of copper-nickel multilayer, surface of the coating is mirror-like and free of porosity while, in its absence, the nickel layer has a large number of cavities and copper mainly grows on the edges of the crystal and the corners of the protruded regions in nickel and makes the surface of the multilayer rough. By adding the brightener, the copper layer becomes more uniform. By adding some brightener to the electrolyte, the smoothness and homogeneity of the deposited multilayer increases. Adding a higher concentration of brightener can prevent the growth of copper crystals on the bright nickel layer. When the brightener is adsorbed on the cathode surface, crystallization is improved and a dense multilayer film with a fine grain structure is obtained. [87] SEM analysis of a Ni/Cu multilayer showed that copper and nickel substrates in the internal regions of the film had the same thickness but the thickness varied in the outer regions. Thickness variations of the layers lead to the increase of the roughness or discontinuity of the multilayer structure in some areas [88].

The effect of layer thickness on the surface topography of the multilayers is not clearly understood. Jikan et.al [117] produced Ni/Cu multilayers with sublayer thicknesses of 1, 5, 10 and 50 μm using a dual bath technique. They observed cauliflower like surface topography for multilayers with sublayers of 50 μm thick, while multilayers with 1, 5 and 10 μm sublayers were smooth. By decreasing the layer thickness, the size of the cauliflower-like grains was reduced on the surface [117]. Such results were confirmed in other studies; at the beginning of deposition, surface roughness was insignificant but with increasing the thickness and growth of dendrites, roughness also increased [93].

The last layer affects the surface characteristics and topography of multilayers. For example in Zn/Ni-Zn multilayers (produced by dual bath), depending on whether the last layer of this multilayer is Zn or the Ni-Zn alloy, the structure of the multilayer will be different (Fig. 15). When the upper layer is zinc, the structure is uniform and silvery-grey, while if the upper layer is zinc-nickel alloy, it will have brighter appearance with a cauliflower-like morphology [118].

In the Ni/Ni-Al_2O_3 multilayered coating, where the nanocrystalline layer of Ni is the upmost layer, the coating has a uniform spherically nodular structure. As the number of layers increases, the size of the nodules decreases. This reduction can be attributed to the reduction of the thickness of each layer. The coating with the nanocomposites layer of Ni-Al_2O_3 at the very top has a polyhedral structure and a number of cavities are also seen on the surface of the coating, which are probably due to the formation of H_2 during deposition [119].

In the case of Fe-Ni-Cu/Cu multilayers, the surface is rough, while the monolithic Ni-Fe-Cu layer has a smoother surface [120]. SEM analysis of the Co-Pt/Pt multilayer showed a filamentous structure. TEM analysis revealed that the thickness of the Co-Pt alloy layer is less than the Pt one. The structure is bamboo-like and the thickness of the layer is controlled by the deposition time [86].

In another study on CoPt/Pt multilayered nanowires, SEM images showed an alternative white-gray bamboo-like structure in each nanowire. On the other hand, neighboring nanowires were grown alongside each other with the same structure and size, but in the farther nanowires there is a difference in size, which could be due to the variation in the resistance of the gold in the substrate. In samples with the same total deposition time, the observed difference in length is due to the growth rate of the nanowires [30]. In the Co-Pt-P/Cu multilayer, the TEM analysis shows that with increasing the thickness of the copper layer, the layers change from the smooth to the waveform [121]. TEM analysis of cobalt/copper multilayer nanowires, showed that the layers are not always perpendicular to the wire axis, these multilayers have regions that are oriented vertically to the axis of the wire. In some cases, the layers have a diagonal orientation, this change of orientation occurring in one or two bilayers. Some of these multilayers have cigar-shape morphology, such that the middle of the nanowires is bigger than their bottom. This heterogeneity is due to the non-uniform growth of nanowires [122].

Another factor closely affecting the surface topography is the topography of the interlayer interface. According to a study on the interface of the Ni/Cu multilayer, there should be an arrangement of misfit dislocations in the interface between two crystals with two different lattice parameters to compensate the mismatch of the lattice parameters. This misfit dislocation existing in all the Cu/Ni interfaces can prevent the movement of dislocations of the lattice to the layers, which lead to increases the strength of the multilayer structure [90]. In very thin multilayers, the lattice planes of layers are slightly tilted with respect to each other which may result in different behavior [93]. however, no clear interface is also possible in some multilayers [107]. It is worth noting that the quality of interfaces can affects the structural properties of multilayers [44]. Since the lattice constants of the layers are different, conditions for formation of edge dislocation can occurs and consequently results in twinning during the growth of multilayers. As an example the interface of two layers of Cu/$Co_{81}Cu_{19}$ multilayer is zig-zag shaped with a sharp edge (Fig. 16) [73].

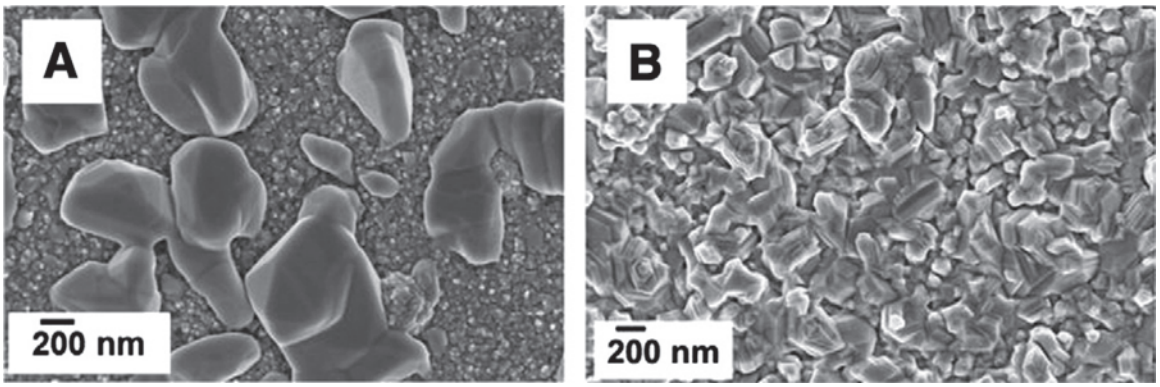

Fig. 14. SEM images showing the morphology of (a) Sn grains on Cu,(b) Zn grains on Cu [107].

Surface roughness of the substrate, as well as the last layer of deposition layer in the multilayer, are also other factors affecting the surface roughness of the multilayer. For example, in the copper-cobalt multilayer when the last deposited layer is copper, the surface roughness is more than when the last deposition layer is cobalt. Lattice mismatch in the multilayer results in surface roughness, because the layer with a larger lattice constant grows only island-like on a layer with smaller lattice constant [69].

The AFM analysis of Fe-Ni-Cu/Cu shows that surface roughness increases with increasing the number of Cu and Fe-Ni-Cu layers. Also higher concentration of Fe makes the surface roughness more pronounced [98]. In relation to FeCoCu/Cu multilayer it is reported that the copper layers are completely separated from the alloy regions of Fe-Co-Cu, which are rough and irregular, which is probably due to the polycrystalline nature of the wires, large grain size and heterogeneity in growth [123]. In Ni-Fe/Pt multilayers, the interface of Ni-Fe/Pt is rougher than that of Pt/Ni-Fe, since at the end of the deposition of NiFe layer, the deposition potential varies from -0.4 –1.4 V then suddenly stops. At the end of platinum layer deposition, the metal can be deposited continuously and, in the range of -0.4 –1.4 V can be deposited even at less negative potentials than -0.4 V [99]. In the Ni-Co/Cu multilayer at more negative potentials, the roughness increases, but at less negative potentials, the roughness decreases and then reaches a constant value. Therefore, in the positive potentials the surface is smoother. In fact, in potentials that are more positive than E_{cu}, cobalt atoms are removed from the surface due to their dissolution and the amount of roughness changes with the chemical composition of the layer. The adsorbed species can block empty areas on the surface and prevent growth. A higher rate of deposition occurs in some areas and leads to more pronounced surface roughness in the more negative deposition potentials of copper. Generally, in this multilayer, in the more negative potentials the roughness increases and, for more positive potentials, roughness first decreases and then remains constant. The effect of potential on roughness is shown in the AFM images of Fig. 17. Surface roughness is related to the simultaneous deposition of nickel and cobalt with copper during the formation of the layer. The highest roughness is obtained in the nickel and cobalt ratio of 1:1 [56]. The individual layers are not perfectly smooth, most layers having a wave-like interface and it is suggested that the surface roughness tends to increase for thinner layers [124].

6.3. *Texture and crystallographic orientation*

Texture is the arrangement of crystal orientation in a polycrystalline material. If crystals are randomly distributed in the structure, the material does not have a texture. However, here could be a preferred orientation parallel to the deposition direction and depending on the distribution; the texture can be loose, moderate or strong. As the

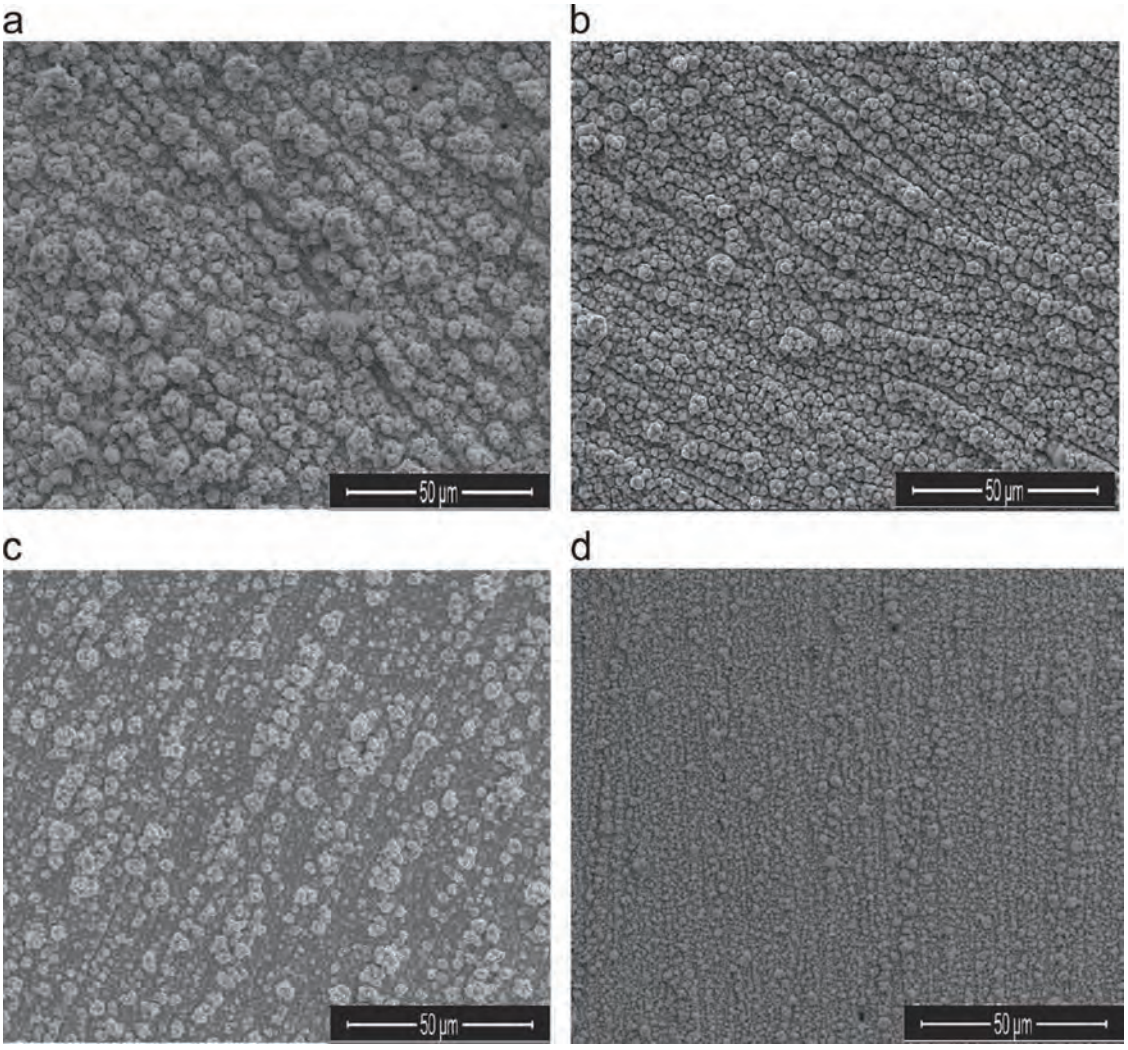

Fig. 15. Effect of increasing copper thickness on Co-Fe/Cu multilayer structure at a Cu thickness of (a) 0 nm. (b) 3 nm, (c) 4.5 nm and (d) 6 nm [75].

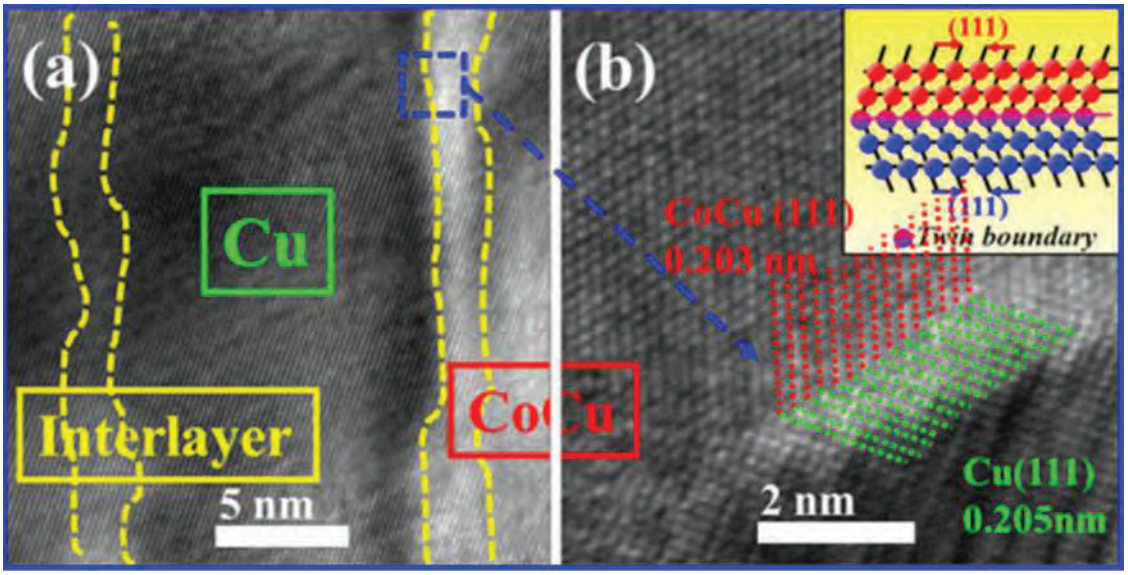

Fig. 16. TEM image of a $Cu/Co_{81}Cu_{19}$ multilayer, (a) the multilayer and the zig-zag interface between layers, (b) the accumulation of layers on each other and twining [73].

distribution becomes more oriented and the texture becomes stronger, anisotropy will increase. The preferred orientation during the deposition in each layer determines the final structure of the layers. This parameter will affect the properties obtained from multilayer coating. By altering the deposition conditions the texture of the deposit alters. Generally, the nucleation and growth process during the deposition is influenced by different parameters such as orientation crystallography of surface, surface energy and kinetic energy of the deposit [125].

The variation in layer thickness can affect the crystallographic orientation of a multilayer. Growth of the thicker layer can be in a preferable direction and growth of the thinner one can be in another preferred direction [29,117,126].

Garcia-Torres et.al [77] reported that in Co-Ag/Ag multilayer nanowires produced by pulsed deposition, with changing the potential, layers are continuous, parallel and have the same thickness. In this multilayer, silver has fcc structure, cobalt has hcp structure and both are polycrystalline. These nanowires have coherent overlapping with continuous nano-channels [77].

In a copper multilayer deposited via ultrasonication, the peak intensity of (200) and (111) copper was stronger than the monolithic copper, while the (220) peak was weak, i.e., the crystalline orientation of the multilayer coating was modified [113].

According to SEM observations, the Co-Zn/Cu multilayer had a homogeneous surface morphology. XRD results have shown strong (111) and (200) Cu diffraction peaks [127].

In a Co-Pt-P/Cu multilayer, the layers grew regularly and parallel to each other due to epitaxial growth; as the deposit became thicker, this regularity persisted [121]. Analysis of the structure of Co-Ag/Ag multilayer produced by smooth DC electrodeposition in a low concentration silver bath by XRD shows that cobalt has a hybrid structure of fcc and hcp. When the concentration of silver is less than (10%), the corresponding XRD peaks were more intense than the cobalt peaks, and simultaneous precipitation of cobalt and silver led to reduction of the cobalt peak intensities [128]. Following XRD of multilayers deposited with thicknesses of 2, 6, and 10 nm for the silver layer, most of the Bragg peaks belonged to silver with FCC structure and cobalt peaks are not detectable or overlap with silver peaks. The fcc silver and hcp cobalt grow to preferable directions of (111) and (001), respectively Several factors can affect the growth way and the deposit structure, particularly, the cathode current density. In a study on Cu/Ni multilayers at a current density of 0.8 $mA{\cdot}cm^{-2}$ or 0.4 $mA{\cdot}cm^{-2}$ for copper deposition and 50 $mA.cm^{-2}$ for nickel deposition, it was observed that when the applied current density for copper was 0.4 $mA{\cdot}cm^{-2}$, the grains had a columnar structure in the [110] direction, the column lengths varying from 200 to

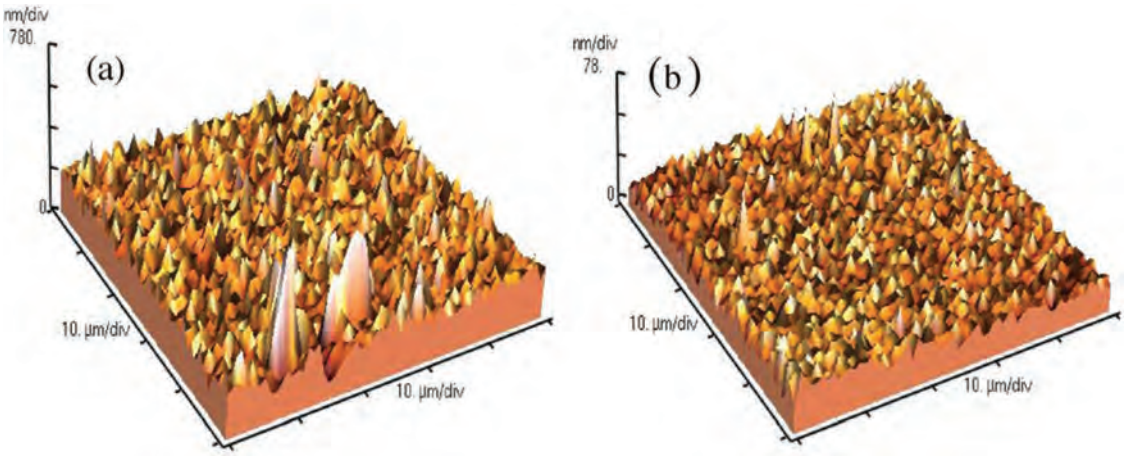

Fig. 17. The effect of potential on surface roughness of a Ni-Co/Cu multilayer (a) E_{Cu} = -0.74 vs. SCE (b) E_{Cu} = -0.26 V vs. SCE [56].

600 nm [116].

In order to investigate the multilayered nanowires of Ni/Pt using XRD analysis, He et.al [129] showed that the structure of nickel and platinum layers is fcc and peak (111) appears very strong for nickel, resulting in the growth of nickel layers in the direction of [111]. The average thickness of the platinum layer and the nickel layer is 35 nm and 60 nm, respectively and each nanowire has a smooth surface. By applying a pulsed current, nickel and platinum layers were alternately deposited [129].

Niu et. al [130] reported that in a multilayered deposit of Ni (normal agitation)/Ni (ultrasonic agitation), SEM analysis showed stacked sandwich layers, the white layers being produced by ultrasonic agitation and the dark layers without ultrasonic agitation. XRD analysis showed that the peak intensity of (111) was stronger for the (200) and (220) orienations [130].

The pH value of the bath can affect the structure and formation of multilayers. For example, the XRD analysis for Co-Fe/Cu multilayer showed that at a pH of 2.7, 3, 3.3 and 3.7, the preferred orientations are (220), (111), (111) and (220), respectively. The multilayers had an FCC structure [76].

The texture can be affected by the substrate at first, but since the subject of coating is continued in the multilayer, each layer is considered as the substrate of the next layer and the layers can mutually interact [123].

Another research group reported that in the Co-Fe/Cu multilayer copper has fcc structure and cobalt has HCP structure; the copper phase grows in the preferred directions of (111) and (220) and cobalt grows in the preferred directions of (022) and (220) [70]. While in Fe-Co-Ni-Cu/Cu multilayers with the same thickness of the alloying layer, due to the enhancement of the thickness of the copper-rich layer, a bcc structure with preferred (110) orientation is observed and in the thinner layers of copper, fcc structure is shown in the (111) direction [29].

In CoFe/Cu multilayers, five diffraction peaks (111), (200), (220), (311) and (222) are related to the fcc structure and no hcp peak for cobalt or bcc peak for iron is detected. It is likely that cobalt and iron adopted the fcc structure of this multilayer, as in the case of copper. The dominant direction for the growth of the sample was [111]. For multilayers in which the thickness of the alloying layers is < 7 nm, a (222) peak appeared, in addition to a (311) one; the latter appeared only in samples having a copper layer thickness > 1 nm [131].

XRD analysis of a Ni/Pd multilayer showed that nickel and palladium have FCC structure and are crystalline with major (111), (200) and (220). The sharp diffraction peaks showed a completely crystalline structure in the multilayer [132].

A comparison of crystalline structure between gradient and homogeneous Ni-Fe nanowires by XRD analysis of the (111), (200) and (220) peaks showed that an FCC structure, with a preferred (110) direction in gradient nanowires [111].

For a Co-Pt-P/Cu multilayer, the crystallographic orientation of the Cu layer with the Co-Pt-P layer is random for a thin copper layer but an increased thickness of the copper layer, resulted growth of (111) planes of copper having a direct impact on the growth of (002) CoPtP planes; both showed epitaxial growth [121].

6.4. Phase and chemical compositions

Multilayered structures usually consist of alternating layers with different chemical compositions and very often layers are thin and nanosized. This opens the possibility of depositing different phases having the same chemical composition. For example, for Co/Cu multilayers, XRD analysis shows three peaks corresponding to the (111), (200) and (220) of copper, and two peaks of (111) and (200) for cobalt (both of them have FCC structure). Some studies on cobalt-copper nanowires have show that growth occurs in the direction of the (111) plane and the peak intensity for cobalt is much lower than copper [133]. Other studies have found that growth of cobalt and copper occurred with fcc and hcp structures, respectively and high intensity [002] peaks for cobalt and [111] for copper indicated preferred orientation of cobalt and copper in these directions [134]. Co/Cu multilayer has FCC structure with (111) planes but this appears in very low thicknesses of HCP structures. On increasing the thickness, the HCP structure is eliminated and grows in the direction of FCC (200) [93]. Similarly, in a Co/Pd nanostructured multilayered system deposited on copper, both Co and Pd showed a fcc arrangement [135].

In the case of alloy layers tailoring the chemical composition to achieve desired phases and hence properties is an interesting prospect, to further enhance materials properties, as reported for many systems such as Ni-W, Ni-Fe, etc. In this respect, deposition of intermetallic phases of multilayered structures is also possible in the Co-Zn/Cu system, where XRD results have shown many Bragg peaks corresponding to the $CoZn_{13}$ polycrystalline, monoclinic phase [127].

In a study on Fe-Ni-Cu/Cu and Ni-Cu/Cu multilayers, it was reported that an increase in the thickness of the layer (Fe-Ni-Cu) resulted in an increase in nickel concentration and abnormal behavior was seen. This has also been seen with an increase in the thickness of the copper layer. With an equal thickness of each layer, the concentration of copper in Fe-Ni-Cu/Cu was lower which is attributable to addition of iron into the electrolyte [98]. In Fe-Ni-Cu/Cu multilayers, all samples along with copper layer contained copper islands on the surface. By increasing the thickness of the copper, according to the EDS analysis in Fig. 18 (a), the iron and copper content in the alloy layer increased but the nickel content was lower [120].

XRD analysis of Co-Pt/Pt multilayer shows that the Co-Pt layer has an irregular FCC structure and no superlattice has found in the alloy layer [86]. As shown in Fig. 18 (b), SEM analysis shows that in Co/Pt multilayer, nanowires are formed very regular and parallel and had a bamboo-like structure. It was reported that platinum had a crystalline

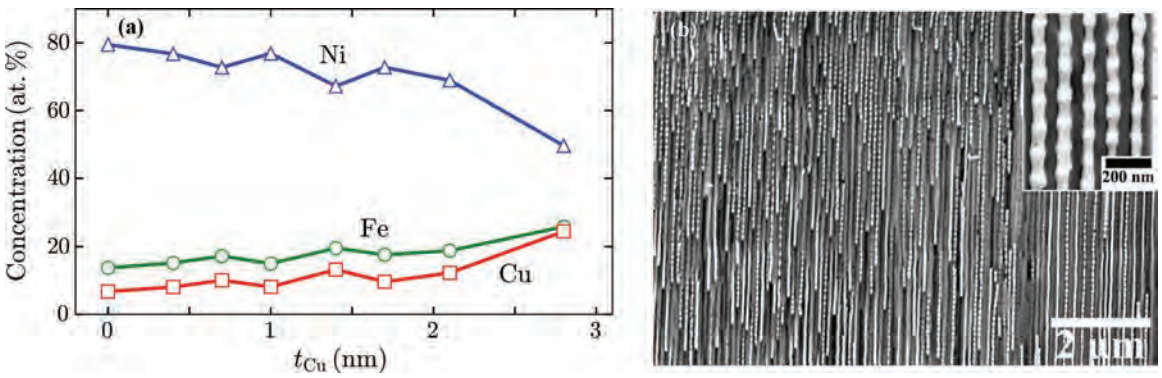

Fig. 18. (a) The effect of copper layer thickness on the concentration of alloying elements in Fe-Ni-Cu/Cu multilayer [120]. (b) SEM image of bamboo-like structure of Co/Pt multilayer [136].

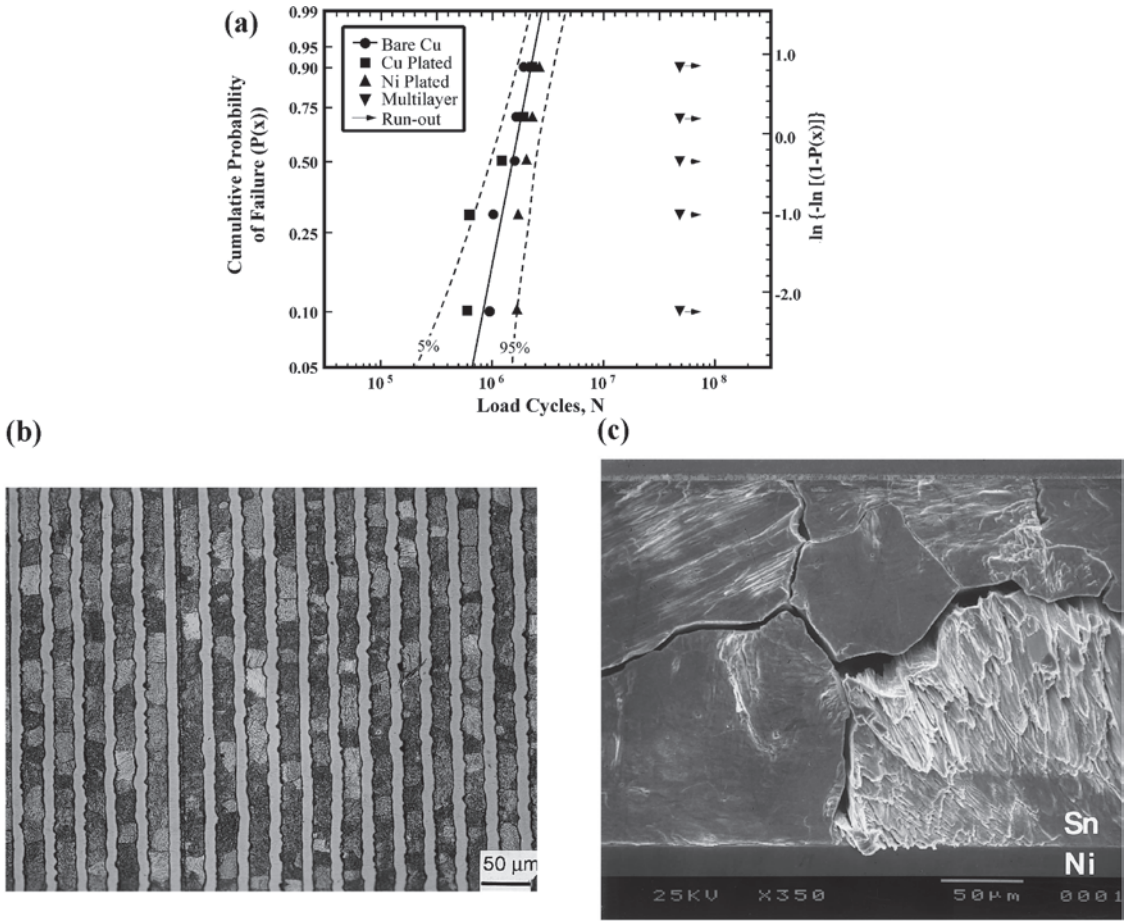

Fig. 19. (a) Comparison of fatigue cycles in multilayer coatings and monolithic nickel and copper films [151]. (b) micrograph of composite Ni/Sn multilayer coating and (c) Surface morphology of electrodeposited Ni/Sn coatings after 4×10^5 cycles [152].

structure whereas Co was amorphous [136].

7. Functional properties of multilayered electrodeposited layers

Gradient and multilayer coatings can improve the mechanical and chemical properties needed for metal surface protection [27] to enhance the corrosion and wear resistance of industrial components [137]. In some cases, due to the presence of impurities and structural defects or due to the nature of the coating (for example, in case of brittle materials), single coatings may not show adequate mechanical properties. This may be overcome by applying multilayer coatings of different metals, different thicknesses, and gradient layers to modify structural defects and improve mechanical properties [55]. Over the last two decades, many studies have focused on magnetic properties and their influence on multilayer coatings and nanowires [115]. Electrodeposited multilayer coatings provide an established method to increase strength and fatigue resistance [138].

7.1. Creep

Creep results from permanent deformation over time in a material subjected to a constant stress or pressure. The effect occurs at high temperatures (above the recrystallization point). In order to obtain the engineering creep curve of a metal, a constant force is applied to a tensile sample at a given temperature. Strain of the sample is determined as a function of time. The resultant stress-strain curves include three separate regions, namely primary creep, secondary creep (steady state creep) and tertiary creep [139].

Prediction of creep behavior and strength of materials at high temperatures is crucial in the design of structures used at elevated temperatures. For instance, oil vessels in a refinery have to be resistant against the stresses caused by hot fluids for long durations [140]. High temperature design employs parameters such as the Larson-Miller, Dorn and Manson-Haferd indices. Creep has been more studied in ceramics than metals as their application at high temperatures is of greater importance [141]. The practical temperature range of electroplated coatings is 400–500 °C while PVD and CVD coatings sometimes experience 1000 °C. On the other hand, creep diffusion mechanisms are naturally more complex in ceramics than metals. This is due to the fact that various diffusive charges for cations and anions have to be neutral. The rate of creep increases with temperature. The required driving force for creep is produced by exile of atoms from regions under compressive stresses and their deposition in regions under tensile stresses. According to the Ashby creep mechanism for pure nickel coatings, five stress regions are based on temperature: Nabarro-Herring creep, Coble creep, boundary slip controlled by boundary diffusion, boundary slip controlled by lattice diffusion and dislocation creep. For example, when grain size was 100 nm, the Nabarro-Herring creep region tended to $1 = \frac{T}{T_m}$ and the dislocation creep region became very small [142].

It was reported that introduction of intermetallic compounds to Cu/Sn and Cu/Ni/Sn multilayer coatings can lead to improvement of nanomechanical properties, particularly creep. the average creep displacement in multilayer coatings (25.71 nm) was less than that in the monolithic coating (33.25 nm) [12].

Transition of creep deformation mechanism from dislocation movement to boundary slip occurs in Ag/Cu multilayer coatings consisting thin layers. In fact, when layers are sufficiently thin, strain rate

becomes sensitive to variations and creep rate in multilayer coatings increases with decrease in thickness of layers. However, an increase in creep rate is also dependent on the structure of layer interfaces [143–145]. Nanocrystalline metallic materials are expected to have higher creep rates than their micro-crystalline counterparts as lattice and boundaries diffusion increase on reduction of grain size [146,147].

7.2. Fatigue and crack propagation

Fatigue is the fracture of a material caused by forces below the final strength and (usually) yield stress. A metal piece subjected to repetitive or fluctuating stresses may eventually undergo fracture at stresses much less than that required for breakdown in a single load. A fracture which occurs under dynamic loading conditions is called a fatigue fracture. No distinct variation in the microstructure of metal that fractured due to fatigue was seen, providing no key to diagnose fatigue fracture [101].

Developments in industries and increase in number of equipment subjected to repetitive and fluctuating loading such as cars, airplanes, compressors, pumps, turbines, etc. led to formation of an understanding according to which fatigue is responsible for at least 90% of fractures occurred during mechanical operations.Three factors are necessary for fatigue fracture: an extremely high maximum tensile stress, great variations in or fluctuating applied stress and numerous cycles of the applied stress.

Other variables such as stress concentration, corrosion, temperature, extra load, metallurgical microstructure, residual stresses and combined stresses may contribute to conditions required for fatigue. Fatigue may be divided into several stages: crack initiation, crack propagation in the slip band, dracture of cracks on the planes with high tensile stresses and final soft fracture [148]. By increasing the resistance against crack propagation, multilayer coatings may improve component lifetime.

Electroplated Ni/Cu multilayer coatings have been used for a wide range of applications and there are many studies on fatigue behavior. For example, it was reported that fatigue wear resistance increased at a smaller distance between layers [149]. On the other hand, Stoudt et al. [150,151] investigated nano-scale crack initiation due to fatigue in thin Ni/Cu multilayer films. It was observed that using copper and nickel with soft FCC atomic arrangements and due to the unique properties of the electrodeposited Ni/Cu multilayer coatings, initiation of fatigue cracks was delayed leading to improvement of fatigue resistance. This requires hardness, toughness, cyclic work hardenability, residual compressive stresses and adherence. According to Fig. 19 (a), multilayer coatings are considerably more resistant than monolithic copper and nickel films [150,151].

In another study on fatigue stability of Ni/Cu multilayer coatings, it was reported that evolution of dislocations in the structure was suppressed by the presence of nanostructured materials at the surface. More investigations revealed that multilayer coatings with layer thickness of 100nm showed a fatigue life ten times longer than simple nickel coatings under a 90MPa stress domain [138].

Lee et al. [27] studied the mechanical properties of electrodeposited thin Ni-W multilayer coatings where the layers were alternatively rich and free of tungsten. They stated that increase in W content in Ni-W alloy led to improvement of hardness; while, fatigue resistance was diminished due to increase in internal stresses [27]. Elsewhere, fatigue crack propagation behavior and resistance of composite Ni-Sn multilayer coatings was investigated by means of three-point bend fatigue test. It was reported that due to presence of inter-granular fatigue cracks as an inherent characteristic of pure tin, the tin layer improves fatigue resistance by preventing propagation of primary fatigue cracks in Fig. 19 (a) SEM image and surface morphology of electrodeposited Ni-Sn sample in Fig. 19 (b) and Fig. 19 (c) illustrate fatigue cracks in boundaries and shear bands across the tin layer after 4×10^5 fatigue cycles [152].

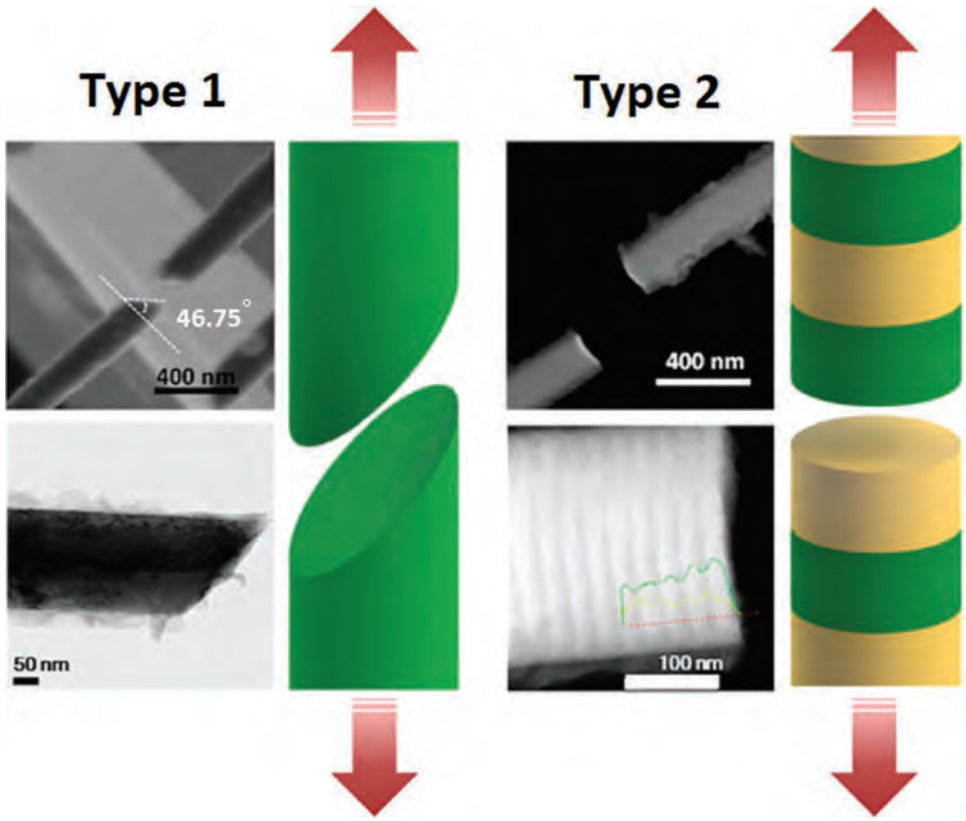

Fig. 20. First type (bulk nickel) and second type (Ni/Ni-Au multilayer coatings) fracture behavior [161]

7.3. Tensile behavior

7.3.1. Stress-strain diagrams

This section is dedicated to elastic strain, tensile, yield and fracture strengths of multilayer coatings produced by electrodeposition process. In the case of removal of strain after loading (with removal of stress); then, the material has an elastic behavior. The largest stress after removal of which the material returns to its primary state is called elastic limit. However, when strain does not disappear after removal of stress (is not zero after loading), the material is said to have a plastic behavior. A well-known method for studying of material's behavior is drawing stress-strain curve obtained through loadings and measurement of deformations in tensile tests. The curve-form of this diagram varies from one material to another [153]. Note that elastic deformation is usually observed as a sort of distortion in the crystalline lattice and disappears after unloading. On the other hand, plastic strain is seen as the movement of dislocations in the crystalline lattice. This form of strains may lead to undesirable cracking within the material structure. Compressive plastic deformation can occur in materials used for reinforcement and performance improvement. This technique is used, for instance, to manufacture semiconductors and in solar cells [153,154].

Fracture occurs whenever a multilayer coating undergoes deterioration or decomposition. This phenomenon is divided to two stages: crack initiation and crack propagation. Fracture is usually observed with plastic deformation before and after crack movement. Within the elastic region, the created deformation disappears after removal of loading. In other words, the whole energy stocked in the coating is released and the piece dimensions would return to their primary values. When the imposed loading is increased, we enter the plastic region where every deformation is permanent. The elastic deformation becomes plastic at the yield point which is 0.002 of the created strain. Homogenous plastic deformation region starts just after the yield point. The volume is constant in this region and the ultimate tensile strength occurs at the end. Next, we have non-homogenous plastic region where the sample undergoes necking and would eventually break. In order to improve mechanical properties, researchers have always tried to mathematically model the mechanical behavior of materials such as elastic strain of various alloys in composition modulated alloy (CMA) multilayer coatings. In regards with the elastic behavior, the modeling addresses the role of inter-atomic forces between layers and interfaces. It was reported that elastic behavior depends on the structure and that is atom- or electron-based. It was reported that an inverse relationship exists between wavelength and strain values. For example, a better stress behavior was seen with reduction of wavelength in Au/Ni and Cu/Ni multilayer coatings [155]. According to Fig. 20, two types of fracture occur in Ni/Ni-Au multilayer nanowires. In fact, fracture behavior is categorized based on fracture surface angle with the tensile axis. Fracture angle with the tensile axis varies between 30° to 50° in the first type of fracture which occurs in Ni/$Ni_{(Au)}$ layers. Fracture in the second type in which the angle is 90° happens in brittle form. Studying the ultimate tensile strength revealed that, for the first type, fracture strength is equal to pure nickel nanowires. Although fracture strength of the second type (multilayer coatings) was higher than bulk nickel, it was brittle and had low formability. Reduction of layer thickness increased fracture strength of the first type, up to a value even higher than that of the second type [156–160].

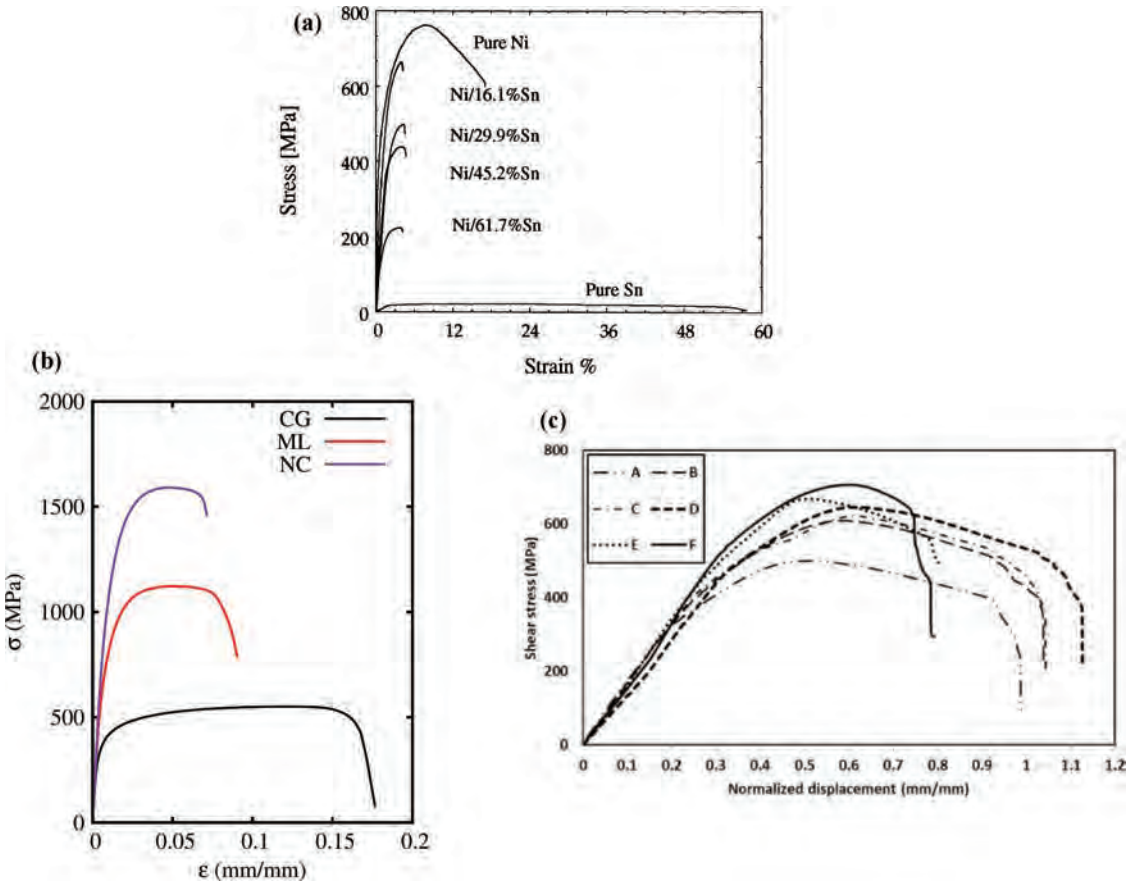

Fig. 21. (a) Comparison of the stress-strain behaviour of Ni/Sn multilayer coatings with pure nickel and tin [159], (b) Stress-strain diagram of Ni/Co multilayer (ML) coating composed of nanocrystalline (NC) and coarse-grained layers(CG) compared with CG and NC monolithics [160] and (c) Stress-strain diagrams of monolithic and multilayer coatings: (A) Ni-Fe-Al_2O_3 90% monolithic: 50 Hz, (B) Ni-Fe-Al_2O_3 20% monolithic: 50 Hz, (C) Ni-Fe-Al_2O_3 20%: 400 Hz, (D) Ni-Fe multilayer: 50 Hz, (E) Ni-Fe-Al_2O_3 multilayer: 50 Hz and (F) Ni-Fe-Al_2O_3: 400 Hz [164]

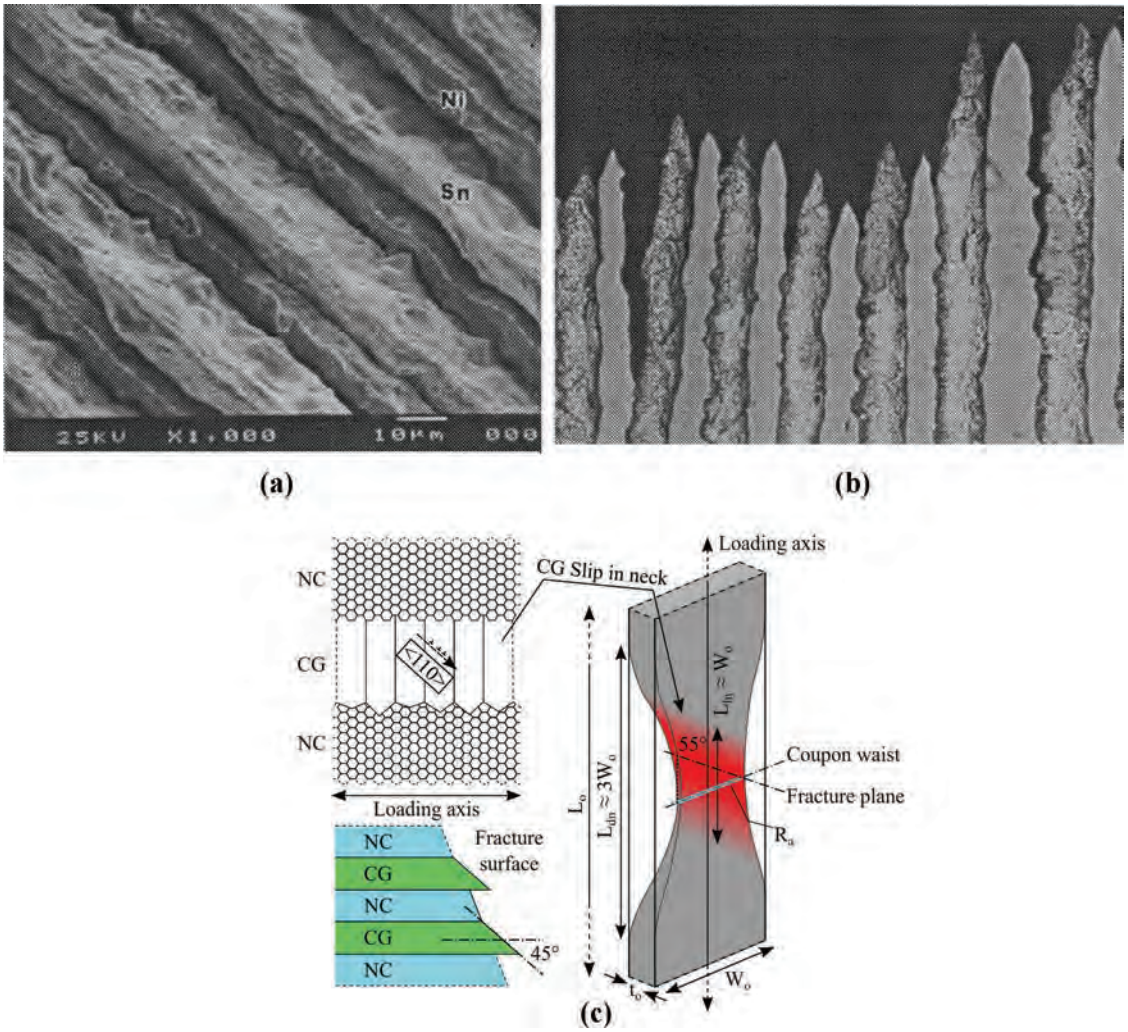

Fig. 22. Tensile fracture in Ni/Sn composite multilayer coatings: (a) SEM morphology, (b) cross section of the fractured samples (optical micrograph, 500 ×) [159] and (c) deformation model and necking in a Ni/Co multilayer coating of nanocrystalline (NC) and coarse-grained (CG) layers [160].

It was reported that an increase in the thickness of the magnetic film in Co-Ni-P/Cu multilayer coatings not only deteriorated magnetic properties (such as maximum energy density) but also induced instability of mechanical properties e.g. corrosion cracking due to increase in elastic strain energy deposited in the films [156]. It is also possible to investigate elastic strain in atomic scale. For instance, there have been some discussions on releasing the elastic strain energy by dislocations due to behavior of atomic planes such as small wedges [157]. Tensile tests on Ni/Cu multilayer coatings showed that there was a sudden increase in yield stress for similar sample's length in both of copper and nickel films. Increase in tensile strength of multilayer coatings is usually associated to grains and interfaces of the structure, which are barriers for the movement of dislocations. The Hall-Petch equation presents the relationship between strength and grain size or distance between layers. The highest tensile strength in Ni/Cu multilayer coatings is achieved in repeat lengths with coherent reduction which alters the deformation mechanism within the spacing between layers. Tensile strength is high in thin layers due to both reinforcement and increase in dislocation locking [158]. Slip bands in various tin grains of the Ni/Sn multilayer coatings change due to plastic deformation induced by the applied axial strength and grain orientation. Cracks initiated in tin grain boundaries after ten thousand cycles and propagated along the boundaries. Intergranular cracks were observed within all tin layers while nickel layers remained absolutely intact. This may be explained by the idea that plastic deformation in Sn layers takes the all energy from internal stresses. It should be mentioned that actual behavior of nickel and tin differs from that seen in the multilayer coatings; the more ductile tin showed a brittle behavior and nickel improved formability [152].

According to tensile tests on samples with nickel and tin layers having constant and variable thicknesses, respectively, elongation of pure nickel and tin samples was higher than composite multilayer coatings. For example, pure nickel elongation was 4.4 times higher than in Ni/Sn multilayer coatings. According to the tensile stress-strain diagram shown in Fig. 21.(a), multilayer coatings are less ductile than pure metals due to the existing barriers at the interfaces between layers for glide dislocations. It is also considered that dislocations may pile up in nickel/tin interfaces but they cannot glide along the interfaces as there is a mismatch between the lattice and elastic moduli. This leads to work-hardening and cleavage cracking at the interfaces which, diminishes the ductility properties of multilayer coatings. The average values of ultimate tensile strength, yield strength and Young's modulus in composite multilayer coatings increase with decrease in the tin content. Tensile fracture morphology of Ni/Sn composite multilayer coatings differ from those of pure tin or nickel samples. Elongation of composites reduced in thinner layers because dislocations had shorter slip distances and plastic deformation became more difficult. The formability of multilayer coatings reduced in thinner layers but the yield strength and ultimate tensile strength of composite multilayer coatings improved with a smaller layer thickness [159].

According to stress-strain diagram of NiCo multilayer coatings in

Fig. 21 (b) (for coarse-grained and nanocrystalline layers), the nanocrystalline layer had a significantly lower formability than coarse-grained layers. However, it enjoyed the highest yield strength. In addition, these multilayer coatings are affected by their nanocrystalline and coarse-grained layers [160].

Decrease in tensile stress in NiP films of CoFe/NiP multilayer coatings due to increase in P content can be justified by several effects, including adsorption/desorption of hydrogen, crystallite joining and the combined effects of texture. The nickel films showed the highest tensile strength provided that H_3PO_3 is not present in the bath. Introduction of p-hydroxybenzhydrazide as stress reliever and softener reduced roughness of the nickel films [162].

It was reported for Ni-Mn multilayer coatings that an increase in heat treatment temperature led to embrittlement and reduction of ultimate tensile strength, yield strength and elongation due to presence of shear bands and twins. On the other hand, a prolonged heat treatment and temperature reduction led to improvement of material strength due to activation of slip systems [163].

According to shear punch studies on multilayer and monolithic Ni-Fe-Al_2O_3 coatings in Fig. 21 (c), the latter had a higher formability and their displacement was larger than multilayer coatings under equal shear stresses. Also, increase in frequency and reduction of duty cycle in monolithic coatings led to increase in shear yield stress and ultimate shear strength but elongation was reduced.

In multilayer coatings, shear yield stress and ultimate shear strength increased with increase in frequency of electrodeposition while elongation decreased. The superior behaviour of multilayer coatings is attributable to grain refinement and improvement of mechanical properties due to locking of dislocations within the interfaces. This occurs via a Frank-Reed mechanism which moves dislocations from grain boundaries towards interfaces and plays a role in continued plastic deformation [164].

7.3.2. Fracture morphology

As seen in Fig. 22 (a) and Fig. 22 (b), both nickel and tin layers show necking after fracture along with plastic deformation. Several bands were disintegrated in interfaces according to cross sections [159].

The residual stress in Ni/Cu multilayer coatings depends on the thickness ratio of nickel to copper (t_{Ni}/t_{Cu}); so that, there were compressive stress when nickel content was less than copper content. However, once nickel content exceeded copper content, nature of residual stress altered and became tensile [165]. In coarse-grained Ni/Co multilayer films, necking took place before fracture; nanocrystalline films did not show such behavior. The multilayer coating showed an intermediate behavior, indicated by expansion of the necking region in the SEM micrograph. It was reported that fracture behavior of multilayer coatings is affected by nanocrystallites. The magnified picture illustrates consecutive presence of fine and coarse pits created by the micro-pores in the coarse-grained and nanocrystalline layers. The multilayer fracture plane occurs at 55° by application of an axial load where the large pits were associated to the coarse-grained layer and small pits were attributed to the nanocrystalline layer. According to Fig. 22 (c), the strain-hardening capability of nanocrystalline layer, leads to microscopic shear bands developing within the local necking region. Transition from uniaxial stress to multi-axial stress leads to plastic deformation between the layers. The deformation causes shear bands activating the slip system in the coarse-grained layer which further develop necking. Elongation in nanocrystalline and coarse-grained layers leads to fracture due to creation of micro-pores. Fracture plane initiates in the thin loading cross section and propagates along the shear band [156–160].

According to fracture analysis in nickel multilayer coatings, fracture area for the sample produced via reverse pulse mechanism occurs on the upper layer of the nickel film. In fact, fracture did not happen at the joint point of the two layers and there were dimples in fracture area of the PR sample. Fracture in the sample treated with HCl (acid was used to remove nickel oxide from the surface) occurs between layers where interfaces are weak and pits are seen. However, interfaces between reverse-pulse-produced layers were stronger. It may be concluded that adhesion of the deposite to the substrate is improved in nickel films produced by a reverse pulsed current technique [166]. It was reported that addition of dimethylformamide to the bath would lead to removal of cracks observed in Ni-Cr multilayer coatings. Hydrogen evolution and adsorption rates were very high in the primary bath so that the highest internal tensile stress inside the coating which initiated cracks. Then, addition of DMF solvent removed the cracks [167]. Fracture analysis on Cu/Sn/(In/Ni/Cu/Ni/In)/Sn/Cu sandwich multilayer coating after shear tests were done at different temperatures. According to Fig. 23, there are some dimples in the fracture plane and the only existing phase is $(Ni,Cu)_3(Sn,In)_4$. Soft fracture planes were observed along the fracture surface with increase in temperature up to 300 °C. In other words, brittle fracture became ductile fracture and the thicker $(Cu,Ni)_6(Sn,In)_5$ phase was seen at interfaces. This is due to the fact that matrices of these three samples are partially rich of indium. The presence of reflow tin and indium after heat treatment contributes to the highest ductility. Indium and tin atoms are distributed over the fracture surface after the shear test [168].

Ni-Fe multilayer coatings include coarse-grained layers which have distortions due to movement of dislocations parallel with slip planes. The segregated distances are controlled by field of internal stresses created by piled-up dislocations near active (compact) planes. Fracture in nanocrystalline monolithic planes occurs with parallel micro-dimples. Dimples size is larger than the average grain size. There were large pores at CG/NC grain boundaries. It was observed that coarse-grained layers were highly formable and coarse-grained substrates did not demonstrate an equal elongation within the first stages. Formability of the multilayer coating depends on the inter-layer interfaces. It was stated that formability of CG layers is due to increase in nucleation of dislocations and their accumulation in the grains. According to Fig. 24 (a), coarse-grained layers form along the preferential (100) direction. During the tensile test, the active slip direction family is (111), which is readily activated by critical resolve shear stress. In general, each dislocation from the coarse-grained layer sticks inside the inter-layer interfaces so that it cannot diffuse into the sidelong grains or disappear in grain boundaries. This is due to presence of internal stresses in interfaces. Studying the

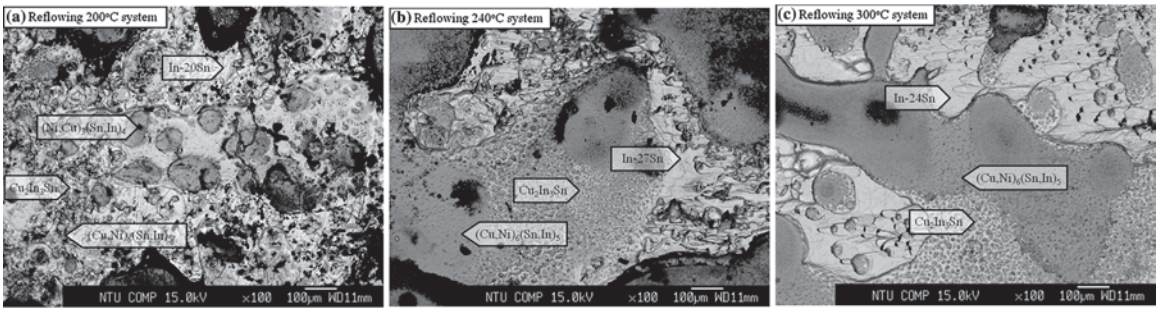

Fig. 23. Fracture surface of the Cu/Sn/(In/Ni/Cu/Ni/In)/Sn/Cu sandwich multilayer coating after the shear test at (a) 200 °C, (b) 240 °C and (c) 300 °C [168].

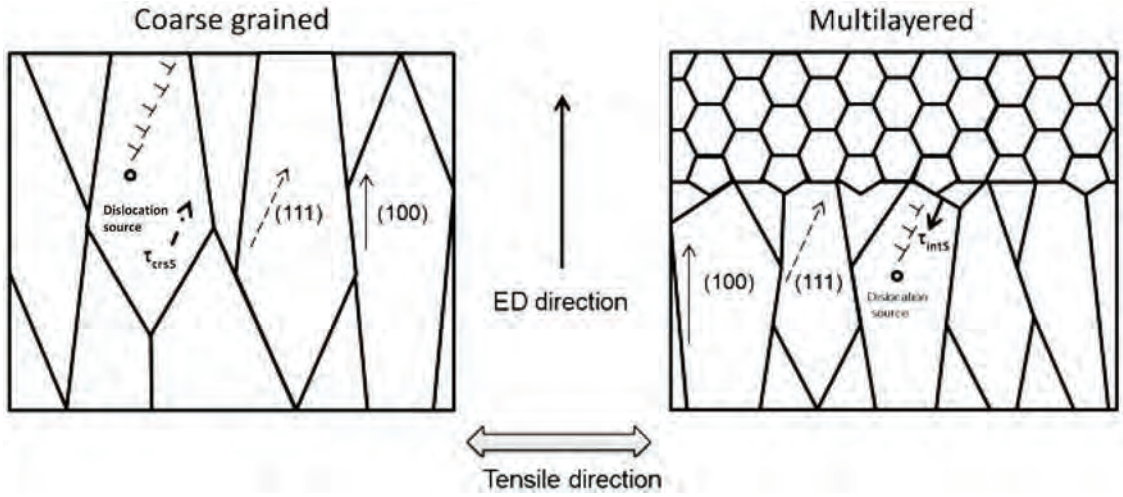

Fig. 24. (a) Schematic illustrating deformation during the tensile test for CG layer and Ni-Fe multilayer coating [169], (b) fracture surface and elongation of multilayer and monolithic coatings.

fracture reveals that the NC substrate was responsible for expansion of micro-dimples along the fracture line while CG layers demonstrated the highest formability [169].

Different types of fracture surfaces and elongation of multilayer and monolithic coatings are illustrated in Fig. 24 (b), the first type of fracture is based on formation of shear bands and slip of grain boundaries. Here, size of shear bands is controlled by thickness of multilayer nanowire films. A transition in grain size usually occurs at interfaces due to their non-coherent nature. The second type of fracture that occurs under high stresses leads to formation of pores and crack initiation inside the interfaces or grain boundaries with the nanostructure [164]. In conclusion, the multilayer coating is more brittle than the monolithic coating and it also has a lower elongation and formability. Besides, reduction of thickness of layers in the multilayer coating increases yield strength. However, it declines elongation and formability even further. Because of brittleness, fracture surface of the multilayer coating is normal to the applied force while that of the monolithic coating is at an angle of 30° to 50° from the applied force.

7.4. Ratio of hardness to elastic modulus

Hardness is a well-known mechanical characteristic which is used to evaluate wear resistance. Wear behavior and life of different materials are determined by means of hardness values. In addition to high hardness, industrial coatings working under harsh situations are now required to have proper toughness and wear resistance properties to guarantee the maximum life expectancy of engineering parts. This is why efforts to obtain coatings made of different types of materials such as ceramics, metals and composites with high hardness and elastic modulus have increasingly continued [170,171]. It is rare to expect high hardness values for electroplated and/or electrodeposited multilayer coatings so that studying the ratio of hardness to elastic modulus (H/E) ratio for these coatings is an uncommon procedure. This feature, actually, is often discussed for PVD and CVD coatings [172]. Nevertheless,

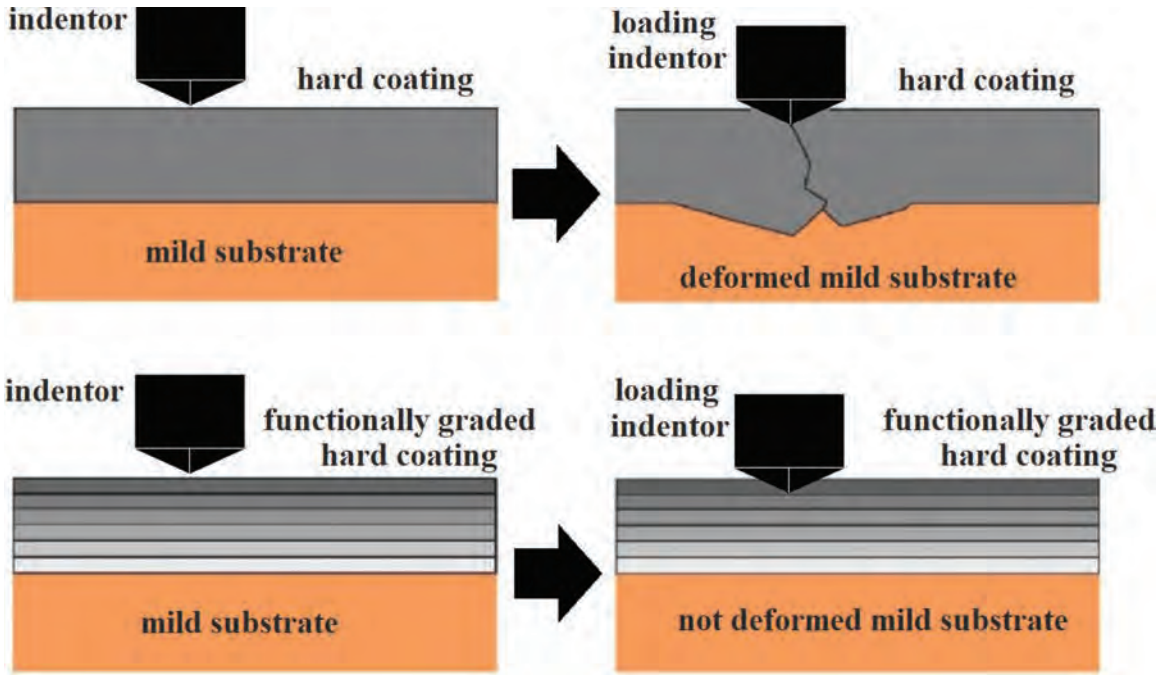

Fig. 25. Schematic showing samples of a higher tolerance gradient coating deposited on a soft substrate.

some studies have examined the H/E ratio to gain more information on mechanical properties, wear resistance and life expectancy of electrodeposited Ni/Cu and Ni-Cu/Cu multilayer coatings. Ghosh et al. produced Ni/Cu multilayer coatings using sulfate bath. Keeping the thickness of copper layers at a constant value, they altered thickness of nickel layers within a given range. It was reported that the average nickel thickness was set as the optimum value to reach the minimum wear rate and maximum H/E ratio (high hardness and low residual stresses). The H/E ratio is discussed as an effective parameter in investigation of tribological properties of metal and ceramic nanocomposite coatings [165]. Similarly, the effects of grain size variation and copper content on the H/E ratio in pulse electroplated multilayer coatings were investigated [173]. Research on Ni/Cu multilayer coatings showed that elastic strain until fracture and fracture toughness are the most useful parameters for evaluation of tribological properties in metal and ceramic nanocomposite coatings. It may be concluded that the highest H/E ratio is associated with the highest wear resistance in a coating [174]. The H/E ratio improved with increase in the nickel at% in Ni/Cu nanocrystalline coatings, implying the increase in wear resistance in comparison to monolithic nickel coatings [175].

7.5. Load bearing ability

An important reason for surface engineers to produce multilayer coatings (both FG and ML) is to enhance load bearing ability [13]. Although this feature is generally known as load bearing ability, it covers practical properties such as increase in hardness and toughness, fracture toughness, low friction coefficient, high wear resistance or a combination of them. In order to provide a better understandingconsider a simple sponge cake which is decorated with a layer of chocolate. The chocolate layer cracks when the cake is being cut since the underlying sponge cake cannot tolerate the force applied by the cutting knife. This is a very simple example that may be used as the main idea for production of gradient coatings in different industries. Hard coatingsexposed to wear or indentation, scarsely,applied on a soft substrate, such as copper unless a gradient is formed from the substrate towards the surface. This is illustrated schematically in Fig. 25. The hard coating fractured during load application since the substrate was soft and the coating could not tolerate a significant load. While, a hardness gradient from the substrate towards the surface improved load bearing ability (LBA), hardness of the bottom layer and substrate remained constant. In a classic study comparing the LBA of monolithic and FG materials, the monolithic coating failed under 9 N load while the FG coating tolerated a 50 N load with no sign of adhesion failure in FG coatings [176].

As mentioned earlier, the development of FG structures increases LBA of coatings since they provide higher fracture toughness [177]. FG structures can tolerate the residual compressive stresses and consequently enhance the fracture toughness, [178]. Numerical studies using the BEM method proved that gradient structures can considerably affect stress intensity factors [179]. In high-temperature applications, FG-structured coatings can reduce thermal and residual stresses as well as provide the required decrease in crack initiation driving force. FG structure is known to play an effective role in improvement of adhesion strength [180]. It was shown in a research on thermal fracture behavior of thermal barrier ceramic coatings that the FG structure had a desirable effect on spallation life of a sample exposed to cyclic thermal loading. According to results, the perpendicular cracks on the surface grew as traverse cracks within the FG structure and crack propagation towards the substrate was prevented. FG structures improve LBA even under cyclic thermal loading though increasing the fracture toughness [181].

In addition to FG, multilayer structures are known as a proper solution in aviation industries for possessing remarkable mechanical properties such as high hardness to toughness ratio, low residual and internal stresses, sufficient adhesion to the substrate, low friction coefficient and consequently, higher LBA [176]. It has been shown for multilayer coatings that lowering the thickness of layers led to improvement of adhesion strength, hardness and Young's modulus as well as reduction of friction coefficient and wear rate. of the presence of interfaces in nano-scaled multilayer coatings caused pile-up of cross-sectional dislocations and/or cracks [176,182,183]. The resistance against crack propagation and movement of dislocations in PVD coatings is due to presence of interfaces and increase in volume energy by interaction of Fermi surfaces with additional Brillouin zones [183,184]. In alumina and zirconia ceramic multilayer structures, toughness values were three times higher than the monolithic coating while work-of-fracture was six times greater than that of the monolithic one [185]. Formation of CVD multilayer coatings on Ti6Al4V alloy led to improvement of static LBA by a factor of four. These coatings enhance the applicability of this alloy for tribological use by reduction of friction coefficient and improvement of wear resistance [186]. Some researchers considered LBA as a distinct mechanism so that limited layered slip mechanism fades with reduction of thickness of layers and mechanism of LBA dominates to improve mechanical properties [187]. Hence, it may be expected that the layered structure in electroplated coatings may lead to stress reduction, increase in fracture toughness and consequently high LBA. However, electroplated coatings possess a lower hardness range than ceramic coatings produced by vapor-phase techniques. The hardness of electroplated ('hard') chromium and nanocomposite coatings can typically reach 1100 and 1250 Hv, respectively. It was also reported that an increase in the diamond nanoparticle content by 64 wt% in Ni-W coatings led to improvement of hardness by 2250 Hv [188]. The formation of nano-scaled Ni/Cu multilayer coatings on titanium alloys led to improvement of hardness, toughness, strength, wear resistance, fretting wear fatigue, and consequently LBA [189]. It was reported, elsewhere, that a layered structure enhanced mechanical and tribological properties of Ni/Fe multilayer coatings [164,190]. However, it was concluded in some cases that electroplated multilayer coatings with a layer below 100 nm have increased residual internal stresses [191]. An increase in LBA due to transformation towards a layered structure (gradient or multilayer coatings) is schematically illustrated in Fig. 26

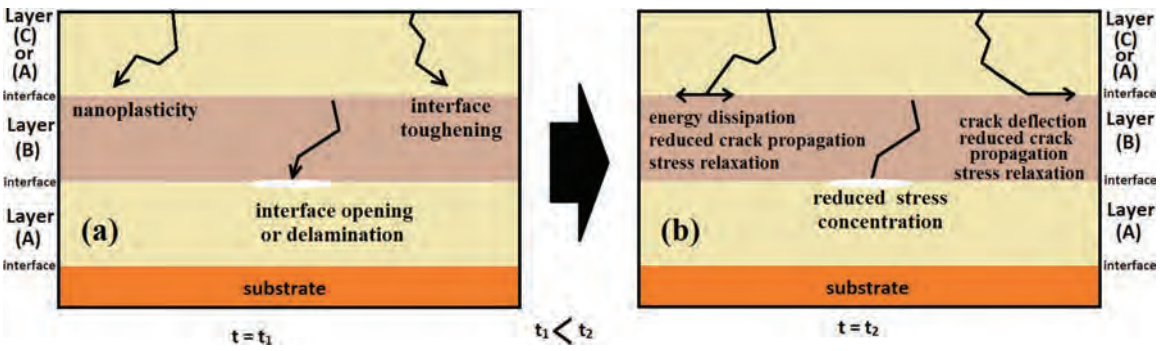

Fig. 26. Some mechanisms for improvement of load bearing ability in multilayer and gradient structures.

[184]. Cracks initiated on the surface would avert or cease as they reached the interface. i.e., sectional cracks directed towards the substrate turned into traverse cracks parallel to the substrate. Crack stopping is justified by a lack of plasticity in interfaces or interface toughening. In both cases, it may improve LBA for FG or ML coatings though increasing the fracture toughness. In addition, those cracks that reach the open area between layers in Fig. 26 (a) may be effectively stopped in Fig. 26 (b) [184].

In conclusion, structure design parameters such as thickness of layers, interfacial toughness and strength of layers may significantly affect toughness, strength and consequently LBA in multilayer coatings, which are known as third generation of coatings [192]. Some research has described the mechanism of LBA as crack aversion along weak interfaces, arguing that crack propagation perpendicularly across the coating would diminish fracture resistance and consequently load bearing ability [193]. Application of multilayer structures improves LBA for low temperature and high temperature use through different mechanisms.

7.6. Wear resistance

Wear resistance has always been a significant characteristic in mechanical properties. Application of multilayer coatings improves wear resistance of the substrate [194]. A very common method to evaluate wear resistance is the ball on disk test, where weight loss of coating results from removal of material from the surface represents coating wear [195].

7.6.1. Wear resistance and friction coefficient

Fretting wear resistance was studied in Ni/Cu multilayer coatings deposited on beryllium-bronze substrates. It was observed that the lowest and the highest wear rates were obtained for the multilayer coatings which their sublayers had the least and the most thicknesses, respectively. It was reported, elsewhere, that Ni/Cu multilayer coating with copper to nickel thickness ratio of 1:2 demonstrated the highest wear rate. Reduction of wear rate, therefore, was obtained through reduction of copper thickness. For example, wear rate of this coating was seven times less than that of nickel monolithic coating. There are two parameters affecting the wear rate in multilayer coatings: (1) increase in interfaces of the substrates with decrease in thickness of the sublayer which causes formation of barriers such as slip dislocations along the interfaces between copper and nickel layers and (2) reduction of grain size with decrease in thickness of the sublayer [87,88,149,196]. The sample with the highest nickel content showed the least friction coefficient so that there was a finer scratch on the surface. Study of wear properties in Ni/Cu multilayer coatings revealed that friction coefficient values and wear rates of all multilayer coatings were lower than that of pure nickel [165]. It was stated in another study on Ni/Cu multilayer coatings of different thicknesses that wear rates of all coatings were lower than pure nickel samples over a range of applied force [197].

Wear resistance of Ni/Cu coatings was not dependent of the composing layers except that of the thick-layered coating which featured a low resistance. It should be mentioned that pure nickel film was entirely removed under a lower force while multilayer coatings endured [82]. Comparing the Ni-Cu monolithic and Ni-Cu/Cu multilayer coatings showed that the multilayer coating had a lower friction coefficient. On the other hand, considering the wear rates in the multilayer coating with low nickel content and the nanocrystalline alloy coating with high copper content, it was shown that wear rate of the multilayer coating was higher and it even increased with increase in the applied force. However, further increase in the applied force lowered the wear rate of the multilayer coating below that of the alloy coating due to the plastic flow formed along the wear direction. Variation of wear rate in the multilayer coating may be attributed to the internal stresses formed in the coating during electrodeposition process. Comparing the multilayer coating with high nickel content and the alloy coating with low copper content, revealed that the alloy coating had a lower wear rate. The constant wear rate of the multilayer coating regardless of nickel content variation is due to its more intensive wearing and lower plastic deformation [173]. The friction coefficient of the Cu/Ni multilayer coating was initially lower than that of the pure nickel coating; however, there was no significant difference in friction coefficient values once stability was reached. According to SEM analysis on the structure with a loaded wear test, there were more wear tracks on the

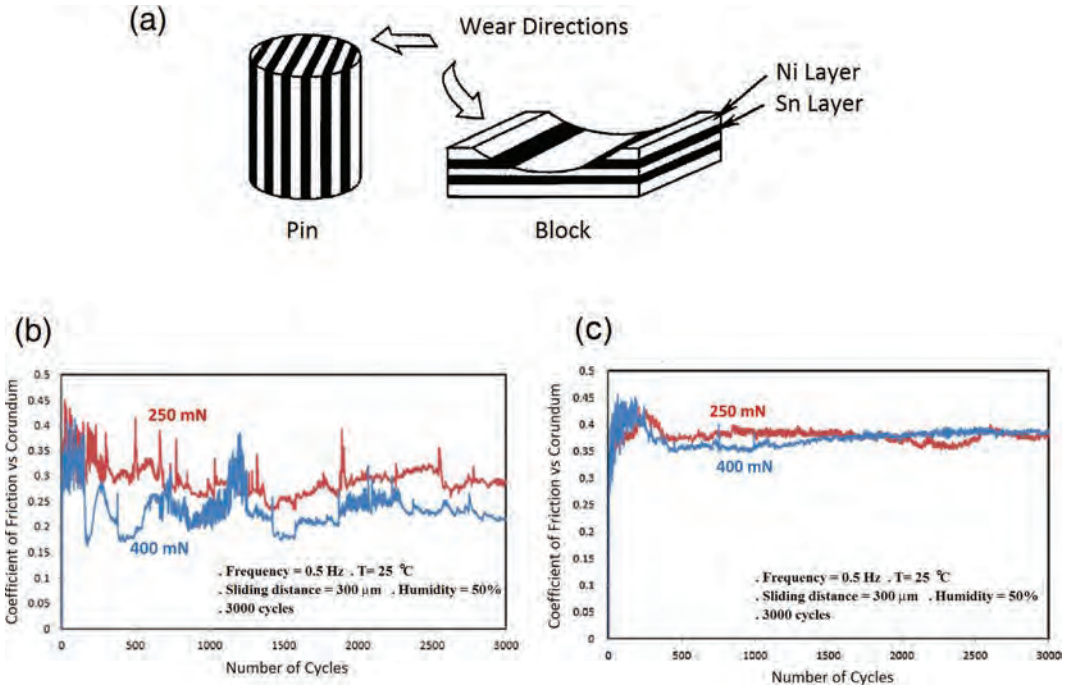

Fig. 27. (a) Schematic illustrations of two kinds of wear tests [198] and the diagrams of friction coefficient per number of cycles in (b) pure tin and (c) gradient Co/Sn coatings [203].

pure nickel deposit than the multilayer one. This is due to the soft and formable nature of copper against the brittle, hard nature of nickel. It may be stated that the multilayer coating had a better fretting wear resistance than pure nickel [92]. It was realized that friction coefficient was a function of the sublayer thickness. The multilayer coating had a higher friction coefficient than copper coating while the nickel monolithic film had the highest friction coefficient of all. The friction coefficient decreased with reduction of the sublayer thickness. Consequently, its highest value was near that of the nickel coating while its lowest value was slightly more than that of copper. According to the analysis results, the wear resistance of multilayer coatings depends on the density of interfaces together with the mechanical and wear properties of nickel and copper. For instance, a multilayer coating with thick layers often provides a wear effect similar to pure nickel. The dominant mechanism is abrasive wear. On the other hand, the multilayer coating with thin sublayers, demonstrating the best wear resistance, underwent delamination. According to EDS analysis, the residual matter on the surface after the wear test was copper because this element improves surface adhesion and reduces friction coefficient by its formability properties. It may be concluded, therefore, that two factors affect wear resistance: 1- increase in interfaces density with reduction of the sublayer thickness and 2- reduction of grain size with reduction of the sublayer thickness (revealed by XRD analysis). Interfaces hinder dislocations slip along the adjacent Ni and Cu layers [83]. Pin-on-disk and block on-ring methods were used to investigate wear properties of Ni/Sn multilayer coatings. For the first, two samples (constant nickel and variable tin contents) were provided. Each sample composed of six nickel and six tin layers which were clamped and placed in cylinder to be worn on a rotating steel disk in Fig. 27 (a). The second method was based on ASTM G77 standard code and included rectangular blocks. The wear ring was exposed perpendicularly to the surface. The thickness of Ni and Sn layers varied in two samples.

In the first test method, the sample with a low tin content initially demonstrated a high friction coefficient. However, the tin phase increased over the contact surface after 230 s, acting as lubricant and reducing the friction coefficient. The friction coefficient raised again on increasing the slip velocity, implying a fading of effect of tin in the multilayer coating. The friction coefficient of the second sample with a high tin content was much lower than the first sample due naturally to its higher tin content. However, wear rate of the second sample was higher than the first sample. This indicates that wear resistance is not necessary dependent on friction coefficient but mechanical strength of the material can be of great importance. Therefore, the second sample was weaker and underwent more intensive plastic deformation during the wear process. SEM analysis in the second test method revealed that Ni and Sn layers were quite distinct in the wear track of the first sample which contained high tin and nickel contents. However, layer boundaries were smeared and could not be observed. Friction coefficient value is fluctuating due to the fact that varying layers are being worn. Peaks and valleys are associated nickel and tin layers, respectively. Friction coefficient of this sample, therefore, rests between those of pure nickel and tin. Friction coefficient of the second sample was lower than the first one due to the lower nickel content. In addition, tin played a more significant role in surface lubrication [198]. It was reported, elsewhere that gradient Ni/SiC coatings improved wear resistance more than pure nickel coatings due to presence of hard silicon carbide particles at the top of the gradient film [25]. Increase in tungsten content in Ni-W multilayer coatings led to improvement of friction coefficient and wear resistance of coatings. On the other hand, reduction of thickness doubled the wear resistance of these coatings [59]. Wear tests in Ni-Fe and Ni-Fe-Al_2O_3 revealed that friction coefficient initially increased. However, it plummeted afterwards and eventually reached a stable value at the end. The average value of friction coefficient for Ni/Fe and Ni/Fe/Al_2O_3 at a constant duty cycle and variable frequency was less than that of the same samples at constant frequency and variable duty cycle.

These results indicate that friction coefficient of multilayer coatings produced with frequency variation was lower than friction coefficient of multilayer coatings deposited with variation of duty cycle. In addition, wear rate and wear profile of samples produced with constant duty cycle and variable frequency was lower than those manufactured by constant frequency and variable duty cycle proving the higher wear resistance of the former [36]. In Ni/Fe/Al_2O_3 gradient coatings, the data obtained for coatings produced with variation of frequency and duty cycle were compared with pure nickel films. Friction coefficient reached the maximum value in both samples and then plummeted. In the end, it arrived at a stable value. Increase in frequency led to decrease in friction coefficient. In general, the multilayer coatings produced with variable frequency showed lower friction coefficient values than pure nickel. On the other hand, reduction of duty cycle was followed by reduction of friction coefficient. This may be due to increase in hard particles content over the coating which reduces the contact area between the alloy substrate and the wearing surface. It was shown that an increase in frequency or duty cycle led to a higher wear rate [36,199]. Ni-Fe-Mn/Al_2O_3 gradient coatings were categorized into two groups including: 1-constant frequency and variable duty cycle and 2- constant duty cycle and variable frequency. Increase in frequency and duty cycle in both cases reduced the wear rate. Increase in surface hardness improved wear resistance. Increase in frequency and grains modification improved hardness in coatings produced at constant frequency and variable duty cycle [48].

It was reported that reduction of duty cycle increased the nanoparticles content while it reduced Mn content in the matrix. Increase in frequency, however, only increased the nanoparticles content with no significant impact on chemical composition of the matrix [61]. It was observed that wear rates of both types of Ni-Fe-Mn-Al_2O_3 coatings were less than Ni-Fe-Al_2O_3 composite coatings. This indicates that presence of manganese in Ni-Fe alloy improved the wear resistance. Ni/Ni-Al_2O_3 multilayer coatings were also studied. The nanocrystalline monolithic coating had the best wear resistance among other types of coatings. The composite multilayer coating did not show desirable wear properties; it suffered delamination with cracks appearing in the surface layer. This is due to the fact that presence of alumina led to increase in surface roughness and friction coefficient. Another reason for deterioration of tribological properties is formation of alumina-nickel bonding. This is why the grained morphology of the nanocrystalline monolithic coating had a higher wear resistance than the cauliflower-like morphology of the nanocomposite monolithic coating. Comparing the nanocrystalline and nanocomposite six-layered coatings with nanocrystalline and nanocomposite monolithic coatings revealed that the wear mechanism is a combination of adhesion and abrasion. Plastic deformation was limited and wear lines became parallel with the wear track. Also, displacement of matter and grooves in nanocrystalline six-layered coating was less than the nanocomposite six-layered coating. It was concluded that presence of interfaces between layers in multilayer coatings with a surface nanocrystalline layer had a desirable impact on tribological properties and wear resistance except for the nanocrystalline monolithic coating. However, presence of interfaces in coatings with a surface nanocomposite layer imposed an adverse impact elevating the wear rate [119,153]. Wear properties of Ni-W monolithic and pure Ni coatings were compared with nanocomposite Ni-W-Al_2O_3 gradient coatings. It was reported that the gradient coating had lower wear rate in comparison with pure Ni and monolithic Ni-W coatings. The highest wear rate was attributed to the pure nickel while the lowest wear rate was attributed to the gradient coating formed at duty cycle of 11%. It was considered that a gradual reduction of tungsten content or the presence on alumina nanoparticles in the coating led to decrease in friction coefficient. Alumina improved the wear resistance by 2 to 4 times in comparison with the Ni-W coating [34,200]. In addition, the primary maximum value of friction coefficient was obtained for the first (constant frequency and variable duty cycle) and second (constant duty cycle and variable frequency) types of gradient coatings referring to the static

friction coefficient. The descending trend of friction coefficient at a longer wear track length may be attributed to reduction of the tungsten content. The wear rate of pure nickel content was 30 percent higher than that of gradient Ni-W coating. Both gradient coatings (first and second types) demonstrated similar wear resistance. It was shown by EDS analysis that W content increased from the substrate towards the surface. Tungsten improved the wear resistance of the gradient coating in comparison with pure nickel [60]. Gradient Ni-Cu-W(alumina) coatings were studied under two groups (variation of frequency and variation of duty cycle). The lower friction coefficient was found for the coatings produced with frequency variation due probably to the high copper or alumina content. There was a primary maximum value for friction coefficient in coatings produced via duty cycle variation namely static friction coefficient [201]. Nickel multilayer coatings which were alternatively composed of ultrasonic and ordinary Ni layers were compared with nickel layers after the wear test. It was observed that weight reduction of the multilayer coating was less than that of the ordinary nickel coating. This implies nickel wear resistance improves through multilayer structure and crack initiation is prevented. It was reported that low thickness of layers improved adhesion to the substrate and increased the wear resistance. Pit damage which occurred on the surface of ordinary nickel coatings was not observed over the multilayer coating [130]. Also, copper multilayer coatings had a better wear resistance than copper ordinary coatings. The multilayer coating also showed a lower weight reduction [113]. Co/Cu multilayer coatings with various thickness values were chosen for wear tests due to their difference in hardness. The sample with the thickest layers demonstrated the best tribological properties as friction force had the longest duration of constancy during the wear test. Wear mechanism changed in the multilayer coating with thin layers leading to minimization of friction and coating destruction [202]. Gradient Co/Sn coatings were compared with pure tin coating in order to achieve a comprehensive understanding on tribological properties. According to Fig. 27 (b), friction coefficient of pure nickel underwent huge fluctuations because of the adhesive wear phenomenon. Analysis of the residual matter in the interface revealed that it contained tin and tin oxide. Friction coefficient of the gradient coating in Fig. 27 (c) was more stable due to the low thickness of top tin layer and intermetallic particles. According to SEM analysis, a very low content of residual matter was seen in the interface. Intermetallic particles improved the wear resistance of the gradient coating by creating a restricted wear depth [203].

Addition of lubricant to Fe-W alloy surfaces led to improvement of tribological properties and reduction of friction coefficient. With electrodeposition under different current densities, these coatings showed higher wear depth than chromium coatings. In fact, increase in current density increased the wear depth by reducing the tungsten content. Fe-W/Cu multilayer coatings were compared with the Fe-W alloy coating. The multilayer coating with thin layers showed similar worn volume to the alloy coating, however, the wear rate and friction coefficient were minimized by increasing the thickness of layers [204].

7.6.2. Worn surface morphology and wear mechanism

Wear resistance of a Ni/Cu layered coating was evaluated by means of a crossed cylinder apparatus. This coating was deposited on the top fixed cylinder. A rotary steel cylinder (covered by abrasive papers up to 4000 grade) approaches the sample and operates the wearing process. SEM analysis revealed that a mild deformation took place under low forces leading to removal of surfaces scratches in Fig. 27). With an increase in the applied force, scratch marks remained smooth yet deformation increased. Under the highest force, the remaining mark was utterly rough with a considerable deformation [158,194]. According to Fig. 28, the wear rate of the copper layer was double that of the nickel layer. The multilayer structure improved the wear resistance of both coatings.

As shown in Fig. 29, a wear test was performed on the Ni/Cu multilayer coating with the lowest Ni content. In addition to the abrasive mechanism, plastic deformation was observed over the surfaces worn by the lower force. Using the higher force, materials were displaced towards the end of the wear track [165].

The multilayer structure prevented deformation and wear of the substrate. The thick-layered coating demonstrated a delaminated microstructure. Grain refinement which was obvious on the underlying

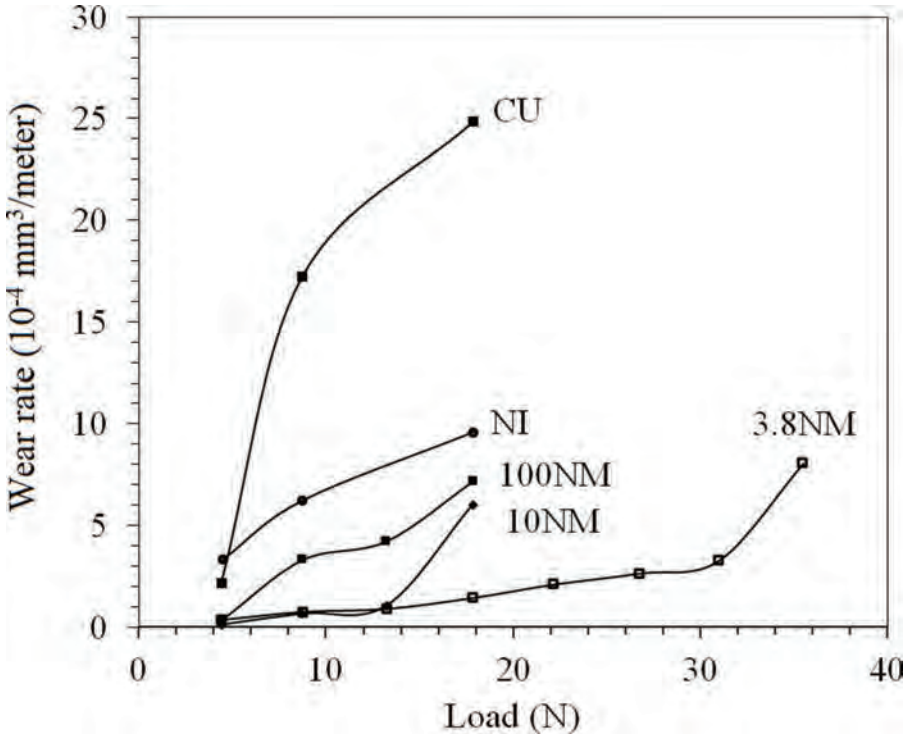

Fig. 28. Comparison of Cu and Ni wear rates with that of Ni/Cu multilayer coatings with different layer distances [194].

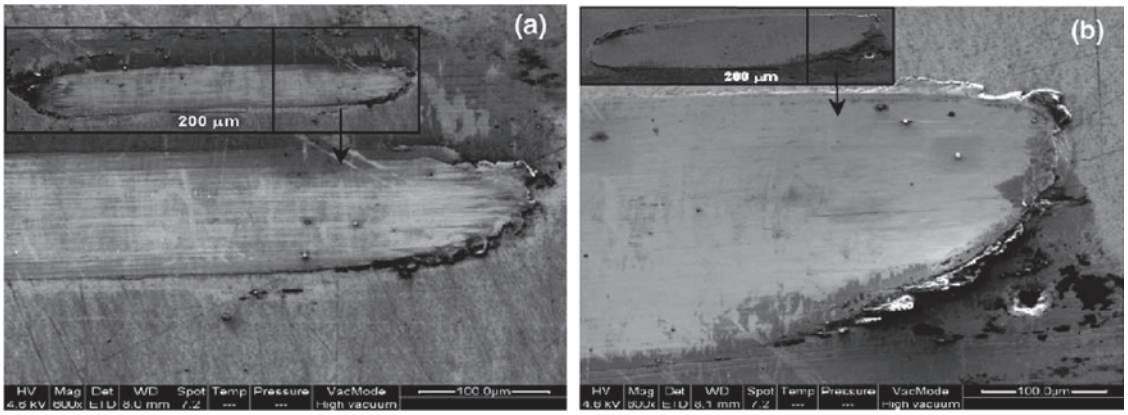

Fig. 29. Morphology of the worn sample with the lowest Ni content using (a) 3 N and (b) 11 N forces [165].

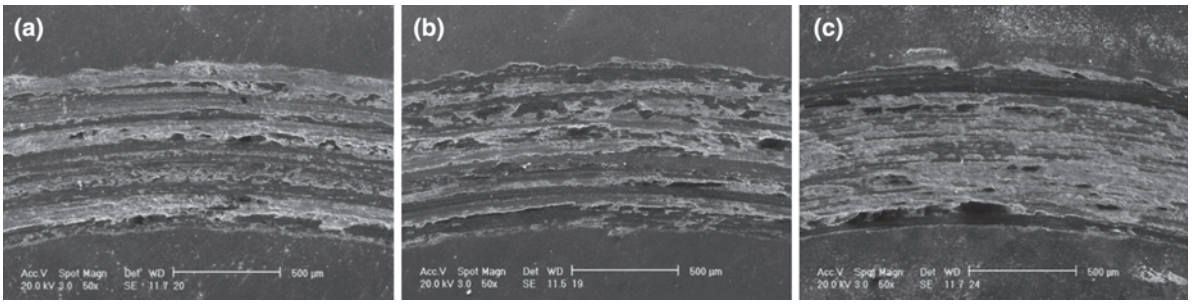

Fig. 30. Surface morphology of Ni-Fe-Mn-Al_2O_3 multilayer coatings after the wear test, (a) constant-duty-cycle and variable-frequency coating, (b) variable-duty-cycle and constant-frequency coating and (c) Ni-Fe-Al_2O_3 monolithic coating [61].

layers is usually observed on worn surfaces of formable materials. However, the lowest wear rate was seen in the thin-layered coating with polycrystalline structure. These coatings were strengthened by Ni/Cu interfaces and grain boundaries caused by the polycrystalline structure. The effect of grain boundaries on hard nano-indentations was less than the interfaces because of the lower density of grain boundaries [197].

It was revealed from the worn surfaces that there was a greater wear impact on Ni-Fe multilayer coatings. The continuous impact on the sample produced by constant duty cycle and variable frequency implies that the dominant wear mechanism was abrasive. Although the adhesion effect is harsh in these coatings, the overall mechanism for both coatings was abrasive while the substrate demonstrated an adhesive mechanism. Increase in frequency was found to modify the grain size. According to previous researches, grain size reduction reduced the wear rate and improved the wear resistance through hindering the motion of dislocations. This may be accounted for the reason of high wear resistance of multilayer coatings produced by variable frequency and constant duty cycle [36].

Fig. 30 illustrates the SEM micrographs of Ni-Fe-Mn-Al_2O_3 multilayer coating produced by constant frequency and variable duty cycle. There were many grooves, boundaries and remaining wear impact marks, implying that abrasive wear was predominant. However, the surface was smoother than the Ni-Fe-Al_2O_3 monolithic coating. Material removal in constant-duty-cycle and variable-frequency coatings was higher than variable-duty-cycle and constant-frequency coatings. Clearly, the monolithic coating showed high plastic deformation [61].

Structure of gradient Ni-Cu-W(alumina) coatings was analyzed by means of SEM (Fig. 31). Typical Ni coatings had non-parallel wear tracks with pits of bulk flake-off. The remaining pores after surface wearing might be due to the low hardness of nickel. The pores surpassed the yield point and formed fatigue-induced cracks. The multilayer coating demonstrated no flake-off but small regions of debris accumulation. In addition, the layers were parallel with no sign of fatigue cracking. The multilayer coating may reduce the stress range effect and divide it between the coating/substrate interfaces. Preventing crack propagation and delamination, the multilayer coating improves wear resistance. The other advantage of multilayer structures is increase in dislocations density in the coating that hinders wear-induced crack growth [130].

In conclusion, formation of multilayer structure improved wear resistance of the underlying substrate by reduction of friction coefficient (see Fig. 32). It may act as a barrier to reduce the stress range among the coating and the substrate. Multilayer structures may also enhance the tribological properties by preventing crack propagation and delamination. The layered structure may either decrease the induced shear stresses and or decrease the depth coatings bearing the shear stress beneath the wear front. In general, multilayer structures have better tribological, wear, and friction characteristics compared to their single layer constituents.

7.7. Scratch resistance

Scratch test is applied for evaluation of scratch resistance and adhesion between the coating and substrate. A diamond pin is dragged over the surface with increasing applied force until fracture happens. The load under which fracture happens is called the critical load. There are various types of fracture such as segregation, cracking along the thickness, plastic deformation or cracking in the coating or substrate.

For example, plastic deformation, groove formation and a few cracking were observed for soft coatings in a typical Rockwell C test. Plastic deformation occurs on soft substrates while the coating might undergo plastic deformation or fracture if it is bent in direction of the groove caused by the plastic deformation. It is possible that the coating becomes very thin with plastic deformation and removal of the coating between the scratcher and the substrate occurs prior to fracture and plastic deformation of the substrate. Plastic deformation is rare in hard coatings deposited on hard substrates. Fracture is induced by scratching;

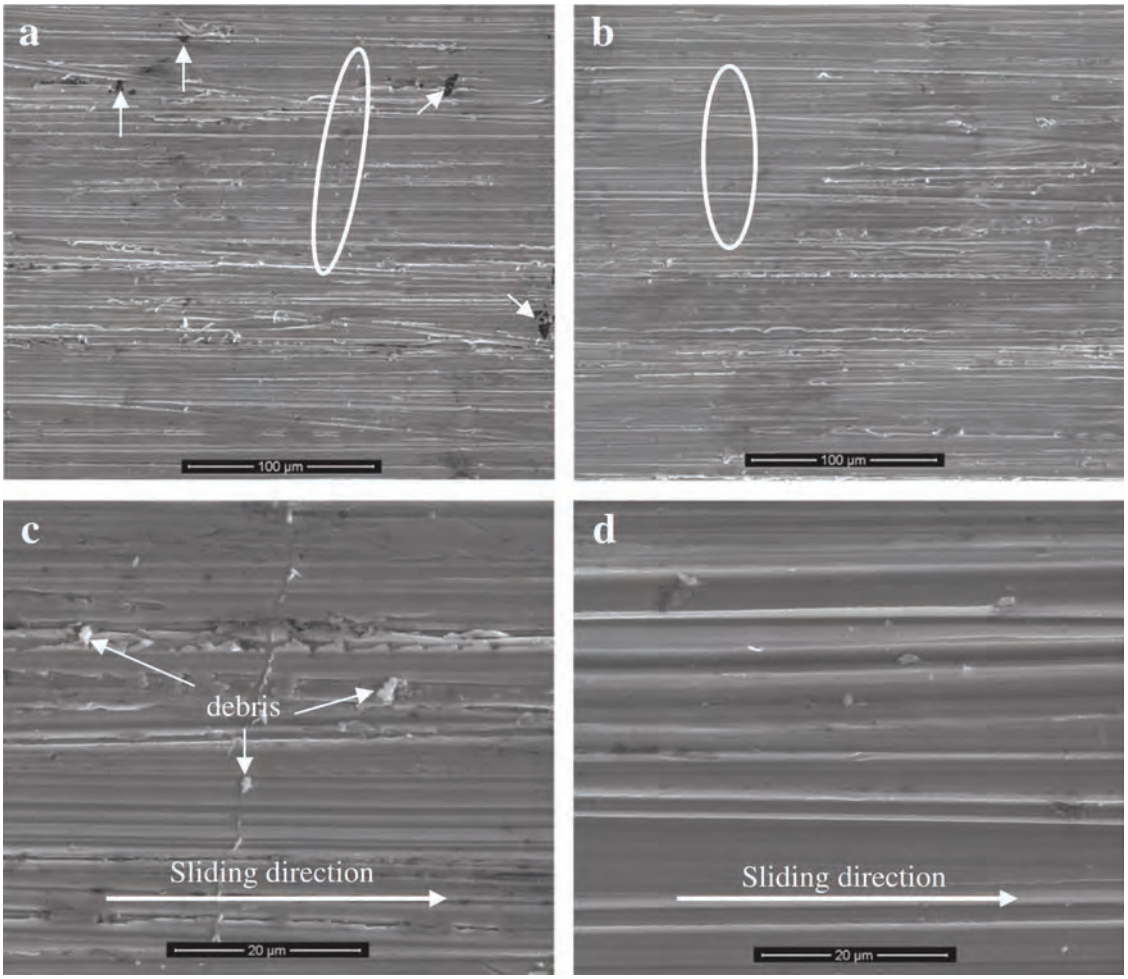

Fig. 31. Surface morphology of gradient Ni-Cu-W(alumina) coatings after the wear test: (a) typical Ni coating, (b) multilayer coating, (c) magnified a and (d) magnified b [61].

for a sharper indenter, more plastic deformation is attributed to the coating than the substrate. If the diamond pin is too sharp, there is an increased risk of its destruction during the test. Pin diameter has to be selected in a way that it is neither damaged nor data analysis becomes too difficult. Hard industrial coatings with thickness of more than one micrometer are tested with Rockwell C pins, while, conical indenters are used for thin coatings. Scratch test is found somewhat useful for evaluation of adhesion in soft coatings. In general, this test is best suitable for a situation where the substrate does not undergo huge plastic deformation and coating is effectively scratched. Characterization of uncoated surfaces can be challenging unless proper chemical analyzing techniques are applied. Provided that the coating and substrate behave differently, the desirable results may be found by measuring wear rate variations during the scratch test. The scratch test is often known as a semi-quantitative method; there are several major and minor parameters which influence the applied critical force. Most of these parameters are apparatus-related and require accurate calibration. Nevertheless, other factors such as coating thickness and substrate hardness should be known for a better realization of the test results. Quantification of the results requires the fracture type associated to adhesion, determination of the fracture mechanism and a method for detection of stresses that induce fracture [205]. This technique is widely used for evaluation of electroplated coatings. For instance, 450 nm nano-scratchers were employed to investigate the mechanical properties of electroplated Ni-W coatings. The obtained results are presented in Fig. 33. It may be observed that scratch depth varied linearly in all samples (with different tungsten contents) with increase in the applied force up to 10 mN. Scratch depth is inversely associated with the hardness of coating. However, such a relationship was not proven for this type of coating. Scratch resistance of Ni-W coatings was compared with a typical nickel coating. Accordingly, scratch resistance of the tungsten carbide coating was significantly higher than the nickel coating which might be due to the coarser grains and lower hardness of the nickel coating [206].

Scratch resistance test is also employed in order to investigate the adhesion of multilayer coatings produced via CVD and PVD techniques. For instance, scratch resistance test was used to study crack initiation and fracture in Ti(C,N) and TiN/Ti(C,N) multilayer coatings. These coatings are generally hard and brittle so that they would undergo fracture when exposed to high stresses. Scratch test was performed using a diamond indenter with a micron-sized peak. Acoustic emission analysis was used for detection of the scratch force at which the first crack occurs [207].

It may be observed that addition of TiN to the coating improved its resistance against crack propagation [207]. Scratch test was used elsewhere, to investigate crack propagation resistance in Ti/TiAlN/TiAlCN multilayer coatings [208]. Micro-scratchers were applied for silicon carbide multilayer coatings deposited via CVD technique. Similar to previous works, the critical force for each coating with different parameters was determined. This technique has been used very rarely in study of multilayer coatings [209]. Papachristos et al. [45] investigated the adhesion of properties of Ni-P-W multilayer coatings by a scratch test. They mentioned that there were two significant critical loads within the scratch test. Cracks initiated under the first critical load, known as the cohesive load. The removal of coating from the surface occurs under

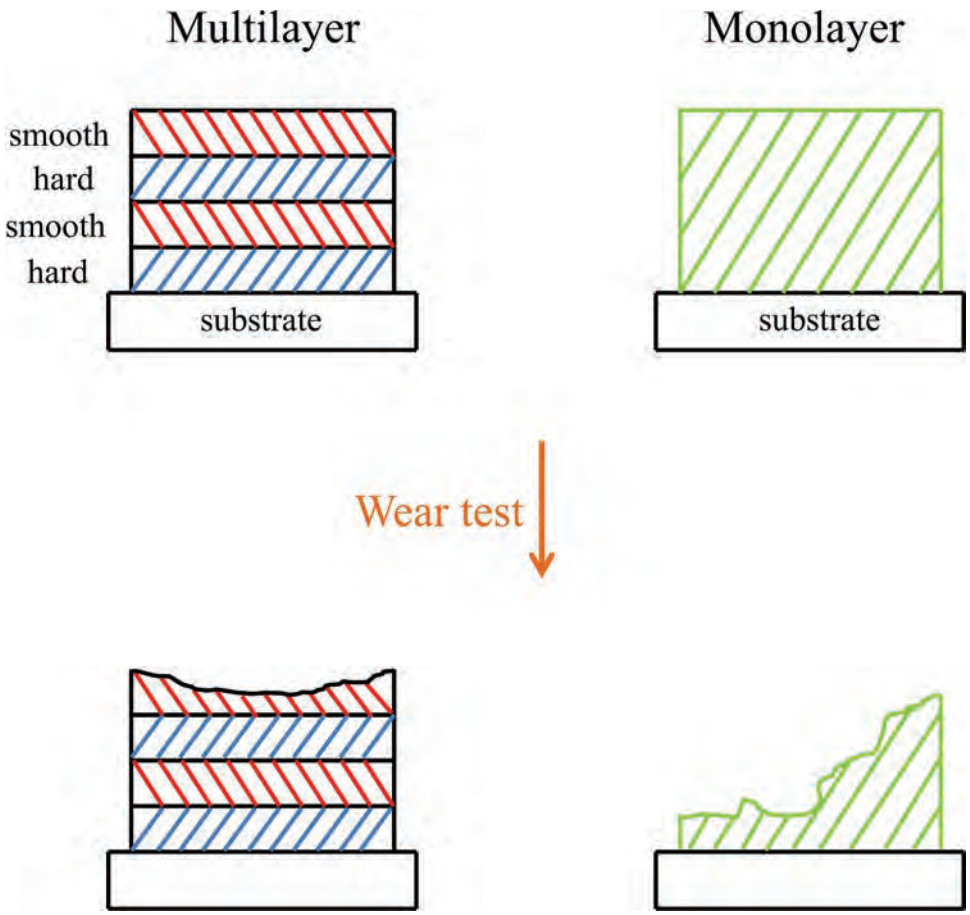

Fig. 32. Wear resistance in single layer and multilayer coatings.

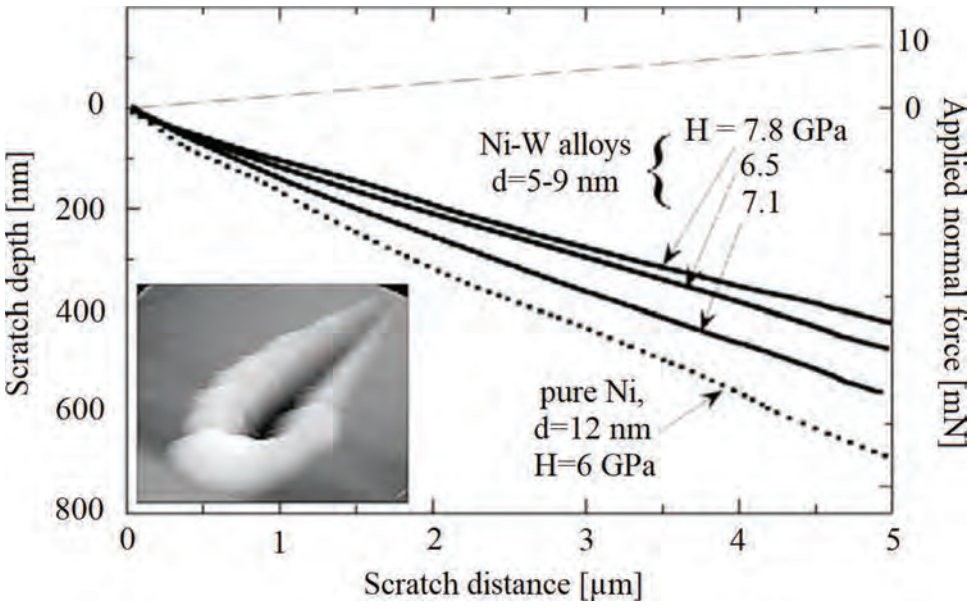

Fig. 33. Scratch depth diagrams based on the position of the diamond cone peak moving over the sample surface. The second traverse axis shows the normal load of the diamond peak. In addition, AFM micrograph illustrates a scratch surrounded by a mass bulk of material. The scratch length in this micrograph is 5 μm [206].

the second critical load known as the adhesive load. The critical loads are determined through acoustic emission technique. The point at which the first acoustic emission is seen indicates the cohesive load. Meanwhile, acoustic emission becomes sharp under the adhesive load. As it was mentioned earlier, adhesion of electroplated Ni-P-W multilayer coatings was investigated by Papachristos et al. [45]. The total increase in acoustic emission was between 25 to 30 N. Removal of coating does not occur frequently due to the soft nature of substrate (copper) and the

hard coating. Destruction, however, was very extensive so that the cohesive load could not be recognized. In addition, high thickness and brittleness of the coating led to formation of deep cracks which produce intense acoustic signals. Hence, the obtained acoustic signal patterns were very complex. Under small loads, the multilayer structure was observed to cause blocking of cracks at the interfaces between layers [45].

7.8. Magnetic properties

Magnetic materials have become extensively interesting over the recent years due to their wide applications in magnetic field sensors, read sensors in high-density magnetic recording systems, magnetic random-access memories, etc. In this regard, magnetic properties of various nanostructured materials such as multilayer coatings and nanowires have been studied. Electroplating is a well-known deposition technique which is used more frequently than as example spraying, chemical vapor deposition (CVD) and molecular beam epitaxial (MBE) due to simplicity, high deposition rate, low costs (as it does not need vacuum equipment) and the ability to produce films on irregular surfaces [210]. Another advantage of this process is the possibility of sample immersion in an electrolyte throughout the preparation process. However, this technique does not provide the feasibility to produce a pure magnetic film from an electrolyte filled with both magnetic and non-magnetic ions. That is, the noble metal always deposits with the other (less noble) metal during the deposition process [211]. In principle, production of multilayer coatings through electroplating can be performed via single- or double-baths procedures. In the latter, the resistance of magnetic materials may decrease because of the possible oxidation of layers during transitions between the baths [212]. Thus, the single-bath method is perceived as a better technique for electroplating of multilayer coatings [213]. In addition to deposition states (galvanostatic/potentiostatic), ion concentration, anion type, modifying additives, current density, overpotential, pH of electrolyte, stirring rate, type of substrate and temperature of electrolyte affect the properties of deposited coatings. Any variation in these parameters may affect magnetic and structural properties. Some of magnetic properties are magneto-resistance, giant magnetoresistance, coercivity (*Hc*), magnetic flux density (*Bs*), saturation magnetization (*Ms*), magnetic remanence (*Mr*), permeability (μ), anisotropy and squareness [158,214–216]. Magneto-resistance (*MR*) is the variation in electrical resistance of a material due to exposure to an external magnetic field. There are many effects that may be called the magneto-resistance [217]. Anisotropic magnetic resistance is attributed to the effect occurring mostly in magnetic materials; while 'giant magneto-resistance' is used to describe effects in multilayer systems. Magnetic resistance is defined as:

$$MR = \frac{\Delta R}{R_0} = (R_H - R_0) \Big/ R_0 \tag{3}$$

Where R_H is the electrical resistance in the presence of a magnetic field and R_0 is the resistance in the absence of a magnetic field. Magnetic field measurement may be performed parallel or perpendicular to the current direction. Longitudinal magnetoresistance (LMR) occurs when the magnetic field is parallel to the current direction. Transverse magnetoresistance (TMR) forms when the magnetic field is perpendicular to the current direction. From these measurements the anistropic magnetoresistance (AMR) effect can be determined. The giant magnetoresistance (GMR) effect is a large change in electrical resistivity due to a small applied magnetic field [65,218].

The current in a multilayer coating may be parallel (current-in-plane) or perpendicular (current-perpendicular-to-plane) to the layers. Magneto-resistance is highly sensitive to growth conditions and may disappear by intermixing magnetic and non-magnetic interfaces. Coercivity indicates the magnetic intensity required for reduction of magnetic flux density in an entirely magnetized sample to zero or demagnetization. In fact, coercivity is the force that must be applied in the opposite direction of the primary field in order to reduce the existing magnetic power to zero. Coercivity is defined as:

$$Hc = \frac{H + Hr}{2} \tag{4}$$

Where H_c is coercivity and H_r is the reversal field. Reversal field is the magnetic intensity required for adjustment of magnetic torques in line with the applied field. Once a ferromagnetic material is exposed to a magnetic field, the torques are set towards the field direction. Magnetic saturation (M_s) is obtained when all of the torques become in line with the field. If a reversal field is applied, some of the torques diverge from the applied field direction and some remain unchanged (magnetic remanence, M_r). Magnetic remanence indicates the magnetic induction that remains in the material. Hysteresis loop squareness is the ratio of M_r to M_s [219]. Increasing attention has been given to multilayer coatings composed of magnetic and non-magnetic layers since a merger of magnetic and non-magnetic metals can confer novel characteristics that may not be present in a single component. Multilayer coatings well-known for their magnetic properties include Co/Cu [87,220], Ni/Cu [98], NiFe/Cu [221], CoNi/Cu [74,124] and CoFe/Cu [131,222]. Magnetic properties of multilayer coatings are affected by many parameters such as the crystalline structure, thickness of layers, deposition potential, orientation, grain size, multilayer coating size, electrolyte composition, pH of electrolyte, temperature of electrolyte, magnetic field and bath additives. The effect of different parameters on magnetic properties of multilayer coatings is explained in the following sections.

7.8.1. The effect of layer thickness on magnetic properties of multilayer coatings

The layer thickness greatly affects the magnetic properties of multilayer coatings. Any alteration in thickness of magnetic and non-magnetic layers as well as that of whole multilayer coating affects the magnetic behavior of the multilayer coating. Highly applied Co/Cu multilayer coatings are composed of magnetic (cobalt) and non-magnetic (copper) layers. Magnetic resistance increases with decrease in thickness of cobalt layers. In fact, the thickness of each layer affects the magnetic properties of the whole multilayer coating. However, MR does not change once the thickness of cobalt is less than 1 nm as the cobalt layer loses its continuity and forms islands having various sizes [87,220]. The maximum magnetic resistance value is generally obtained when the thickness of cobalt layer ranges from 1 to 1.5 nm [223,224]. It was reported elsewhere that under a constant thickness of copper layer (4 nm) and an increase in thickness of the cobalt layer from 0.2 to 1 nm, GMR value demonstrated an ascending trend, except within 0.5-0.6 nm range. The lowest GMR was found at 0.6 nm [225]. In fact, the multilayer coating displayed a great magnetic resistance and anisotropic magnetic resistance at low and high thicknesses of the cobalt layer. LMR and TMR values increase with increase in cobalt layer thickness leading to increase in AMR [6,226]. It was reported by Pandya et al. [227] that GMR increased with increase in thickness of the cobalt layer from 5 to 20 nm due to the increase in surface roughness [227]. As seen in Fig. 34, an increase in the cobalt layer thickness led to reduction of the coercivity force due to increase in grain size [38,68,226,228]. The cobalt layer thickness also affects saturation magnetization. Reduction of thickness leads to a lower saturation magnetization and consequent increase in squareness [38,220].

In CoNi/Cu multilayer coatings, MR increased under a constant thickness of copper layer and an increasing thickness of the CoNi layer from 2 to 17 nm. However, the MR value dropped after further increase in thickness from 17 to 510 nm. The reduction in MR is due to the discontinuity of extra-thin CoNi layers. MR remained constant above 510 nm due to the presence of anisotropic magnetic resistance [74]. The thickness of the magnetic CoNi layer affects magnetic behavior and coercivity of CoNi/Cu multilayer nanowires; at a constant copper layer

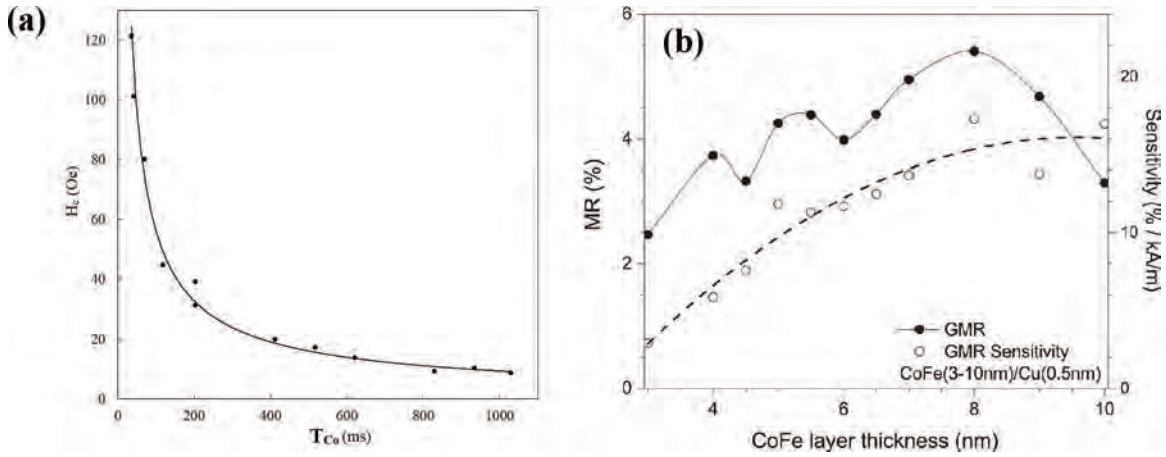

Fig. 34. (a) Dependency of coercivity to the thickness of cobalt layer in Co/Cu multilayer coatings [38]. (b) The great magnetic resistance of CoFe/Cu multilayer coating as a function of thickness of CoFe layers [222].

thickness and with a variable CoNi layer thickness (from 1 to 17 nm), magnetic behavior varies. Nanowire showed a superparamagnetic behavior when the thickness of the magnetic layer was lower than 6.8 nm; ferromagnetic behavior was seen once the thickness exceeded 6.8 nm. Discontinuity of layers may be responsible for the super paramagnetic behavior. Coercivity increased for thinner CoNi layers from 17 to 6.8 nm. However, further decrease in thickness of the magnetic layer from 6.8 to 1 nm led to decline of coercivity due to the discontinuity of layers; maximum coercivity was obtained at a thickness of 6.8 nm [124].

The thickness of the magnetic layer in FeCoNiCu/Cu multilayer coatings affects the great magnetic resistance. GMR reached the maximum value (6%) once the thickness of the copper-rich layer reached 1.8 nm due to the large grain size. A slight increase or decrease in thickness of the copper layer leads to a plummeting GMR value [29]. CoFe/Cu multilayer coating demonstrated a fluctuating magnetic behavior with copper layers of constant thickness and thickness of CoFe layers increasing from 3 to 10 nm in Fig. 34 (b) [222]. A thicker CoFe ferromagnetic layer increased the coercivity of the multilayer coating due to strengthening

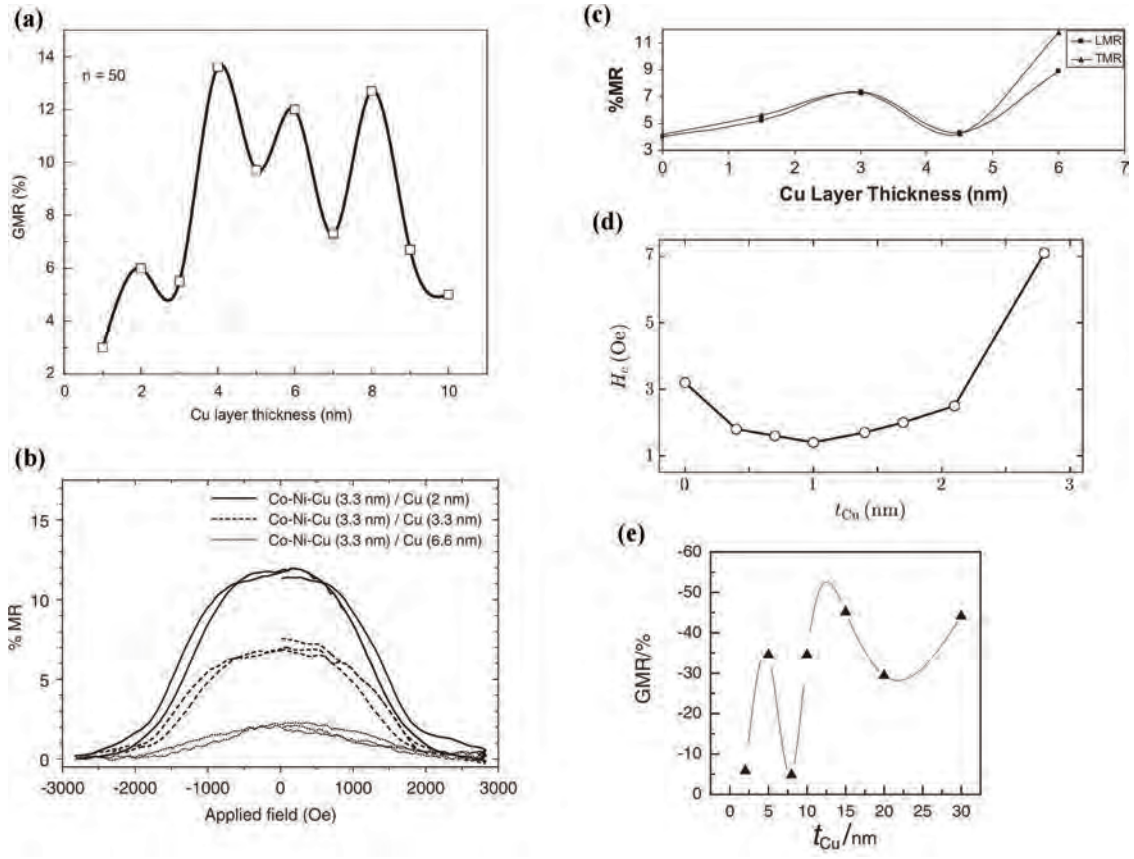

Fig. 35. (a) GMR variations versus the thickness of copper layer in Co/Cu multilayer coating [227]. (b) The magnetic resistance percentage measured for CoNiCu/Cu multilayer nanowires with CoNiCu and copper layers of constant and varied thicknesses [234]. (c) MR variations versus thickness of the copper layer in FeCo/Cu multilayer coating [75]. (d) Coercivity as a function of thickness of the copper layer [120] and (e) GMR variations versus the thickness of copper layer in NiFe/-Cu/Co/Cu multilayer coating [236].

of ferromagnetic bonds between the magnetic layers [131].

Magnetic anisotropy of CoCuP/Cu multilayer coatings decreased with reduction of thickness of CoCuP layers, reaching a minimum value at thickness of 3 nm. This may be attributed to the decline of columnar growth and increase in the demagnetizing agent perpendicular to the sample surface. Magnetic anisotropy increased with further reduction of thickness due probably to the discontinuities in ferromagnetic layers [229]. The cobalt layer thickness affects coercivity and magnetic remanence in Co/Pd multilayer coatings. The facile axis for magnetization is on-plane when the cobalt layer thickness exceeds 0.6 nm. The magnetic remanence ratio increases with decrease in the cobalt layer thickness until it reaches 1 at a thickness of 0.4 nm. This indicates that the easy magnetization axis of the multilayer coating changes from parallel with the film plane to perpendicular to it. In fact, the easy magnetization axis of the multilayer coating changes from on-plane to perpendicular with decrease in thickness of the cobalt layer [135]. The Ni/Cu multilayer coating had a lower great magnetic resistance than the Co/Cu multilayer coating. Replacement of cobalt by nickel significantly reduces the GMR [84,110]. In Ni/Cu multilayer nanowires, a thicker nickel layer increases shape anisotropy and coercivity. The latter increases with increase in thickness of the NiCu magnetic layer in NiCu/Cu multilayer coatings. Introduction of Fe to the NiCu magnetic layer and formation of FeNiCu/Cu multilayer coatings leads to decrease in coercivity and increase in GMR and saturation magnetization. Similar to NiCu/Cu multilayer coatings, increase in thickness of the FeNiCu layers leads to improvement of coercivity. $Ni_{80}Fe_{20}$/Cu multilayer nanowire has GMR properties. However, its value is very small due to the wavy interface [97]. Ni/Cu/Fe multilayer nanowire shows a lower coercivity than Cu/Ni nanowires [230]. Thickness of the magnetic layer (Fe) affects the magnetic behavior of Fe/Cu multilayer nanowires such as coercivity. The easy magnetization orientation is perpendicular to the nanowire axis when the iron layers are thin. However, increase in thickness of the iron layer changes the easy magnetization orientation to parallel [231]. In Ni/Pd multilayer nanowires, increase in ratio of nickel deposition time to palladium deposition time reduces saturation magnetization and consequently improves magnetic properties since the weight percentage of nickel increases at the expense of decrease in weight percentage palladium [132].

7.8.2. The effect of non-magnetic layer thickness on magnetic properties of multilayer coatings

Thickness of non-magnetic layers affects the magnetic properties of multilayer coatings. The effect of non-magnetic layers thickness is bold in Co/Cu multilayer coatings where the GMR behavior has a fluctuating behavior in regards with the thickness of copper layer in Fig. 35 (a). The magnetic resistance in CoCu/Co multilayer coatings depends on the composition of ferromagnetic cobalt-rich layer and thickness of the non-magnetic copper layer.The MR ratio is a maximum (15%) when the thickness of copper layer reaches 1.4 nm, cobalt composition is 86% (layer thickness of 0.9 nm) and temperature is 300 K; magnetization is a minimum. In fact, increase in thickness of the copper layer up to 1.4 nm leads to improvement of the MR ratio but this ratio begins to fall with further increase in thickness. This is due to a decline in antiferromagnetic interactions between the ferromagnetic Co layers near the non-magnetic Cu layers [232].

Addition of nickel to CoCu alloy layers and formation of CoNiCu/Cu multilayer coatings leads to increase in GMR. When the nickel content reaches 3.5%, GMR may increase by 11% [233]. In Fig. 35 (b), an increase in thickness of the copper layer in CoNiCu/Cu multilayer nanowires from 2 to 7 nm is followed by reduction of magnetic resistance [234]. Magnetic resistance also decreases with increase in thickness of the copper layer in CoNi/Cu multilayer nanowires. That is, increase in thickness of the copper layer from 4.2 to 42 nm (with the CoNi layer thickness being constant) lead to reduction of magnetic resistance [74].

In Fig. 35 (c), an increase in thickness of the copper layer leads to a fluctuating magnetic behavior in the FeCo/Cu multilayer coating. This is caused by microstructural defects such as roughness of the interface [75, 131]. Increase in thickness of the copper layer in FeCoCu/Cu multilayer nanowires is followed by increase in coercivity and squareness properties [235].

The effect of non-magnetic layer thickness on magnetic behavior of FeNiCu/Cu multilayer coatings is important. An increase in the copper layer thickness up to 1 nm is followed by reduction of coercivity but further increase in thickness of the copper layer from 1 to 2.8 nm leads to an increased coercivity in Fig. 35 (d) [120]. An increase in the copper layer thickness in Ni/Cu multilayer coatings is found to increase the magnetic remanence due to dipolar interactions between the nickel layers caused by reduction of the copper layers thickness [89].

It can be seen in Fig. 35 (e) that the GMR of NiFe/Cu/Co/Cu multilayer coating, similar to Co/Cu and FeCo/Cu multilayer coatings, demonstrates a fluctuating behavior with an increase in copper layer thickness [236].

While the thickness of the CoPtP layer is maintained constant in CoPtP/Cu multilayer coatings, an increase in thickness of the copper layer leads to elevation of vertical coercivity whereas in-plane coercivity is inversely related to thickness of the copper layer. In addition, increase

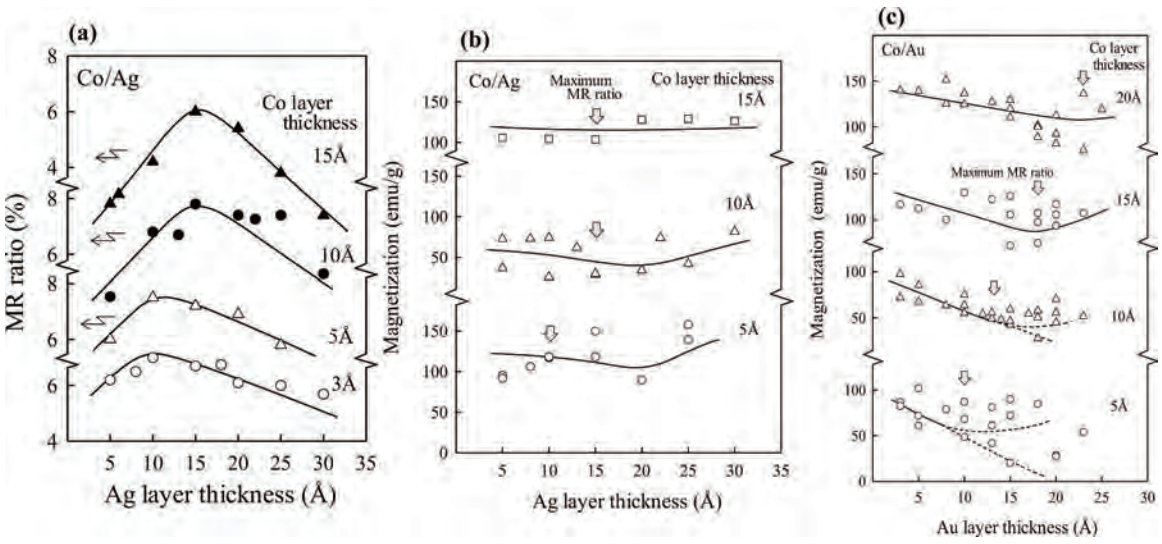

Fig. 36. (a) MR ratio in Co/Ag multilayer coating as a function of sliver layer thickness. (b) dependence of the silver layer thickness to magnetization at any cobalt content in Co/Ag multilayer coating and (c) dependence of the gold layer thickness to magnetization at any cobalt content in Co/Au multilayer coating [57].

in thickness of the copper layer declines the in-plane coercivity [121]. In a multilayer coating of 10 layers with a thickness of 100 nm (CoPtP and copper), the optimum coercivity and squareness values were 4130 Oe and 0.7, respectively [237]. MR ratio depends on thickness of cobalt and silver layers in Co/Ag multilayer coating. The maximum MR ratio is obtained with increase in thickness of cobalt and silver layers up to 1.5 nm in Fig. 36 (a) [57,213].

Generally, magnetization of Co/Ag and Co/Au depends on thickness of the cobalt, silver and gold layers. Increase in thickness of the cobalt layer improves magnetization in both multilayer coatings. It may be seen in Fig. 36 (b) that the magnetization is minimum when thicknesses of cobalt and silver layers are 1 nm and 2 nm respectively. The minimum magnetization in Co/Au coatings is obtained when thicknesses of cobalt and gold layers are 1.5 nm and 2 nm, respectively in Fig. 36 (c). Magnetization fluctuation is immense at high thickness of gold layers and low thickness of cobalt layers. Magnetism of cobalt layers becomes highly influenced by the surrounding gold atoms as thickness of the cobalt layer decreases [57]. Saturation magnetization of Co/Ag multilayer nanowire is generally lower than Co nanowires [238].

An increase in the thickness of cobalt- and silver-rich layers affects MR ratio in $Co_{70}Ag_{30}/Co_8Ag_{92}$ multilayer coatings. The highest MR ratio is obtained when thicknesses of cobalt- and silver-rich layers are 0.8 nm and 1.2 nm, respectively. Under equal conditions (at room temperature and in magnetic field of 21 kOe), the maximum MR values for $Co_{70}Ag_{30}$ (0.8 nm)/Co_8Ag_{92} (1.2 nm) multilayer and Co/Ag monolithic coatings were 8.7% and 5%, respectively. It may be concluded that forming a multilayer structure increased the MR in Co/Ag coating [52]. Increase in thickness of the silver layer in CoAg/Ag multilayer nanowires alters the magnetic properties from AMR to GMR [77]. The effect of non-magnetic layer thickness on magnetic properties of Co/Zn multilayer coatings is notably significant. In a research on these multilayer coatings where thickness of the cobalt layer was maintained constant (5 nm) and thickness of the zinc layer was increased from 0.1 to 7 nm, the highest GMR value was observed at thickness of 0.8 nm (30%) [106]. In addition, coercivity reduces with decrease in thickness of the zinc layer [239]. The GMR is affected by whether the first deposited layer is cobalt or zinc. In fact, the GMR shows a higher level when cobalt is deposited as the first layer. CoZn/Cu multilayer coatings had a lower magnetic resistance than Co/Cu multilayer coatings so that magnetization did not reach saturation under a high magnetic field (14 kOe) [115].

7.8.3. The effect of number of layers

Total number of layers is another factor affecting the magnetic properties of multilayer coatings. It was mentioned earlier that thickness of magnetic and non-magnetic layers in Co/Cu coatings affects several magnetic properties such as magnetic resistance, coercivity and saturation magnetization. Increase in number of bilayers up to 50 led to increase in the great magnetic resistance of Co/Cu coatings. However, further increase in number of bilayers (from 50 to 75) declined the GMR. This is due to formation of non-specular Co-Cu interfaces [240]. The same behavior was observed by Haciimailoglu et al. [241] as they reported that increase in number of bilayers up to 222 layers leads to increase in the GMR; while, further increase caused a fluctuating behavior. In addition, GMR occurs with a slight AMR when number of layers is below 111.

Increase in number of bilayers in CoCu/Cu multilayer coatings led to reduction of magnetic resistance as the structure of coating evolved with growth of the sample [28]. These multilayer coatings also possess anisotropic magnetic resistance [242]. Increase in total thickness of NiFe/Cu multilayer coatings leads to increase in thickness of copper layers and decrease in thickness of nickel-iron layers which, in turn, affect the coercivity of multilayer coatings. Increase in total thickness of the coatings from 0.3 to 5 nm leads to decrease in coercivity by 50% [243]. Increase in number of bilayers leads to increase in magnetic resistance of Fe/Pt multilayer coatings as well as increase in anisotropy of $Co_{83}P_{17}/Co_{74}P_{26}$ multilayer coatings [114,244]. Increase in thickness of $Fe_{50}Pt_{50}$ layer leads to increase in vertical coercivity of $Fe_{50}Pt_{50}/Fe_2Pt_{98}$ multilayer coatings. However, it does not influence the parallel coercivity. Also, these multilayer coatings possess magnetic anisotropy [245,246].

7.8.4. The effect of deposition potential on magnetic properties

Deposition potential plays an important role in magnetic properties of multilayer coatings. This parameter affects the great magnetic resistance of Co/Cu and NiCo/Cu multilayer coatings. Increase in copper potential deposition in Co/Cu multilayer coatings towards more positive values leads to increase in the ferromagnetic GMR and decrease in the superparamagnetic GMR [247]. Besides, the GMR was approximately 13% in the same multilayer nanowires at deposition potential of -0.9/–0.4 V. However, GMR plummeted within a more negative potential (-1.0/–0.5 V) due to increase in structural defects. Further, even a more negative potential (-0.8/–0.3 V) leads to a very tiny magnetic resistance due to dissolution of cobalt.

Moving from the optimum potential towards more positive values led to decrease in surface roughness of NiCo/Cu multilayer coatings which, in turn, improved the GMR [56].

7.8.5. The effect of electrolyte additives on magnetic properties

Introduction of various additives/bath formulations to the electroplating bath affects magnetic properties of multilayer coatings. For instance, addition of NaCl to the electroplating bath of CoCu/Cu multilayer coatings leads to alteration of magnetic properties. In fact, NaCl addition reduces the GMR as adsorption of chlorine during deposition leads to grain refinement in the multilayer coatings. Grain refinement, increase in nucleation rate and change deposition mechanism lead to formation of an irregular structure which consequently reduce the great magnetic resistance [101]. It has been shown that presence of DPSA in the electroplating bath of Co/Cu multilayer coatings affects the magnetic properties. Introduction of DPSA to the electrolyte reduces surface roughness and coercivity [248]. Addition of silver to Co/Cu multilayer coatings alters the GMR. Increase in the silver content up to 1at% alters the microstructure so that the GMR would increase. The presence of Ag^+ ions influences the nucleation and growth of layers. On the other hand, silver can modify Co/Cu interfaces. In other words, silver improves magnetic properties by reducing lattice misfits between cobalt and copper. An increase in silver content above 1 at%, however, is followed by reduction of the GMR [40]. Addition of lead to these multilayer coatings reduces the GMR. Magnetic behavior of coatings changes from GMR to AMR with increase in Pb^+ concentration above 0.2% [20]. Introduction of polyethylene glycol (PEG) to the electroplating bath of NiFe/Cu multilayer coatings increases the MR. Coercivity is decreased on addition of the PEG as it causes reduction of the crystallite size [249].

7.9. Hardness

A major application of hardness measurement is in quality control of metallic parts. Hardness is known as an important feature in materials that depends on strength, elastic and plastic properties. Hardness is often defined as the capability of a material to resist against scratch, wear, cutting and indentation. The higher the hardness of a material, the more resistant is against indentation. Hardenability is defined as the degree of hardness that materials obtain during a hardening process. There are many techniques proposed for measuring hardness of materials by means of various loading conditions. Some of the most prevailing hardness testing methods are Brinell test, Rockwell test, Vickers test, Knoop test, scleroscope and Mohs hardness. These processes vary in terms of test conditions and parameters and each may be used in

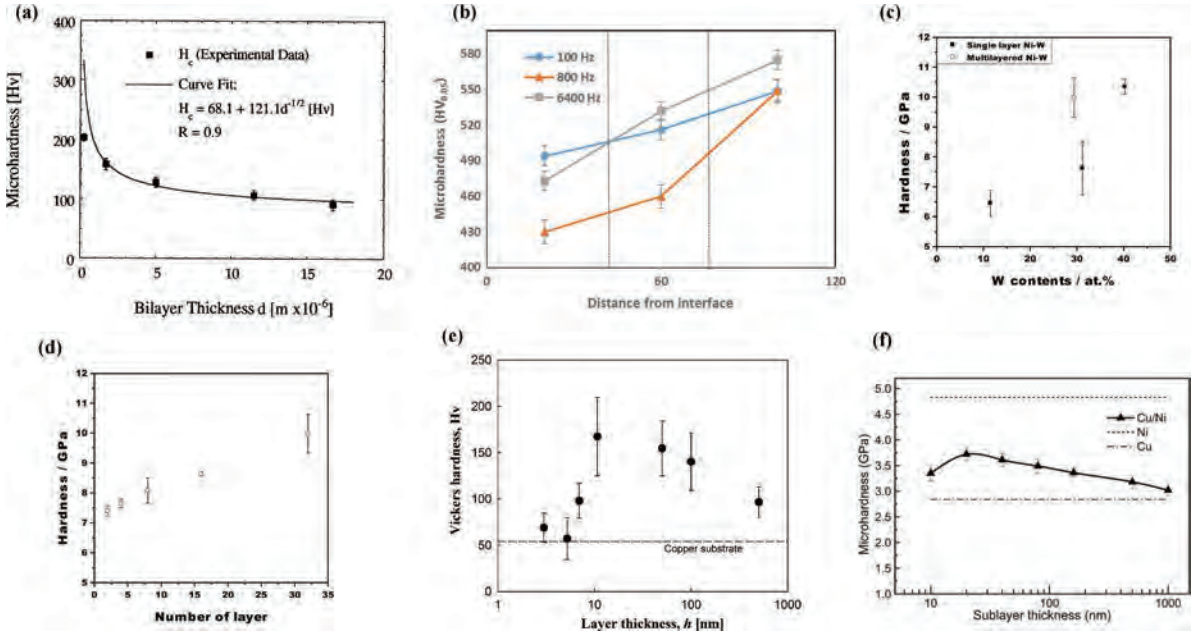

Fig. 37. Vickers microhardness of (a) Ni-30%Sn multilayer coatings in accordance with thickness of layers (d) [159] and (b) Ni-Fe-Al_2O_3 gradient coatings at different distances under the sublayer [36,199]. the effect of (c) tungsten content and (d) number of bilayers on the hardness of Ni-W multilayer coatings [27]. hardness of (e) Ni/Cu nano-scaled multilayer coatings versus thickness of layers [93], (f) Cu/Ni multilayer and copper and nickel monolithic coatings Hardness versus thickness of the sublayer [83].

accordance to the requirements desired by the researcher. For instance, Mohs hardness is based on the ability of material to scratch another material while scleroscope measures hardness based on return of the hammer after impact with sample surface. Broad usage of hardness tests is because of the easy correlation between hardness test results and tensile/yield strength of steels. Many metals and alloys have been subjected to hardness and microhardness testing leading to acquirement of a great deal of findings. In the present work, hardness of different multilayer coatings electrodeposited under various conditions is studied. Wang and Singh [159] investigated the mechanical properties (including microhardness) in Ni/Sn multilayer coatings. According to Fig. 37 (a), an increase in the thickness of bilayers led to a reduction of the Vickers microhardness in Ni-30%Sn multilayer coatings. Microhardness of pure nickel and tin coatings were 274.2 Hv and 7.5 Hv, respectively; while, the maximum hardness value for the alloyed coatings was 203 Hv. Fig. 37 also shows the Hall-Petch equation which represents hardness values based on different thicknesses (d) with a correlation coefficient (R) of 0.9 [159]. Panayotova [250] investigated the effects of different parameters such as additives contents (succinic acid, asparaginic, ascorbic acid), temperature, pH and current density on microhardness of Fe-C multilayer coatings. The optimum conditions to reach maximum hardness (600-710 Hv) and the best wear and corrosion resistance are pH = 3, $T = 45\ ^{\circ}C$ and current density = 35 mA. cm^{-2} in a bath containing succinic acid or a mixture of succinic acid and ascorbic acid [250].

Due to the increasing advances in nickel-based alloys, particularly Ni-W, in terms of mechanical properties, researchers studied the properties of Ni-P-W multilayer coatings. These coatings were produced through pulse electroplating procedure where wavelength ranged from 8 to 4000 nm. It was reported that hardness increased with gradual reduction of the wavelength. Increase in hardness was even more considerable under 120 nm. The amorphous coatings were compared with the similar crystalline coatings which showed the same increasing trend for hardness. The only difference was that the maximum hardness within the 2 to 5 nm range in crystalline coatings that was 30% higher than the other wavelength. In amorphous coatings, the wavelength of 8 nm gave the maximum hardness about 13% above other wavelengths. The hardness of the above coatings does not follow the Hall-Petch equation [45]. Ni-W multilayer coatings showed relatively higher hardness than Ni-W monolithic coatings. It may be seen in Fig. 37 that number of layers and tungsten content affects hardness of these multilayer coatings. Hardness is found to improve with increase in number of bilayers [27,60]. It also increases with increase in electroplating current density, tungsten content and thickness of layers. Ni-W gradient coatings which are produced via low duty cycles or high frequencies demonstrate higher hardness values due to having high content of alumina nanoparticles and tungsten. Ni-Cu-W-Al_2O_3 gradient coatings which are produced via high duty cycles and frequencies have high microhardness values. Being deposited under a constant frequency, the zones in coating near substrate shows a higher hardness that the top surface of coating. Tungsten and nickel contents near the surface are lower than near the substrate [201].

Presence of Al_2O_3 nanoparticles in Ni-Fe multilayer coatings leads to decline of plastic deformation of the matrix metal, on the one hand, and prevention of grain growth and reduction of grain size, on the other hand. Hence, it improves hardness of the coatings [36]. As it may be seen in Fig. 37 (b), hardness is higher near the surface of Ni-Fe-Al_2O_3 coatings than near the coating/substrate interface. This is due to the higher Al_2O_3 nanoparticles content near the surface [36,199]. It was reported that presence of Mn in the gradient coating led to increase in hardness by 150 Hv. Like nanoparticles, presence of manganese improves microhardness. Increase in duty cycle leads to increase in manganese content, in one hand, and reduction of alumina content, on the other hand, leaving no significant impact on microhardness [48]. Nucleation rate increase at high frequencies so more nanoparticles are incorporated into the coating. Hence, high frequencies lead to formation coatings with high hardness values [61]. Decrease in thickness of the sublayer in Ni-Fe multilayer coatings leads to increase in the hardness [251].

Decrease in thickness of layers in Ni/Cu nano-sized multilayer coatings leads to increase in hardness in Fig. 37 (e). This may be justified using the Hall-Petch equation as thickness of layers is equivalent with the average grain size. Hardness decreases, however, with further decrease in thickness after the first peak. Non-compliance of the Hall-

Petch equation in small thicknesses is attributed to lamellar slip mechanism. When the thickness is lowered below 100 nm, confined layer slip mechanism is activated so that hardness no longer follows the Hall-Petch equation. Therefore, hardness value smaller than that predicted value by the Hall-Petch equation is observed. It is believed that, within a thickness range of 10 to 100 nm, dislocation locking on a given plane is not possible due to the strong repulsive forces between dislocations on the same plane. The repulsive forces, therefore, lead to deformation with confined layer slip mechanism that includes propagation of dislocation loops parallel with the layer's interfaces [252,253].

As shown in Fig. 37 (f), that hardness plummeted when the layer thickness fell below 10 nm. This may be attributed to annihilation of the misfit dislocation lattice which preserves the interface against shearing dislocations. It was also declared in literature that hardness does not alter with further decrease in thickness [254]. It was stated, elsewhere, that brush plated Cu/Ni multilayer coatings had a lower hardness than nickel but higher than copper. Hardness gradually increases with decrease in thickness of the sublayer. On the other hand, increase in the interface density between layers led to increase in hardness. This was achieved by reduction of wavelength modulus or decrease in thickness of the sublayer [83].

Hardness of composite nickel-copper multilayer coatings increased with decrease in thickness of layers and increase in the interfaces. Hardness of copper films was lower than nickel. It was also observed that hardness of the composite multilayer coatings was higher than the same coating with an extra copper content. Increase in thickness of nickel layers and decrease in thickness of copper layers led to increase in hardness of the multilayer coating so that it even surpassed nickel. Hardness of Cr/Ni multilayer coating was improved with heat treatment and increase in temperature. Phase analysis through XRD revealed that increase in hardness was obtained due to formation of a diamond structure at high temperatures. The highest hardness value was obtained at 550 °C due to the presence of fine crystallites in the multilayer coating. Note that nucleation in chromium layers occurred in a dense form with no preferential orientation towards the nickel interfaces. The surface energy between nickel and chromium was insufficient to provide the required energy for nucleation [255]. Increase in thickness of layers led to improvement of hardness in both multilayer and monolithic nickel coatings. Due to finer grains and the layered structure, the multilayer coating featured a higher hardness than monolithic films. A small grain size leads to dislocation pile-up that in turn, increases the yield stress. On the other hand, the difference in elastic modulus and grain size of interfaces is in fact a barrier for dislocation movement that increases hardness of multilayer coatings higher than monolithic coatings. This phenomenon cannot be clearly explained; however, according to Koehler's theory, hardness improvement is obtained through the differences occurred in values of Young's modulus of layers. That said, we have seen no difference between Young's modulus values of layers in the present work. Thus, this might be the reason for the lower hardness of multilayer coating than monolithic films [130]. The hardness of the Co/Cu multilayer coating was higher than Ni/Cu multilayer coating for the same layer thickness. Hardness of Co/Cu multilayer coatings gradually decreases with increase in the annealing temperature. However, further increase in temperature leads to increase in hardness. Excessive temperature increase eventually removes the interfaces between layers causing the hardness to fall again. Annealing diminishes the hardness of Ni/Cu multilayer coating more quickly than Co/Cu multilayer coatings [81].

Hong et al. [256] produced printed circuit board (PCB) copper bump micro-sized multilayer coatings by means of reverse pulse electrodeposition technique. They investigated the effects of forward-to-reverse current ratio and brightener concentration in the bath on hardness values. It was reported that the maximum hardness was achieved in a current ratio of 1:1 (forward/reverse) and brightener concentration of 700 ppm. An increase in brightener concentration improves hardness by refining the copper grain size. An excessive concentration of brightener causes diffusion of sulfur atoms through the copper crystallites and consequently reduction of copper density. It is assumed that reduction of hardness is led by formation of copper sulfide over the cathode surface. In addition, surface roughness and grain size were improved by increase in reverse pulse current density; while, it reduces hardness and copper density in the coating [256]. In addition to multilayer coatings, hardness of gradient electrodeposited metals such as nickel has been studied. For instance, gradient increase in SiC content towards the surface as well as increase in thickness of the coating improved hardness of Ni/SiC coatings by 700 Hv. Increase in ZrO_2 content in Ni/ZrO_2 composite multilayer coatings improved microhardness from the substrate interface towards the surface. This may be attributed to the gradient in deposited ZrO_2 particles and reduction of Ni grain size in the matrix [257]. It should be noted that hardness values of electrodeposited coatings are commonly lower than PVD and CVD coatings. That is, further research and analysis is required to minimize the existing difference and even obtain harder coatings at lower costs in specific cases.

7.10. Corrosion resistance

Corrosion means a metal degradation due to reactions with its surrounding medium. The most common media for corrosion are aqueous solutions. There is often a thin, aqueous film on the surface in atmospheric corrosion. Corrosion of metals has been paid a great deal of attention for a long time. Protective methods such as hard chromium electroplating have been employed in order to preserve the substrate against corrosive attacks. Corrosion of electroplated coatings is studied by means of various analytical approaches. The most common techniques to investigate corrosion of electroplated coatings include direct current polarization methods and electrochemical impedance spectroscopy (EIS). Polarization is the resistance against an electrical current. For an electrochemical reaction controlled by activation, polarization curves are linear in a coordinate plane where E is plotted versus $\log(j)$. Corrosion potential (E_{corr}) may be found by extrapolation of slopes of cathodic and anodic curves. In addition, the intersection point represents corrosion current density (j_{corr}) or corrosion rate. EIS is a powerful tool in study of corrosion (corrosion rate determination, passive layers investigation, performance of corrosion inhibitors and determination of electrochemical reactions mechanism) in various electrochemical systems. Electrical impedance, or simply stated as impedance, is the resistance against an alternative sinusoidal current. There is no difference between resistance and impedance in direct current as the former may be described as impedance at zero-degree phase. This technique includes application of a slight potential over a given amount of time, measurement of the exchanging current density and determination of system impedance and phase. In an EIS analysis, system impedance (Z) and the angle between impedance and the applied potential are calculated as functions of the applied frequency. Increase in corrosion resistance is one of the major aims of manufacturing of electroplated coatings. Nickel-, chromium- and zinc-based coatings are amongst the most common products on the market which are used for corrosion prohibition. Corrosion studies on electroplated Ni-Cu multilayer coatings using polarization curves and electrochemical impedance revealed that these coatings had a much higher corrosion resistance than typical monolithic copper films [258]. The best corrosion performance was observed with a nickel film once compared with chromium and Ni(20 nm)/Cu(20 nm) multilayer coatings. The inferior performance of chromium was attributed to the grid of cracks that facilitates penetration of solution throughout the coating. Presence of cracks (in a smaller extent) in the multilayer coating also contributed to its lower corrosion performance than the nickel film. In addition, introduction of copper and nickel to cobalt during the electroplating process led to improvement of corrosion properties. It may be observed in Fig. 38 that corrosion was significantly reduced with increase in thickness of the Ni layer from 20 to 50 nm. Improvement of corrosion resistance was due to decrease in porosities and crystallite grain boundaries. However, further increase in thickness

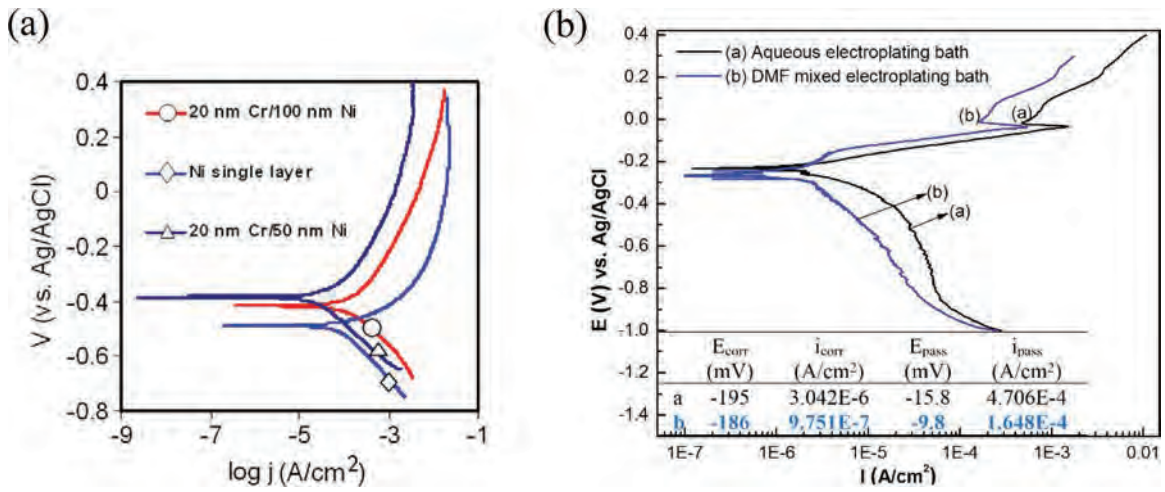

Fig. 38. Polarization curves of (a) Ni, Ni (50 nm)/Cr and Ni (100 nm)/Cr coatings in 0.1 M sulfuric acid solution [55] and (b) coatings obtained in aqueous and DMF baths [167].

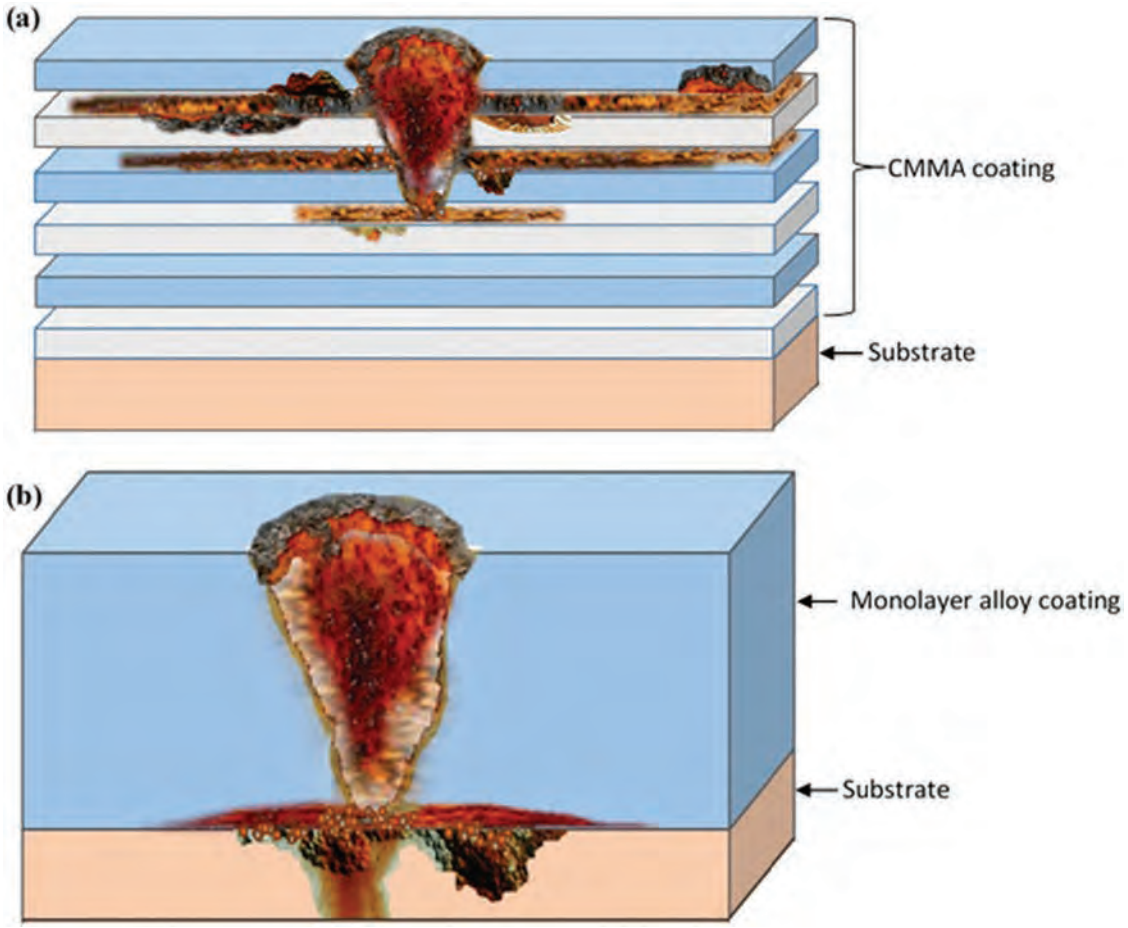

Fig. 39. Corrosion schematics for (a) multilayer and (b) monolithic alloy single layer coatings [26].

up to 100 nm led to deterioration of corrosion resistance. Corrosion behavior of Ni(100 nm)/Cr multilayer coatings is similar to nickel monolithic films because of the lower number of internal layers and more nickel layers [55].

The effect of electroplating bath on corrosion behavior of Ni-Cr multilayer coatings has been investigated. In addition to the aqueous bath, a mixed dimethylformamide (DMF) bath was used. Fig. 38 (b) shows that the coating deposited in the DMF bath had higher corrosion resistance than the coating produced in the aqueous bath. This was justified by the fact that more hydrogen entered in the coating surface in the aqueous bath leading to formation of residual stresses and cracks which act as conveying channels for penetration of chloride ions towards the substrate. The DMF deposited coating, however, did not show any of these cracks so that corrosion behavior was improved. It may be

observed that the passive behavior was not complete and corrosion current density rose as soon as passivity was obtained. This is attributable to an incomplete passive layer [167].

Introduction of iron to Ni/Cr multilayer coatings was observed to improve corrosion resistance in comparison with monolithic and non-alloy coatings. It has been revealed in pulse electroplated Ni/Fe/Cr multilayer coatings that chromium content increased with increase in duty cycle. High chromium content contributes to formation of microcracks that would eventually diminish the corrosion resistance. Chemical composition of layers, density of microcracks and structural differences lead to diversion of cracks on interfaces. In result, corrosion products accumulate in the region and cause delamination of the uppermost layer of coating [49].

It has been shown that number of layers is effective in corrosion resistance of Ni-W multilayer coatings so that corrosion behavior constantly improved with increase in the number of layers up to 300. Further increase in number of layers, however, led to deterioration of corrosion resistance. This is due to the inter-layer diffusion behavior. Increase in number of layers basically increases the required time for diffusion of the corrosive agent. Hence, corrosion resistance is better than bulk materials or monolithic coatings. On the other hand, a multilayer structure increases the interface so that the corrosive agent has to move in various directions and within the interfaces. Such behavior is demonstrated in Fig. 39 [26].

Allahyarzadeh et al. [60] studied the effect of presence of nanoparticles in electroplated Ni-W coatings. It was reported that corrosion resistance of Ni-W coated samples may be lower than pure nickel films if no nanoparticles were introduced to the multilayer coating [60]. Essentially acting as barriers, nanoparticles restrain diffusion of corrosive agents and consequently improve corrosion resistance [36,199]. Mohajeri et al. [259] used direct, pulse and reverse pulse current techniques in manufacturing of nickel-titania/titania multilayer coatings and studied their corrosion behavior in sulfuric acid and sodium chloride solutions. In the sodium chloride solution, the best corrosion resistance was featured by Ni-Ti monolithic alloy single layer coatings produced by reverse pulse technique that had a lower corrosion current than coatings deposited by pulse and direct currents. However, the pulsed current electroplated Ni-TiO_2 multilayer coating had a better corrosion behavior due to contribution of titania nanoparticles in the coating. In fact, preferential corrosion sites are filled by titania nanoparticles. Nanoparticles prevent dissolution of preferential sites and reduce the grain size. Although it is expected that corrosion becomes harsh with increase in grain boundaries, presence of nanoparticles leads to formation of many microcells on the coating that reduce grain size and anode-to-cathode ratio, leading to reduction of corrosion. Similar results were observed in the sulfuric acid solution where a passive layer covered the surface and nanoparticles hindered formation of a continuous nickel oxide film which is why the corrosion current in the coating with titania nanoparticles was higher than electroplated pure Ni coatings [259]. It was observed that frequency and duty cycle did not impose considerable effects on corrosion behavior of Ni-Fe-alumina multilayer coatings. In fact, potential moved towards noble values under a constant duty cycle and variable frequency. This is mainly due to formation of the passive layer [36]. It was stated, elsewhere, that presence of alumina nanoparticles in Ni-W-alumina multilayer coatings led the corrosion potential towards noble values. In addition, corrosion resistance of coatings produced at low frequencies was high as high frequencies lead to grain refinement which, in turn, raises the corrosion rate through increase in grain boundaries. Alumina nanoparticles presence is bolder under low duty cycles so that corrosion potential becomes noble [34]. Increase in frequency reduced corrosion resistance of Ni/Fe/Mn (alumina) multilayer coatings by adversely affecting the grain size [48]. Corrosion resistance was improved by ultrasonic assisted electrodeposition of copper multilayer coatings. In fact, corrosion resistance of these coatings surpassed that of typically electroplated copper coatings. Corrosion potential increased while corrosion current was significantly diminished. Under the same period of time, weight loss of the ultrasonic sample was half that of the typical coating [113]. Corrosion properties of Al/Zn and Al/Zn/Zr multilayer coatings have been investigated. According to immersion tests results, the maximum protection period for monolithic single-layer coatings was 49 days. However, multilayer coatings provided minimum and maximum protection periods of 51 and 69 days, respectively [260]. Corrosion resistance of Zn/Cr multilayer coatings was 40 times higher than monolithic single-layer coatings of the same substance. Increase in corrosion resistance was attributed to the Cr content variation in layers. It is believed that layers containing high Cr contents provided protection against corrosion. Corrosion performance of Co-Sn coatings in a 3.5 wt% NaCl solution was studied. It was observed that corrosion behavior improved with decrease in cobalt content. Corrosion potential of coatings electroplated at negative potentials moved towards noble values. The difference in corrosion potentials from one layer to another, due to formation of a dense coating, is very important in protection of the substrate. The Co/Sn coating had a more noble corrosion potential than iron, indicating that few porosities existed over the surface. Alloy and composite Ni/Zn multilayer coatings are also reported to provide significant corrosion resistance. There have been many studies conducted on electroplating and characterization of corrosion behavior of Ni/Zn multilayer coatings. These coatings are usually deposited on steel substrates with various thicknesses (for the whole coating or each layer) and chemical compositions. Corrosion resistance was evaluated through electrochemical experiments. It was revealed that Ni-Zn multilayer coatings are better than nickel or zinc monolithic single-layer films in terms of corrosion resistance [261,262]. Although Ni/Zn multilayer coatings feature desirable corrosion properties and may replace cadmium coatings [263, 264], their protective capabilities may be improved even further by replacement of the zinc layer with either Zn-Fe/Zn or Zn/Zn-Fe layers since zinc may more effectively fulfill its sacrificial role when it is adjacent to iron [265]. It may be concluded that, under the same conditions, the best corrosion resistance of Ni/Ni-Zn is obtained once the uppermost layer is made of Ni-Zn due to sacrificial properties of zinc [266]. Introduction of phosphorus to the nickel layer in Ni-Zn multilayer coatings may improve corrosion resistance of multilayer coatings owing to the inhibition effect on white rust forming [267]. According to a wide range of experiments, including cyclic voltammetry in chloride and sulfate solutions, electrochemical analysis and salt-spray tests in a 5 wt.% NaCl solution, corrosion resistance improved with increase in nickel content. Electrochemical analysis and slat-spray tests showed that the coating with 20 wt.% Ni had excellent corrosion properties as the red rust of zinc appeared on surface after 48 h. In addition, increase in number of layers (or reduction of thickness of layers while the whole thickness remained constant) improved corrosion resistance [261,266]. Electrochemical impedance tests revealed that Ni/Zn multilayer coatings provided better protection for steel substrates than monolithic single-layer coatings. It was shown that multilayer coatings had lower Warburg admittance over a long duration in comparison with monolithic single-layer coatings. That is, corrosive agents penetrated towards the depth by a small extent. In addition, reduction of Warburg admittance over time in Ni/Zn multilayer coatings proved that corrosive agents could not deeply penetrate into the coating. This is probably due to filling of porosities by corrosion products. Note that this phenomenon was not observed with the monolithic single-layer coating; hence, there may be other parameters involved. Polarization test results indicate that the passive layer formed on Ni/Zn multilayer coatings in the anodic polarization lead to reduction of corrosion rate. However, the anodic branch of the zinc monolithic single-layer coating did not possess such characteristics and corrosion processes actively occurred in anodic zones. The passive layer formation may be justified by accelerated corrosion of zinc in adjacent with nickel and increase in pH due to escalation of cathodic reactions over the surface. Rahsepar and Bahrololoom [261] stated that a larger number of layers (achieved by a reduction of layer thickness) leads to a smaller grain size in Ni/Zn multilayer coatings. Hence, a larger number

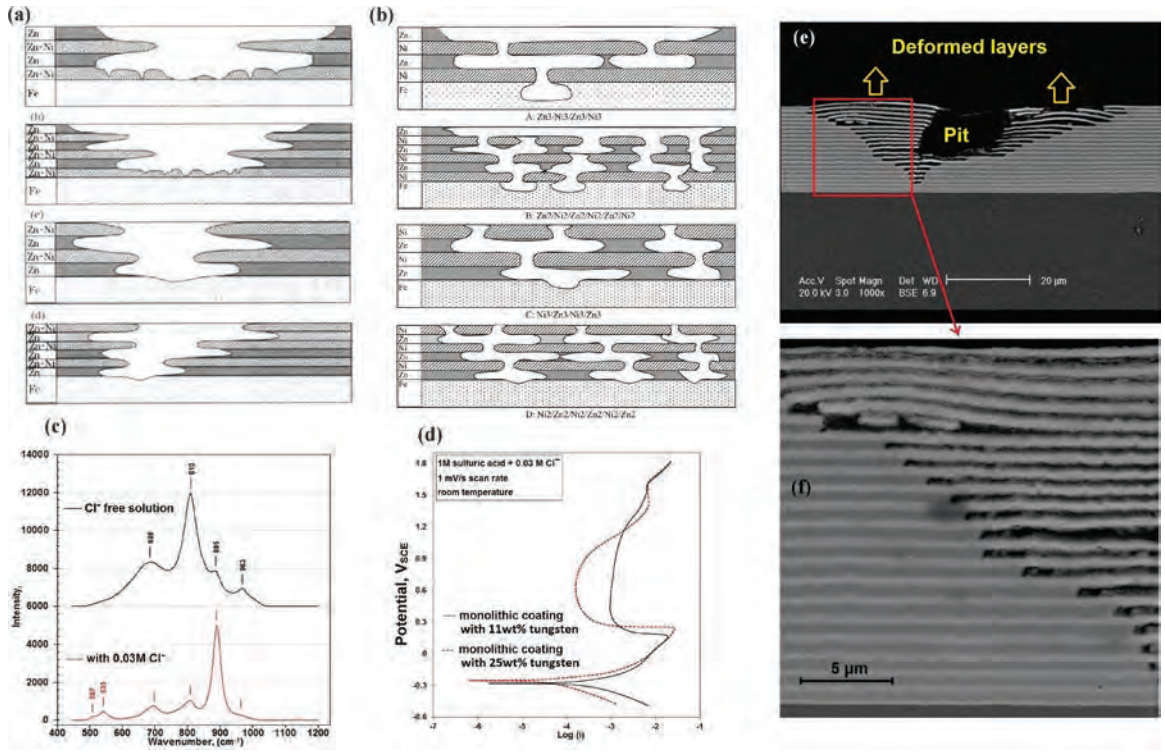

Fig. 40. Schematic illustration of corrosion mechanism in (a) Zn/Ni-Zn [266] and (b) Zn/Ni [268] multilayer coatings, (c) Raman spectroscopy for analysis and comparison of corrosion products over the corroded surface of Ni-W multilayer coatings in 1 M sulfuric acid solutions with/without chloride. (d) Polarization curves of monolithic layers with 11 wt.% W and 25 wt.% W, produced by a 10 and 90% duty cycle of pulsed current in a 1 M sulfuric acid solution containing (0.03 M) chloride ions at 25 °C (e) and (f) Backscattered electron micrographs of cross sections of Ni-W multilayer coatings after the corrosion test at two magnifications [14].

of layers (or reduction of thickness) is not always followed by improvement of corrosion resistance in saline media. In fact, corrosion resistance begins to fall after an optimum number of layers. However, a larger number of layers significantly reduced the passivation current and consumption of electrons in anodic branches of polarization curves. The corrosion mechanism in Ni/Zn and Ni/Ni-Zn coatings may vary depending on whether the zinc-containing layer is the uppermost layer or not. Generally, formation of a barrier layer may reduce anodic dissolution rate when corrosion is controlled by anodic reactions and dezincification. As it is schematically illustrated in Fig 40 (a,b), corrosion process continues after dissolution of the zinc sublayer and involves the underlying Ni-Zn or Ni layer. Due to the higher corrosion resistance of Ni-Zn layer, the underlying zinc layers undergo corrosion once reached by corrosive agents through pores and microcracks. When the uppermost layer is nickel or nickel-zinc, the underlying zinc layers are affected by corrosion via penetration of attacking agents [266,268]. The processes are shown in Fig. 40.

The simultaneous effect of multilayer structure and nanoparticles in Ni-Zn-SiO_2 multilayer coatings has been studied. It was revealed that producing multilayer structure and incorporating of nanoparticles may lead to desirable effects on protection against corrosion. The corrosion resistance of the Ni-Zn-SiO_2 multilayer coating was 10^7 times greater than the same monolithic single-layer film. In addition, corrosion resistance of the monolithic single-layer with nanoparticles was 1.5 times greater than the same with no nanoparticles [262]. It may be concluded that the effect of multilayer structure in improvement of corrosion resistance is greater than that of nanoparticles. Presence of alumina nanoparticles in Ni-Zn multilayer coatings led to improvement of corrosion resistance in chloride solutions. It was stated that increase in number of layers (or interfaces) of nanocomposite Ni-Zn-Al_2O_3 multilayer coatings improved anti-corrosion properties [269,270]. Corrosion mechanisms in multilayer coatings have been studied by Allahyarzadeh et al. [14]. According to Raman spectroscopy studies Fig. 40 (c) and the corroded cross sections in Fig. 40 (e,f), preferential corrosion of nickel in Ni-rich layers was the main parameter controlling the corrosion mechanism. SEM micrographs of corroded cross sections of Ni-W multilayer coatings. Fig. 40 (e,f) show that the corrosive solution passed through the Ni-rich layers (after preferential solution of nickel) but could not reach the underlying substrate. However, Elias and Chitharanjan Hegde [26] and Shourgeshty et al. [270] had previously expressed that it is the expansion of corrosive agents through consecutive interfaces that improves corrosion resistance in Ni-W and Ni-Zn multilayer coatings, respectively. Similar results were obtained in Ni-W multilayers in sulfuric acid media in other research [271]. A study of corroded cross sections of multilayer coatings (especially in presence of chloride ions) revealed that mechanistic corrosion studies cannot be completed without considering the galvanic effect between layers in Fig. 40 (d). In fact, Ni-rich layers act as sacrificial anode for W-rich layers and improve corrosion resistance by preferential dissolution. In addition, accumulation of corrosion products is another important matter in corrosion of multilayer coatings. Three major parameters affect corrosion behavior of multilayer coatings: 1) multilayer structure and penetration and expansion of the corrosive medium among layers, 2) the galvanic effect between layers and 3) destruction of layers due to accumulation of corrosive products Figs. 15 and 16.

8. Technological developments

In recent decades, a number of scientific and technology enterprises have focused on advancing the knowledge of nanostructure electrodeposited multilayer coatings with superior functional properties. The concepts discussed earlier have been used to develop specific coatings. For example, the Xtalic Corporation has developed a coating under the trade name Xtalic Xbright^{TM}, to serve as an alternative to the mainstream chromium coatings. This proprietary coating is a tailored metallic nanostructured Ni-W alloy [3] comprising of 11 alternating

Fig. 41. Haulage truck bumpers coated with a Ni-W multilayer coating, which are claimed to have double the lifetime of conventional hard chromium coatings.

Fig. 42. Potential applications of multilayer electrodeposited coatings for various industrial components, indicating the number of layers, their thickness and improved properties compared to monolithic layers.

high and low W concentration layers for different assets, namely truck bumpers (see Fig. 41). This application required a high level of mechanical ballistic impact resistance, as the bumper was exposed to a barrage of rocks and road debris which could impact its surface. The multilayered coatings were discovered to extend the lifetime of the bumper for about twice as long. The enhanced performance is attributed to the many redundant layers which involve many interfaces, and the elastic absorbing nature of variable acoustic impedance between the layers. The wear resistance of such multilayer Ni-W coating, which is produced *in-situ* by altering the periodic pulse reverse waveform, is

about ten orders of magnitude higher than conventional hard chromium coatings together with improved corrosion resistance. The higher cathodic current efficiency of this coating in comparison with the hard chromium electroplating is important in minimizing energy losses and avoiding electrolyte mist. The bath used in this coating is less toxic and environmentally hazardous than chromic acid baths used in traditional chromium electroplating [272].

Monolithic layers were conventionally electroplated on different industrial equipment and tools, owing mainly to their mechanical properties, hardness, corrosion resistance, such as the surface of industrial shafts, cylinders, and pistons, cutting tools, engraving rollers, textile rollers, ball valves, dental and medical tools, injection screws, gun grooves, roll and ball bearings, car wheels, engine valves, crankshafts, pulley, gears, etc. Nowadays, with improved technology, it is possible to replace old and conventional electroplated coatings with novel micro/nanostructured electrodeposited multilayer coatings (Fig. 42). In each case, the surface coatings with different multilayers can be successfully applied on specified equipment, considering its mission, with intended properties as well as sustaining the environmental concerns. For instance, cutting tools can be supplied with Ni-W multilayers with superior hardness, gun grooves can be upgraded with multilayer Ni-P coatings, injection screws can be electrodeposited with Ni-Co multilayers.

In addition to providing coatings for low temperature applications, electrodeposited layered structures are being used as high temperature coatings. For example, high temperature aluminide coatings modified by Pt/Pd and Pt/Ru layers were electroplated on nickel-based super alloy prior to pack cementation. Such coatings were reported to show superior resistance to cyclic oxidation and a less rumpled surface [273].

A major success of electrodeposited multilayers has been the development of measurement technologies and magnetic field sensors used in a wide range of measuring devices. In particular, higher measurement resolution and superior magnetic properties are of wide interest; giant magneto-resistive films of Cu/Co multilayers have been developed. Sensors manufactured by such multilayers offer advantages such as small size, low cost, the capability of integration with signal processing circuits and contributions to the advent of wearable electronic devices.

Regarding the mechanical behavior of multilayers, especially fracture toughness and durability/load-bearing capabilities, the ceramic-based multilayers coatings, such as TiN and TiC, fabricated using CVD and PCD processes, are well-known to materials and mechanical engineers and scientists due to their outstanding properties. In ceramic coatings, multilayer structures have been deployed to upgrade the toughness/fracture toughness through the crack deflection at the interfaces between layers as well as crack tip blunting due to nanoplasticity at the interface. The layer thickness, number of layers, and also the multilayer system are effective parameters that independently influence the coating toughness/fracture toughness. Cutting tools technology is one of the most common applications of these coatings due to their wear resistance and toughness [274–277]. It is possible to develop metallic, alloy, and micro/nanocomposite electrodeposited coatings with layered structures through dynamic nanostructure control (DNC). In addition to corrosion resistant, magnetic, and decorative films with superior wear resistance, outstanding load-bearing capabilities, as well as excellent toughness can be achieved for industries such as cutting tool technologies.

9. Summary

In this review we have discussed a wide range of examples of functional materials, connected by the general configuration of a layered structure, on a nanomtre scale in many cases. While multilayers have been first grown by physical and vapour deposition methods, electrodeposition over the years has been used extensively, due to its simplicity and moderate operational costs. Another feature of electrodeposition is ability to control the finished quality of the final coating. The wide opportunities to control electroplating conditions will provide an arena capable to generate a variety of useful multifunctionality. Several points may be summarised:

1 Multilayer electrodeposition can be traced back to a patent involving Cu-Ni multilayers in 1905 but continues to grow and diversify.
2 Early studies of multilayer deposits were often motivated by the possibility of producing higher tensile strength and ductility; modern endeavours tend to focus on the promise of particular electronic, magnetic or optical properties, better corrosion protection or modified tribological surfaces.
3 Earlier studies also tended to consider different metals then compositionally modulated alloy compositions; diversification now includes particle-metal matrix composites.
4 The choice of a single or dual electroplating bath is well established since a single bath has simplicity, facile processing and ease of scale-up. Differences between adjacent layers may be induced by step changes in electrode potential, current density, pulsed current parameters or operational variables including agitation or electrode movement.
5 While multi-layered electrodeposits remain specialised, their use has diversified to industries ranging from speciality electronic materials to engineering coatings experiencing arduous tribological service and aerospace.
6 Progress in multi-layered electrodeposition has incorporated current trends in electroplating research, including self-assembled layers and the use of deep eutectic solvents for electrolytes.
7 Some of the literature on electrodeposited multilayers is poorly documented. Substrate material and geometry, the composition of layers, their thickness, the number of layers, the thickness of any separating layer, the microstructure and phase composition of layers should always be specified as well as the total deposit thickness.

Further research and development

Several aspects require particular attention in laboratory research and industrial development.

Comparison of coating techniques

1. A systematic study of multilayer coatings from liquid electrolytes and a comparison of deposit properties with vapour deposition techniques is overdue to stimulate progress in electrodeposited multilayer processing.

Electrochemical aspects

2. Electrode kinetics data essential to an improved understanding of multilayer deposition, such as polarisation and current vs. time behaviour, are missing in many reports.

3. The effect of bath additives on the morphology, phase composition and continued nucleation/growth of successive layers.

Deposit characterisation

4. Continued diversity of coating materials, e.g., doped ceramic, conductive polymer and polymer-metal or ceramic-metal composite multilayers by appropriate anodic and/or cathodic electrodeposition.

5. Despite through-porosity being a particular problem in thin coatings and those used in corrosion protection but a systematic, quantitative treatment of porosity measurements in multilayer deposits does not exist.

6. Combinations of materials alternately deposited cathodically or anodically, coupled with a degree of control over their nanostructure and porosity, even from a single bath, opens the door to many coating materials and architectures. The possibility of using open-circuit,

including electroless deposition and other application techniques, such as sol-gel and electrophoresis, markedly increases coating diversity and applications.

Substrate surface condition

7. Pretreatment of the substrate has become increasingly important in early nucleation and growth to achieve ever thinner coatings, faster layer deposition and multiple, but well-defined, successive layers.

Future coatings

8. Electrodeposition is increasingly competing with vacuum deposition methods for deposition of multilayered biomaterials, including hydroxyapatite.

9. Improved diversity of fabrication together with fine control over operating conditions can be used to realise more complex surfaces and even complete devices (possibly for MEMS applications) via electrodeposition of multilayers, possibly in combination with electrochemical surface finishing-assisted 3D printing.

10. Many modern materials demand high purity or fine control of dopant levels together with tailored morphology, elemental/phase composition and nanostructure. Examples include semiconductors, speciality electrocatalysts, magnetic and optical materials.

Process control

11. To electrodeposit engineered multilayers of such materials, it seems likely that bath additives will be limited and electrolyte flow/agitation conditions, as well as pulsed waveform parameters, will need careful tuning. Such stringent control of operating conditions is poorly met by traditional processing in open-topped, rectangular cross-section vats. Instead, tailored ultrasonic transducers, electrolyte flow tube (eductor) networks or controlled flow past planar cathodes in rectangular channel cells may be needed.

12. Digital control of operational parameters and computational modelling of multilayer electrodeposition will be important activities in achieving a suitable reaction environment at the cathode surface.

13. Increasingly stringent legislation and rising environmental concern are likely to restrict the choice of bath additives for multilayered electrodeposition. This seems likely to provide a stronger focus on additive-free electrolytes, closer control over operational conditions and more consideration of the mode of current control.

Declaration of Competing Interest

The authors declare that they have no known competing financial interests or personal relationships that could have appeared to influence the work reported in this paper.

Acknowledgment

M. Aliofkhazraei would like to thank Dr. H. Alimadadi for his comments during preparation of the initial draft of this paper.

References

[1] A. Haseeb, B. Blanpain, G. Wouters, J.P. Celis, J. Roos, Electrochemical deposition: a method for the production of artificially structured materials, Mater. Sci. Eng. A 168 (1993) 137–140.
[2] M. Allahyarzadeh, M. Aliofkhazraei, A.S. Rouhaghdam, V. Torabinejad, Electrochemical tailoring of ternary Ni-W-Co(Al_2O_3) nanocomposite using pulse reverse technique, J. Alloys Compd. 705 (2017) 788–800.
[3] A.J. Detor, C.A. Schuh, Tailoring and patterning the grain size of nanocrystalline alloys, Acta Mater. 55 (2007) 371–379.
[4] T.J. Rupert, C.A. Schuh, Sliding wear of nanocrystalline Ni–W: structural evolution and the apparent breakdown of Archard scaling, Acta Mater. 58 (2010) 4137–4148.
[5] A. Kanthiah, E.I. Manimaran, R. Pactulingam, Microstructural and magnetic properties of cadmium incorporated magnetic alloys as monolayer and multilayer coatings, J. Mate. Sci. Mater. Electron. 31 (2020) 19332–19342.
[6] S. Zsurzsa, L. Péter, L.F. Kiss, I. Bakonyi, Magnetic and magnetoresistance studies of nanometric electrodeposited Co films and Co/Cu layered structures: Influence of magnetic layer thickness, J. Magn. Magn. Mater. 421 (2017) 194–206.
[7] J.S. Koehler, Attempt to design a strong solid, Phys. Rev. B 2 (1970) 547–551.
[8] E. Wilhelms, F. Dehchar, R. Jordberg, M. Kjellberg, J. Stjärnesund, P. Söderbäck, Electrochemical deposition of multi-and single layer coatings: a study of hardness, wear and corrosion resistance for different electrodeposited, (2015) Uppsala Universitet.
[9] Q. Ye, Q. Fu, F. Lei, S. Yang, Analysis of electric explosion performance of Ni/Cu multilayer foil, propellants, Explos. Pyrotech. 45 (2020) 1436–1442.
[10] S. Hertel, K. Vogel, M. Wiemer, T. Otto, Electroplating of Pd/Sn multilayers for reactive bonding in packaging and assembly applications, in: Proceedings of the 2020 IEEE 8th Electronics System-Integration Technology Conference (ESTC), IEEE, 2020.
[11] K.R. Pirota, M. Vazquez, Arrays of electroplated multilayered Co/Cu nanowires with controlled magnetic anisotropy, Adv. Eng. Mater. 7 (2005) 1111–1113.
[12] A.Z.M.S. Rahman, P.Y. Chia, A. Haseeb, Nanomechanical properties of intermetallic compounds formed in electrodeposited Cu/Sn and Cu/Ni/Sn multilayer interconnects, in: Proceedings of the 36th International Electronics Manufacturing Technology Conference, IEEE, 2014, pp. 1–4.
[13] M. Allahyarzadeh, M. Aliofkhazraei, A.S. Rouhaghdam, H. Alimadadi, V. Torabinejad, Mechanical properties and load bearing capability of nanocrystalline nickel-tungsten multilayered coatings, Surf. Coat. Technol. 386 (2020), 125472.
[14] M. Allahyarzadeh, M. Aliofkhazraei, A.S. Rouhaghdam, V. Torabinejad, H. Alimadadi, A. Ashrafi, Electrodeposition mechanism and corrosion behavior of multilayer nanocrystalline nickel-tungsten alloy, Electrochim. Acta 258 (2017) 883–899.
[15] S. Zhang, S. Kobayashi, Multilayering process of electrodeposited nanocrystalline iron–nickel alloys for further strengthening, J. Mater. Sci. 55 (2020) 5627–5638.
[16] W.Y. Chen, H.W. Chen, W.P. Li, J.C. Huang, H.S. Yu, J.G. Duh, S. Lan, T. Feng, Compositionally modulated microstructure in nano-layered Ni-P metallic glass composite coating prepared by electrodeposition, Surf. Coat. Technol. 389 (2020), 125636.
[17] M. Khadem, O.V. Penkov, H.K. Yang, D.E. Kim, Tribology of multilayer coatings for wear reduction: a review, Friction 5 (2017) 248–262.
[18] G.F. Wang, L.D. Shen, L.M. Dou, Z.J. Tian, Z.D. Liu, Research on preparation of multilayers by the multiple jet electrodeposition, Int. J. Electrochem. Sci. 9 (2014) 220–226.
[19] A. Karimzadeh, M. Aliofkhazraei, F.C. Walsh, A review of electrodeposited Ni-Co alloy and composite coatings: microstructure, properties and applications, Surf. Coat. Technol. 372 (2019) 463–498.
[20] M.J. Fesharaki, K. Neuróhr, L. Péter, Á. Révész, L. Pogány, G. Molnár, I. Bakonyi, Influence of Pb additive to the spacer layer on the structure and giant magnetoresistance of electrodeposited Co/Cu multilayers, J. Electrochem. Soc. 163 (2016) D485–D492.
[21] M. Schlesinger, M. Paunovic, Modern electroplating, John Wiley & Sons, 2011.
[22] M.H. Allahyarzadeh, M. Aliofkhazraei, A.R. Rezvanian, V. Torabinejad, A.R. S. Rouhaghdam, Ni-W electrodeposited coatings: characterization, properties and applications, Surf. Coat. Technol. 307 (2016) 978–1010.
[23] N.S. Nia, J. Creus, X. Feaugas, C. Savall, The effect of tungsten addition on metallurgical state and solute content in nanocrystalline electrodeposited nickel, J. Alloys Compd. 609 (2014) 296–301.
[24] S. Ruan, C.A. Schuh, Mesoscale structure and segregation in electrodeposited nanocrystalline alloys, Scr. Mater. 59 (2008) 1218–1221.
[25] H. Wang, S. Yao, S. Matsumura, Electrochemical preparation and characterization of Ni/SiC gradient deposit, J. Mater. Process. Technol. 145 (2004) 299–302.
[26] L. Elias, A. Chitharanjan Hegde, Electrodeposition of laminar coatings of Ni-W alloy and their corrosion behaviour, Surf. Coat. Technol. 283 (2015) 61–69.
[27] S. Lee, M. Choi, S. Park, H. Jung, B. Yoo, Mechanical properties of electrodeposited Ni-W ThinFilms with alternate W-rich and W-poor multilayers, Electrochim. Acta 153 (2015) 225–231.
[28] L. Péter, A. Cziráki, L. Pogány, Z. Kupay, I. Bakonyi, M. Uhlemann, M. Herrich, B. Arnold, T. Bauer, K. Wetzig, Microstructure and giant magnetoresistance of electrodeposited Co-Cu/Cu multilayers, J. Electrochem. Soc. 148 (2001) C168–C176.
[29] Q. Huang, D.P. Young, J.Y. Chan, J. Jiang, E.J. Podlaha, Electrodeposition of FeCoNiCu/Cu compositionally modulated multilayers, J. Electrochem. Soc. 149 (2002) C349–C354.
[30] Y. Peng, T. Cullis, G. Möbus, X. Xu, B. Inkson, Nanoscale characterization of CoPt/Pt multilayer nanowires, Nanotechnology 18 (2007), 485704.
[31] H.H. Lou, Y. Huang, Electroplating. Encyclopedia of Chemical Processing, Taylor and Francis, New York, 2006, pp. 839–848.
[32] D.S. Iyer, Electrodeposited nanoscale multilayers of Invar with copper, Thesis for the MS degree, Bangalore University, 2005, p. 153.
[33] D. Gupta, A.C. Nayak, D. Kaushik, R.K. Pandey, Investigation of Cu and Co multilayer deposition in aqueous ambient, J. Phys. Chem. Solids 66 (2005) 861–868.
[34] M.H. Allahyarzadeh, M. Aliofkhazraei, A.R.S. Rouhaghdam, V. Torabinejad, Electrodeposition of Ni-W-Al_2O_3 nanocomposite coating with functionally graded microstructure, J. Alloys Compd. 666 (2016) 217–226.

[35] M.A. Khazrayie, A.S.R. Aghdam, Characterization of Ni-W/MWCNT nanocomposite layers formed by pulsed electrochemical deposition, Prot. Metals Phys. Chem. Surf. 47 (2011) 63–67.
[36] V. Torabinejad, A.S. Rouhaghdam, M. Aliofkhazraei, M.H. Allahyarzadeh, Electrodeposition of Ni-Fe and Ni-Fe-(nano Al_2O_3) multilayer coatings, J. Alloys Compd. 657 (2016) 526–536.
[37] J.U. Cho, Q.X. Liu, J.H. Min, S.P. Ko, Y.K. Kim, Synthesis and magnetic anisotropy of multilayered Co/Cu nanowire array, J. Magn. Magn. Mater. 304 (2006) e213–e215.
[38] V.M. Fedosyuk, O.I. Kasyutich, N.N. Kozich, Electrodeposition and study of multilayered Co/Cu structures, J. Mater. Chem. 1 (1991) 795–797.
[39] Y. Ueda, T. Houga, H. Zaman, A. Yamada, Magnetoresistance effect of Co-Cu nanostructure prepared by electrodeposition method, J. Solid State Chem. 147 (1999) 274–280.
[40] K. Neuróhr, L. Péter, L. Pogány, D. Rafaja, A. Csik, K. Vad, G. Molnár, I. Bakonyia, Influence of Ag additive to the spacer layer on the structure and giant magnetoresistance of electrodeposited Co/Cu multilayers, J. Electrochem. Soc. 162 (2015) D331–D340.
[41] N. Rajasekaran, L. Pogány, Á. Révész, B. Tóth, S. Mohan, L. Péter, I. Bakonyi, Structure and giant magnetoresistance of electrodeposited Co/Cu multilayers prepared by two-pulse (G/P) and three-pulse (G/P/G) plating, J. Electrochem. Soc. 161 (2014) D339–D348.
[42] D. Rafaja, C. Schimpf, T. Schucknecht, V. Klemm, L. Péter, I. Bakonyi, Microstructure formation in electrodeposited Co–Cu/Cu multilayers with GMR effect: influence of current density during magnetic layer deposition, Acta Mater. 59 (2011) 2992–3001.
[43] M. Agarwal, V. Kumar, S.R.K. Malladi, R. Balasubramaniam, K. Balani, Effect of current density on the pulsed co-electrodeposition of nanocrystalline nickel-copper alloys, JOM 62 (2010) 88–92.
[44] S. Valizadeh, G. Holmbom, P. Leisner, Electrodeposition of cobalt-silver multilayers, Surf. Coat. Technol. 105 (1998) 213–217.
[45] V.D. Papachristos, C.N. Panagopoulos, L.W. Christoffersen, A. Markaki, Young's modulus, hardness and scratch adhesion of Ni–P–W multilayered alloy coatings produced by pulse plating, Thin Solid Films 396 (2001) 174–183.
[46] H. Alimadadi, M. Ahmadi, M. Aliofkhazraei, S.R. Younesi, Corrosion properties of electrodeposited nanocrystalline and amorphous patterned Ni–W alloy, Mater. Des. 30 (2009) 1356–1361.
[47] M. Aliofkhazraei, S. Ahangarani, A.S. Rouhaghdam, Effect of the duty cycle of pulsed current on nanocomposite layers formed by pulsed electrodeposition, Rare Metals 29 (2010) 209–213.
[48] V. Torabinejad, M. Aliofkhazraei, A. Rouhaghdam, M. Allahyarzadeh, Electrodeposition of Ni–Fe–Mn/Al_2O_3 functionally graded nanocomposite coatings, Surf. Eng. 33 (2017) 122–130.
[49] V. Torabinejad, M. Aliofkhazraei, A. Sabour Rouhaghdam, M. Allahyarzadeh, Corrosion properties of Ni-Fe-Cr (III) multilayer coating synthesized via pulse duty cycle variation, Mater. Corros. 68 (2017) 347. -254.
[50] M. Chandrasekar, M. Pushpavanam, Pulse and pulse reverse plating—conceptual, advantages and applications, Electrochim. Acta 53 (2008) 3313–3322.
[51] Y. Ueda, N. Hataya, H. Zaman, Magnetoresistance effect of Co/Cu multilayer film produced by electrodeposition method, J. Magn. Magn. Mater. 156 (1996) 350–352.
[52] H. Zaman, S. Ikeda, Y. Ueda, Magnetoresistance in Co-Ag multilayers and granular films produced by electrodeposition method, IEEE Trans. Magn. 33 (1997) 3517–3519.
[53] J. Lamovec, V. Jović, I. Mladenović, M. Sarajlić, V. Radojević, Assessment of the composite behavior of different Ni/Cu multilayer composite systems, in: Proceedings of the 2014 29th International Conference on Microelectronics Proceedings - MIEL 2014, 2014, pp. 183–186.
[54] W. Cai, C.A. Schuh, Tuning nanoscale grain size distribution in multilayered Al–Mn alloys, Scr. Mater. 66 (2012) 194–197.
[55] M.R. Etminanfar, M.Heydarzadeh Sohi, Corrosion resistance of multilayer coatings of nanolayered Cr/Ni electrodeposited from Cr(III)–Ni(II) bath, Thin Solid Films 520 (2012) 5322–5327.
[56] B.G. Tóth, L. Péter, J. Dégi, Á. Révész, D. Oszetzky, G. Molnár, I. Bakonyi, Influence of Cu deposition potential on the giant magnetoresistance and surface roughness of electrodeposited Ni–Co/Cu multilayers, Electrochim. Acta 91 (2013) 122–129.
[57] C.L.S. Rizal, A. Yamada, Y. Hori, S. Ishida, M. Matsuda, Y. Ueda, Magnetic properties and magnetoresistance effect in Co/Au, Ag nano-structure films produced by pulse electrodeposition, Phys. Status Solidi (c) 1 (2004) 1756–1759.
[58] Q. Huang, D. Davis, E.J. Podlaha, Electrodeposition of FeCoNiCu nanowires, J. Appl. Electrochem. 36 (2006) 871–882.
[59] N. Udompanit, P. Wangyao, S. Henpraserttae, Y. Boonyongmaneerat, Wear response of composition-modulated multilayer Ni-W coatings, Adv. Mater. Res. 1025-1026 (2014) 302–309.
[60] M.H. Allahyarzadeh, M. Aliofkhazraei, A.R. Sabour Rouhaghdam, V. Torabinejad, Functionally graded nickel–tungsten coating: electrodeposition, corrosion and wear behaviour, Can. Metall. Q. 55 (2016) 303–311.
[61] V. Torabinejad, M. Aliofkhazraei, A. Sabour Rouhaghdam, M.H. Allahyarzadeh, Ni–Fe–Mn–(nano)Al_2O_3 coating with modulated composition and grain size, Trans. Indian Inst. Metals 70 (2017) 1199–1207.
[62] M. Alper, Electrodeposited magnetic superlattices, HH Wils Physics Laboratory, University of Bristol, 1995.
[63] A. Tekgül, M. Alper, H. Kockar, H. Kuru, Facile electrodeposition CoCu/Cu multilayers: deposition potentials for magnetic layers, J. Mater. Sci. 52 (2016) 3368–3374.
[64] A. Tekgül, H. Kockar, H. Kuru, M. Alper, C.G. ÜnlÜ, Electrochemical, structural and magnetic analysis of electrodeposited CoCu/Cu multilayers: influence of Cu layer deposition potential, J. Electron. Mater. 47 (2017) 1896–1903.
[65] I. Bakonyi, W.E.G. Hansal, Development of pulse-plating technology for the preparation of coatings with varying composition along their thickness: a historical overview, Trans. IMF 96 (2018) 237–243.
[66] J.Y. Xue, J.X. Wu, D.J. Yang, Structure and properties of Cu-Co multilayer films produced by electrodeposition, Acta Metall. Sin. (Eng. Lett.) 10 (1997) 115–119 [d].
[67] Á. Cziráki, I. Geröcs, B. Fogarassy, B. Arnold, M. Reibold, K. Wetzig, E. Tóth-Kádár, I. Bakonyi, Correlation of microstructure and giant magnetoresistance in electrodeposited Ni-Cu/Cu multilayers, Z. für Metallkunde 88 (1997) 781–789.
[68] T. Ohgai, K. Hashiguchi, T. Morimura, K. Takao, A. Kagawa, Fabrication of Co/Cu multilayered nanowires using a pulsed current deposition technique, Mater. Sci. Forum (2010) 1728–1731.
[69] B.G. Tóth, L. Péter, I. Bakonyi, Magnetoresistance and surface roughness study of the initial growth of electrodeposited CoCu multilayers, J. Electrochem. Soc. 158 (2011) D671–D680.
[70] N. Rajasekaran, S. Mohan, A comparative study of Cu-Co alloys versus Cu/Co multilayered coatings obtained by electrodeposition techniques, J. Electrochem. Soc. 159 (2012) D577–D581.
[71] N. Takane, H. Narita, X. Liu, S. Arai, Magnetic properties and microstructure of electrodeposited Co/Cu multilayers, Electrochemistry 81 (2013) 966–970.
[72] M. Uhlemann, A. Gebert, M. Herrich, A. Krause, A. Cziraki, L. Schultz, Electrochemical deposition and modification of Cu/Co-Cu multilayer, Electrochim. Acta 48 (2003) 3005–3011.
[73] J. Zhang, H. Ma, S. Zhang, H. Zhang, X. Deng, Q. Lan, D. Xue, F. Bai, N.J. Mellors, Y. Peng, Nanoscale characterisation and magnetic properties of $Co_{81}Cu_{19}$/Cu multilayer nanowires, J. Mater. Chem. C 3 (2014) 85–93.
[74] X.T. Tang, G.C. Wang, M. Shima, Layer thickness dependence of CPP giant magnetoresistance in individual CoNi/Cu multilayer nanowires grown by electrodeposition, Phys. Rev. B Condens. Matter Mater. Physics 75 (2007) 1–10.
[75] T. Sahin, H. Kockar, M. Alper, Properties of electrodeposited CoFe/Cu multilayers: the effect of Cu layer thickness, J. Magn. Magn. Mater. 373 (2015) 128–131.
[76] T. Sahin, H. Kockar, M. Alper, Giant magnetoresistance and magnetic properties of CoFe/Cu multilayer films: dependence of electrolyte pH, J. Supercond. Novel Magn. 26 (2013) 825–829.
[77] J. Garcia-Torres, E. Gomez, E. Valles, Electrochemical synthesis of Co–Ag/Ag multilayered nanowires for GMR applications, Mater. Lett. 111 (2013) 101–103.
[78] Y. Hayashi, S. Kashiwabara, Y. Jyoko, Preparation and characterization of electrodeposited metallic multilayers, Phys. B Condens. Matter 239 (1997) 35–40.
[79] Y. Jyoko, W. Schwarzacher, Characterization of electrodeposited magnetic Co/Pt multilayered nanostructures, Electrochim. Acta 47 (2001) 371–378.
[80] P. Cojocaru, A. Leserri, L. Magagnin, M. Vázquez, G. Carac, Electrodeposition of Ni/Cu multilayer nanowires using alumina template, ECS Trans. 33 (2011) 43–49.
[81] Y. Kaneko, H. Sakakibara, S. Hashimoto, Dependence of vickers hardness on annealing temperature at Co/Cu multilayered films, Mater. Sci. Forum 561-565 (2007) 2399–2402.
[82] Y. Kaneko, H. Sakakibara, S. Hashimoto, Microstructure and Vickers hardness of Co/Cu multilayers fabricated by electrodeposition, J. Mater. Sci. 43 (2008) 3931–3937.
[83] Y. Qian, J. Tan, Q. Liu, H. Yu, R. Xing, H. Yang, Preparation, microstructure and sliding-wear characteristics of brush plated copper-nickel multilayer films, Surf. Coat. Technol. 205 (2011) 3909–3915.
[84] K.D. Bird, M. Schlesinger, Giant magnetoresistance in electrodeposited Ni/Cu and Co/Cu multilayers, J. Electrochem. Soc. 142 (1995) L65–L66.
[85] D. Pullini, G. Innocenti, D. Busquets, A. Ruotolo, Investigation of multilayer local tilt within long portion of single Co/Cu nanowires, Appl. Phys. Lett. 90 (2007), 133106.
[86] Y.K. Su, D.H. Qin, H.L. Zhang, H. Li, H.L. Li, Microstructure and magnetic properties of bamboo-like CoPt/Pt multilayered nanowire arrays, Chem. Phys. Lett. 388 (2004) 406–410.
[87] Q. Xue, W. Zhang, The electrodeposition of a copper/nickel multilayer alloy on beryllium bronze substrate, J. Phys. D Appl. Phys. 30 (1997) 3301–3306.
[88] W. Zhang, Q. Xue, Tribological properties of nickel-copper multilayer film on beryllium bronze substrate, Thin Solid Films 305 (1997) 292–296.
[89] M. Chen, P.C. Searson, C.L. Chien, Micromagnetic behavior of electrodeposited Ni/Cu multilayer nanowires, J. Appl. Phys. 93 (2003) 8253–8255.
[90] Y. Kaneko, T. Sanda, S. Hashimoto, Microstructures of Ni/Cu and Ni-Co/Cu multilayers produced by electrodeposition method, Adv. Mater. Res. 26-28 (2007) 1321–1324.
[91] Y. Rheem, Electrodeposition of GMR Ni/Cu multilayers in a recirculating electrochemical flow reactor, Korean J. Mater. Res. 20 (2010) 90–96.

[92] Y. Qian, J. Tan, H. Yang, Z. Hu, Brush plated multilayered Cu/Ni coating from a single electrolyte and its fretting wear behaviors, Adv. Mater. Res. 97-101 (2010) 1467–1470.

[93] Y. Kaneko, Y. Mizuta, Y. Nishijima, S. Hashimoto, Vickers hardness and deformation of Ni/Cu nano-multilayers electrodeposited on copper substrates, J. Mater. Sci. 40 (2005) 3231–3236.

[94] H. Yang, M. Zeng, R. Yu, Magnetic properties of the NixCo1-x/Cu multilayer nanowires, Mater. Res. Bull. 57 (2014) 249–253.

[95] L. Péter, J. Pádár, E. Tóth-Kádár, A. Cziráki, P. Sóki, L. Pogány, I. Bakonyi, Electrodeposition of Co-Ni-Cu/Cu multilayers. 1. Composition, structure and magnetotransport properties, Electrochim. Acta 52 (2007) 3813–3821.

[96] P. Shakya, B. Cox, D. Davis, Giant magnetoresistance and coercivity of electrodeposited multilayered FeCoNi/Cu and CrFeCoNi/Cu, J. Magn. Magn. Mater. 324 (2012) 453–459.

[97] K.Y. Kok, C.M. Hangarter, B. Goldsmith, I.K. Ng, N.B. Saidin, N.V. Myung, Synthesis and characterization of electrodeposited permalloy ($Ni_{80}Fe_{20}$)/Cu multilayered nanowires, J. Magn. Magn. Mater. 322 (2010) 3876–3881.

[98] K. Hedayati, Structural and magnetic characterization of electrodeposited Ni–Cu/Cu and Fe–Ni–Cu/Cu multilayer, Appl. Phys. A Mater. Sci. Process. 118 (2014) 975–979.

[99] M. Elawayeb, Y. Peng, B.J. Inkson, Nanostructure and chemical characterisation of individual NiFe/Pt multilayer nanowires, J. Nanosci. Nanotechnol. 11 (2011) 7777–7782.

[100] C. Low, R. Wills, F. Walsh, Electrodeposition of composite coatings containing nanoparticles in a metal deposit, Surf. Coat. Technol. 201 (2006) 371–383.

[101] L. Péter, Z. Kupay, Á. Cziráki, J. Pádár, J. Tóth, I. Bakonyi, Additive effects in multilayer electrodeposition: properties of Co-Cu/Cu multilayers deposited with NaCl additive, J. Phys. Chem. B 105 (2001) 10867–10873.

[102] C.A. Ross, L.M. Goldman, F. Spaepen, Electrodeposition technique for producing multilayers of nickel-phosphorus and other alloys, Journal of the Electrochemical Society 140 (1993) 91–98.

[103] D.S. Stoychev, E.A. Stoyanova, S. Rashkov, Deposition of thin tin coatings on aluminium alloys, Surf. Technol. 23 (1984) 127–141.

[104] J. Lamovec, V. Jovic, M. Vorkapic, B. Popovic, V. Radojevic, R. Aleksic, Microhardness analysis of thin metallic multilayer composite films on copper substrates, J. Min. Metall. Sect. B Metall. 47 (2011) 53–61.

[105] W. Zhang, W. Li, L. Zhang, S. Yao, Electrodeposition of ordered arrays of multilayered Cu/Ni nanowires by dual bath technique, Acta Phys. Chim. Sin. 22 (2006) 977–980.

[106] P. Pascariu, S.I. Tanase, D.P. Tanase, A.V. Sandu, V. Georgescu, Preparation and magnetic properties of electrodeposited [Co/Zn] multilayer films, Mater. Chem. Phys. 131 (2012) 561–568.

[107] R.A. Wibowo, R. Hamid, T. Maier, T. Dimopoulos, Galvanostatically-electrodeposited Cu–Zn–Sn multilayers as precursors for crystallising kesterite Cu_2ZnSnS_4 thin films, Thin Solid Films 582 (2015) 239–244.

[108] D. Banga, J.L. Lensch-Falk, D.L. Medlin, V. Stavila, N.Y.C. Yang, D.B. Robinson, P. A. Sharma, Periodic modulation of Sb stoichiometry in $Bi_2Te_3/Bi_{2-x}Sb_xTe_3$ multilayers using pulsed electrodeposition, Cryst. Growth Des. 12 (2012) 1347–1353.

[109] V.S. Protsenko, F.I. Danilov, The corrosion-protective traits of electroplated multilayer zinc-iron-chromium deposits, Metal Finish. 108 (2010) 28–32.

[110] G.R. Nabiyouni, Design and fabrication of Nanomagnetic sensors based on electrodeposited GMR materials, Metrol. Meas. Syst. 16 (2009) 1–11.

[111] H. Yang, Y. Li, M. Zeng, W. Cao, W.E. Bailey, R. Yu, Static and dynamic magnetization of gradient FeNi alloy nanowire, Sci. Rep. 6 (2016).

[112] A. Bastos, S. Zaefferer, D. Raabe, C. Schuh, Characterization of the microstructure and texture of nanostructured electrodeposited NiCo using electron backscatter diffraction (EBSD), Acta Mater. 54 (2006) 2451–2462.

[113] R. Cui, Z. Yu, Y. He, W. Shu, Copper multilayer coating prepared by ultrasonic-electrodeposition, Adv. Mater. Res. (2010) 1348–1351.

[114] D. Pinzaru, S.I. Tanase, P. Pascariu, A.V. Sandu, V. Nica, V. Georgescu, Magnetic properties and giant magnetoresistance effect in [Fe/Pt]n granular multilayers, Optoelectron. Adv. Mater. Rapid Commun. 5 (2011) 235–241.

[115] D. Pinzaru, S.I. Tanase, P. Pascariu, L. Vlad, C. Pirghie, V. Georgescu, Microstructure, magnetic and magnetoresistance properties of electrodeposited [Fe/Pt] granular multilayers, J. Supercond. Novel Magn. 24 (2011) 2145–2152.

[116] C. Bonhôte, D. Landolt, Microstructure of Ni-Cu multilayers electrodeposited from a citrate electrolyte, Electrochim. Acta 42 (1997) 2407–2417.

[117] S.S. Jikan, S.S. Abdullah, M.H. Ismail, N.A. Ismail, N.A. Badarulzaman, Multilayer of Ni/Cu coating produced via electroplating process, Appl. Mech. Mater. (2014) 891–895.

[118] J. Fei, G. Liang, W. Xin, W. Wang, J. Liu, Corrosion behaviors of zinc and Zn-Ni alloy compositionally modulated multilayer coatings, J. Univ. Sci. Technol. Beijing Miner. Metall. Mater. (Eng. Ed.) 12 (2005) 545–552.

[119] Z. Shafiee, M.E. Bahrololoom, B. Hashemi, Electrodeposition of nanocrystalline $Ni/Ni–Al_2O_3$ nanocomposite modulated multilayer coatings, Mater. Des. 108 (2016) 19–26.

[120] B. Silva, D. Gonzalez-Chavez, J. Gomes Filho, R. Sommer, Microwave absorption of electroplated NiFeCu/Cu multilayers deposited directly on Si (100) substrates, J. Magn. Magn. Mater. 420 (2016) 23–27.

[121] K.H. Lee, G.H. Kim, W.Y. Jeung, Epitaxial growth and magnetic properties of electrochemically multilayered [CoPtP/Cu]n films, Electrochem. Commun. 6 (2004) 115–119.

[122] D. Pullini, D. Busquets, A. Ruotolo, G. Innocenti, V. Amigó, Insights into pulsed electrodeposition of GMR multilayered nanowires, J. Magn. Magn. Mater. 316 (2007) e242–e245.

[123] S. Kim, M. Jung, M. Kim, J. Choi, Bi-functional anodic TiO_2: Nanotubes for wettability control and barrier oxide for uniform coloring, Appl. Surf. Sci. 407 (2017) 353–360.

[124] X.T. Tang, G.C. Wang, M. Shima, Superparamagnetic behavior in ultrathin CoNi layers of electrodeposited CoNi/Cu multilayer nanowires, J. Appl. Phys. (2006) 99.

[125] D. Bera, S.C. Kuiry, S. Seal, Synthesis of nanostructured materials using template-assisted electrodeposition, JOM 56 (2004) 49–53.

[126] N. Maleak, P. Potpattanapol, N.N. Bao, J. Ding, W. Wongkokuo, I.M. Tang, S. Thongmee, Fabrication and magnetic properties of electrodeposited Ni/Cu nanowires using the double bath method, J. Magn. Magn. Mater. 354 (2014) 262–266.

[127] T. El Bahraoui, H. Errahmani, A. Berrada, A. Dinia, G. Schmerber, F. Cherkaoui El Moursli, F. Hajji, H. Lassri, Structural, magnetic and transport properties of CoZn/Cu electrodeposited multilayers, J. Magn. Magn. Mater. 272-276 (2004) e955–e957.

[128] J. García-Torres, L. Péter, Á. Révész, L. Pogány, I. Bakonyi, Preparation and giant magnetoresistance of electrodeposited Co-Ag/Ag multilayers, Thin Solid Films 517 (2009) 6081–6090.

[129] L. He, L. Qin, J. Zhao, Y. Yang, Y. Yin, Preparation of Pt/Ni multilayer nanowires with enhanced magnetic property and electrocatalytic activity, J. Nano Res. 40 (2016) 20–28.

[130] Y. Niu, J. Wei, Y. Yang, J. Hu, Z. Yu, Influence of microstructure on the wear mechanism of multilayered Ni coating deposited by ultrasound-assisted electrodeposition, Surf. Coat. Technol. 210 (2012) 21–27.

[131] A. Tekgül, M. Alper, H. Kockar, M. Haciismailoglu, The effect of ferromagnetic and non-ferromagnetic layer thicknesses on the electrodeposited CoFe/Cu multilayers, J. Mater. Sci. Mater. Electron. 26 (2015) 2411–2417.

[132] B. Jaleh, F. Koosha, A.O. Dezfuli, Preparation and magnetic properties of Ni/Pd multilayer nanowire arrays, J. Superconduct. Novel Magn. 27 (2014) 1065–1071.

[133] S. Kumar, D. Saini, Structural and magnetic characterization of electrochemically deposited Co-Cu multilayer nanowires, J. Mater. Sci. Mater. Electron. 24 (2013) 1086–1089.

[134] Z. Song, Y. Xie, S. Yao, H. Wang, W. Zhang, Z. Tang, Microstructure and magnetic properties of electrodeposited Co/Cu multilayer nanowire arrays, Mater. Lett. 65 (2011) 1562–1564.

[135] K. Kudo, K. Kobayakawa, Y. Sato, Preparation of multilayered Co/Pd nanostructure films by electroplating and their magnetic properties, Electrochim. Acta 47 (2001) 353–357.

[136] L.F. Liu, W.Y. Zhou, S.S. Xie, O. Albrecht, K. Nielsch, Microstructure and temperature-dependent magnetic properties of Co/Pt multilayered nanowires, Chem. Phys. Lett. 466 (2008) 165–169.

[137] H. Fauser, C. Poizat, M. Grimm, H. Knoll, W. Schmitt, R. Freudenberger, Electrodeposition of Gradient Layers for Improved Impact Load Resistance, Functionally Graded Materials VIII, Trans Tech Publications Ltd 492-493, Mater. Sci. Forum, 2005, pp. 53–58.

[138] Y. Kaneko, Y. Nishijima, T. Sanda, S. Hashimoto, Fatigue life enhancement by surface coating of Ni/Cu multilayered films. Materials Science Forum 561-565, Trans Tech Publications Ltd., 2007, pp. 2393–2398.

[139] D.R. Askeland, P.P. Fulay, W.J. Wright, The science and engineering of materials, SI Edition, CL-Engineering00, 2011.

[140] M.E. Kassner, M.T. Pérez-Prado, Erratum to “five-power-law creep in single phase metals and alloys” [progr. mater. sci. 45 (2000) 1–102], Prog. Mater. Sci. 45 (2000) 273.

[141] M. Barsoum, Fundamentals of Ceramics, CRC Press, 2002.

[142] N. Wang, Z. Wang, K.T. Aust, U. Erb, Room temperature creep behavior of nanocrystalline nickel produced by an electrodeposition technique, Mater. Sci. Eng. A 237 (1997) 150–158.

[143] X. Zhu, X.J. Liu, R.L. Zong, F. Zeng, F. Pan, Microstructure and mechanical properties of nanoscale Cu/Ni multilayers, Mater. Sci. Eng. A Struct. Mater. Prop. Microstruct. Proc. Mater. Sci. Eng. A Struct. Mater. 527 (2010) 1243–1248.

[144] X. Zhu, J. Luo, G. Chen, F. Zeng, F. Pan, Size dependence of creep behavior in nanoscale Cu/Co multilayer thin films, J. Alloys Compd. J. Alloys Compd. 506 (2010) 434–440.

[145] Y. Liu, Y. Chen, K. Yu, H. Wang, J. Chen, X. Zhang, Stacking fault and partial dislocation dominated strengthening mechanisms in highly textured Cu/Co multilayers, Int. J. Plast. 49 (2013) 152–163.

[146] R.C. Gifkins, Diffusional creep mechanisms, J. Ame. Ceram. Soc. 51 (1968) 69–72.

[147] H. Lüthy, R.A. White, O.D. Sherby, Grain boundary sliding and deformation mechanism maps, Mater. Sci. Eng. 39 (1979) 211–216.

[148] B.I. Sandor, Book Reviews : Metal Fatigue in Engineering, 14, John Wiley & Sons, 1982, pp. 36–37.

[149] W. Zhang, Q. Xue, Fretting wear characteristics of Ni/Cu multilayers electrodeposited on beryllium bronze substrate, Wear 214 (1998) 23–29.

[150] M.R. Stoudt, R.C. Cammarata, R.E. Ricker, Suppression of fatigue cracking with nanometer-scale multilayered coatings, Scr. Mater. 43 (2000) 491–496.
[151] M.R. Stoudt, R.E. Ricker, R.C. Cammarata, The influence of a multilayered metallic coating on fatigue crack nucleation, Int. J. Fatigue 23 (2001) 215–223.
[152] W. Wang, R.N. Singh, Fatigue crack growth in a Ni–Sn multilayered composite, Mater. Sci. Eng. A 251 (1998) 184–191.
[153] Z.P. Bažant, L. Cedolin, Stability of Structures, World Scientific, 2010.
[154] M. Aliofkhazraei, Modern Surface Engineering Treatments, ed, InTechOpen, 2013.
[155] D.R. Gabe, W.A. Green, The mathematical modelling of CMA multilayered coatings, Surf. Coat. Technol. 105 (1998) 195–201.
[156] Y. Li, J. Kim, M. Kim, A. Armutlulu, M.G. Allen, Thick multilayered micromachined permanent magnets with preserved magnetic properties, J. Microelectromech. Syst. 25 (2016) 498–507.
[157] S.-I. Baik, A. Duhin, P.J. Phillips, R.F. Klie, E. Gileadi, D.N. Seidman, N. Eliaz, Atomic-scale structural and chemical study of columnar and multilayer Re-Ni electrodeposited thermal barrier coating, Adv. Eng. Mater. 18 (2016) 1133–1144.
[158] C.A. Ross, Electrodeposited multilayer thin films, Ann. Rev. Mater. Sci. 24 (1994) 159–188.
[159] W. Wang, R.N. Singh, Influence of the microstructure on the mechanical properties of Ni/Sn multilayered composites, Mater. Sci. Eng. A 271 (1999) 306–314.
[160] M. Daly, J.L. McCrea, B.A. Bouwhuis, C.V. Singh, G.D. Hibbard, Deformation behavior of a NiCo multilayer with a modulated grain size distribution, Mater. Sci. Eng. A 641 (2015) 305–314.
[161] B.H. An, I.T. Jeon, J.H. Seo, J.P. Ahn, O. Kraft, I.S. Choi, Y.K. Kim, Ultrahigh tensile strength nanowires with a Ni/Ni–Au multilayer nanocrystalline structure, Nano Lett. 16 (2016) 3500–3506.
[162] S. Riemer, M. Sun, I. Tabakovic, Role of p-hydroxybenzhydrazide additive in electrodeposition of thin NiP film used as a nonmagnetic spacer in laminated (CoFe/NiP) nano structures, J. Electrochem. Soc. 163 (2016) D239–D246.
[163] B. Tunaboylu, Electrodeposition of multilayer NiMn beams for probes, Mater. Lett. 70 (2012) 51–53.
[164] V. Torabinejad, M. Aliofkhazraei, A.S. Rouhaghdam, M.H. Allahyarzadeh, T. Kasama, H. Alimadadi, Mechanical properties of multilayer Ni-Fe and Ni-Fe-Al_2O_3 nanocomposite coating, Mater. Sci. Eng. A 700 (2017) 448–456.
[165] S.K. Ghosh, P.K. Limaye, S. Bhattacharya, N.L. Soni, A.K. Grover, Effect of Ni sublayer thickness on sliding wear characteristics of electrodeposited Ni/Cu multilayer coatings, Surf. Coat. Technol. 201 (2007) 7441–7448.
[166] H. Wang, R. Liu, W.Q. Jiang, J. Zhu, J.Z. Feng, G.F. Ding, X. Zhao, A novel method for improving the adhesion strength of the electrodeposited Ni films in MEMS, Appl. Surf. Sci. 257 (2011) 2203–2207.
[167] H. Zhang, L. Liu, J. Bai, X. Liu, Corrosion behavior and microstructure of electrodeposited nano-layered Ni–Cr coatings, Thin Solid Films 595 (2015) 36–40.
[168] Y.W. Yen, H.M. Hsiao, P.S. Shao, Y.W. Chang, A novel electronic packaging method to replace high-temperature Sn-Pb solders, J. Electron. Materials 44 (2015) 3914–3919.
[169] L. Kurmanaeva, H. Bahmanpour, T. Holland, J. McCrea, J.H. Lee, J. Jian, H. Wang, E.J. Lavernia, A.K. Mukherjee, Room temperature mechanical behaviour of a Ni-Fe multilayered material with modulated grain size distribution, Philos. Mag. 94 (2014) 3549–3559.
[170] A. Leyland, A. Matthews, On the significance of the H/E ratio in wear control: a nanocomposite coating approach to optimised tribological behaviour, Wear 246 (2000) 1–11.
[171] J. Musil, F. Kunc, H. Zeman, H. Poláková, Relationships between hardness, Young's modulus and elastic recovery in hard nanocomposite coatings, Surf. Coat. Technol. 154 (2002) 304–313.
[172] A. Leyland, A. Matthews, Design criteria for wear-resistant nanostructured and glassy-metal coatings, Surf. Coat. Technol. 177-178 (2004) 317–324.
[173] S.K. Ghosh, P.K. Limaye, C. Srivastava, R. Tewari, Comparison of sliding wear behaviour of pulse electrodeposited Ni–Cu nanocrystalline alloys and Ni–Cu/Cu multilayers, Trans. IMF 88 (2010) 158–162.
[174] S.K. Ghosh, P.K. Limaye, B.P. Swain, N.L. Soni, R.G. Agrawal, R.O. Dusane, A. K. Grover, Tribological behaviour and residual stress of electrodeposited Ni/Cu multilayer films on stainless steel substrate, Surf. Coat. Technol. 201 (2007) 4609–4618.
[175] E. Pellicer, A. Varea, S. Pané, B.J. Nelson, E. Menéndez, M. Estrader, S. Suriñach, M.D. Baró, J. Nogués, J. Sort, Nanocrystalline electroplated Cu-Ni: metallic thin films with enhanced mechanical properties and tunable magnetic behavior, Adv. Funct. Mater. 20 (2010) 983–991.
[176] J.S. Zabinski, A.A. Voevodin, Recent developments in the design, deposition, and processing of hard coatings, J. Vac. Sci. Technol. A Vac. Surf. Films 16 (1998) 1890–1900.
[177] Y. Zhang, M.J. Sun, D. Zhang, Designing functionally graded materials with superior load-bearing properties, Acta Biomater 8 (2012) 1101–1108.
[178] K. Tohgo, M. Iizuka, H. Araki, Y. Shimamura, Influence of microstructure on fracture toughness distribution in ceramic–metal functionally graded materials, Eng. Fract. Mech. 75 (2008) 4529–4541.
[179] X. Gao, C. Zhang, J. Sladek, V. Sladek, Fracture analysis of functionally graded materials by a BEM, Compos. Sci. Technol. 68 (2008) 1209–1215.
[180] F. Erdogan, Fracture mechanics of functionally graded materials, Compos. Eng. 5 (1995) 753–770.
[181] A. Kawasaki, R. Watanabe, Thermal fracture behavior of metal/ceramic functionally graded materials, Eng. Fract. Mech. 69 (2002) 1713–1728.
[182] X. Guan, Y. Wang, Q. Xue, L. Wang, Toward high load bearing capacity and corrosion resistance Cr/Cr2N nano-multilayer coatings against seawater attack, Surf. Coat. Technol. 282 (2015) 78–85.
[183] A.A. Voevodin, S.D. Walck, J.S. Zabinski, Architecture of multilayer nanocomposite coatings with super-hard diamond-like carbon layers for wear protection at high contact loads, Wear 203-204 (1997) 516–527.
[184] H. Holleck, V. Schier, Multilayer PVD coatings for wear protection, Surf. Coat. Technol. 76-77 (1995) 328–336.
[185] R. Bermejo, Y. Torres, A. Sanchezherencia, C. Baudin, M. Anglada, L. Llanes, Residual stresses, strength and toughness of laminates with different layer thickness ratios, Acta Mater. 54 (2006) 4745–4757.
[186] W. Pawlak, B. Wendler, Multilayer, hybrid PVD coatings on Ti6Al4V titanium alloy, J. Achiev. Mater. Manuf. Eng. 37 (2009).
[187] K. Hu, L.J. Xu, Y.Q. Cao, G.J. Pan, Z.H. Cao, X.K. Meng, Modulating individual thickness for optimized combination of strength and ductility in Cu/Ru multilayer films, Mater. Lett. 107 (2013) 303–306.
[188] X. Zhang, J. Qin, M.K. Das, R. Hao, H. Zhong, A. Thueploy, S. Limpanart, Y. Boonyongmaneerat, M. Ma, R. Liu, Co-electrodeposition of hard Ni-W/diamond nanocomposite coatings, Sci. Rep. 6 (2016) 22285.
[189] X. Zhang, D. Liu, G. Liu, Z. Wang, B. Tang, Improvement of the fretting damage resistance of Ti-811 alloy by Cu/Ni multilayer films, Tribol. Int. 44 (2011) 1488–1494.
[190] V. Torabinejad, M. Aliofkhazraei, A.S. Rouhaghdam, M.H. Allahyarzadeh, Tribological performance of Ni-Fe-Al_2O_3 multilayer coatings deposited by pulse electrodeposition, Wear 380-381 (2017) 115–125.
[191] M. Allahyarzadeh, Corrosion and Wear Behaviours of Pulse Reverse Electrodeposited Multilayer Nanocrystalline Ni-W And Ni-W-Al_2O_3 Nanocomposite Coatings, Department of Materials Engineering, Tarbiat Modares University, Tehran, Iran, 2017.
[192] C. Subramanian, K.N. Strafford, Review of multicomponent and multilayer coatings for tribological applications, Wear 165 (1993) 85–95.
[193] H. Liu, S.M. Hsu, Fracture behavior of multilayer silicon nitride/boron nitride ceramics, J. Am. Ceram. Soc. 79 (1996) 2452–2457.
[194] A.W. Ruff, D.S. Lashmore, Effect of layer spacing on wear of Ni/Cu multilayer alloys, Wear 151 (1991) 245–253.
[195] K.H. Hou, T. Han, H.H. Sheu, M.D. Ger, Preparation and wear resistance of electrodeposited Ni–W/diamond composite coatings, Appl. Surf. Sci. 308 (2014) 372–379.
[196] Z. Wei, X. Qunji, Z. Xushou, The influence of brighteners on the friction and wear of electrodeposited multilayer films, Wear 214 (1998) 74–78.
[197] T. Hattori, Y. Kaneko, S. Hashimoto, Tribological Properties of Ni/Cu Multilayers. Mater. Sci. Forum 561-565, Trans Tech Publications Ltd., 2007, pp. 2451–2454.
[198] W. Wang, R.N. Singh, Tribological behavior of Ni/Sn metallic multilayer composites, J. Mater. Eng. Perform. 7 (1998) 27–32.
[199] V. Torabinejad, A.S. Rouhaghdam, M. Aliofkhazraei, M.H. Allahyarzadeh, Ni–Fe–Al_2O_3 electrodeposited nanocomposite coating with functionally graded microstructure, Bull. Mater. Sci. 39 (2016) 857–864.
[200] E. Beltowska-Lehman, P. Indyka, A. Bigos, M. Kot, L. Tarkowski, Electrodeposition of nanocrystalline Ni–W coatings strengthened by ultrafine alumina particles, Surf. Coat. Technol. 211 (2012) 62–66.
[201] M.H. Allahyarzadeh, M. Aliofkhazraei, A.R.S. Rouhaghdam, V. Torabinejad, Gradient electrodeposition of Ni-Cu-W(alumina) nanocomposite coating, Mater. Des. 107 (2016) 74–81.
[202] A. Tokarz, P. Wieczorek, T. Fra˛czek, Z. Nitkiewicz, Preparation, structural and mechanical properties of electrodeposited Co/Cu multilayers, Phys. Status Solidi (c) 5 (2008) 3526–3529.
[203] E.P. Georgiou, J.G. Buijnsters, H. Wang, D. Drees, A.K. Basak, J.P. Celis, Nanostructured gradient Co-Sn electrodeposits as alternative to Sn connector contacts, Surf. Coat. Technol. 271 (2015) 148–155.
[204] N.I. Tsyntsaru, Z.I. Bobanova, D.M. Kroitoru, V.F. Cheban, G.I. Poshtaru, A. I. Dikusar, Effect of a multilayer structure and lubrication on the tribological properties of coatings of Fe-W alloys, Surf. Eng. Appl. Electrochem. 46 (2010) 538–546.
[205] S.J. Bull, E.G. Berasetegui, An overview of the potential of quantitative coating adhesion measurement by scratch testing, Tribol. Int. 39 (2006) 99–114.
[206] C.A. Schuh, T.G. Nieh, H. Iwasaki, The effect of solid solution W additions on the mechanical properties of nanocrystalline Ni, Acta Mater 51 (2003) 431–443.
[207] L. Chen, S.Q. Wang, S.Z. Zhou, J. Li, Y.Z. Zhang, Microstructure and mechanical properties of Ti(C,N) and TiN/Ti(C,N) multilayer PVD coatings, Int. J. Refract. Metals Hard Mater. 26 (2008) 456–460.
[208] M.A. Al-Bukhaiti, K.A. Al-hatab, W. Tillmann, F. Hoffmann, T. Sprute, Tribological and mechanical properties of Ti/TiAlN/TiAlCN nanoscale multilayer PVD coatings deposited on AISI H11 hot work tool steel, Appl. Surf. Sci. 318 (2014) 180–190.
[209] F. Rebib, T. Gaudy, A. Soum-Glaude, I. Caron, T. Da Silva, C. Picard, F. Cournut, L. Thomas, Mechanical study of high resistance silicon carbide based multi-nano-layers grown by multifrequency PACVD, Plasma Process. Polym. 6 (2009) S917–S922.

[210] D.H. Mosca, F. Petroff, A. Fert, P.A. Schroeder, W.P. Pratt, R. Laloee, Oscillatory interlayer coupling and giant magnetoresistance in Co/Cu multilayers, J. Magn. Magn. Mater. 94 (1991) L1–L5.

[211] S. Esmaili, M.E. Bahrololoom, C. Zamani, Electrodeposition of NiFe/Cu multilayers from a single bath, Surf. Eng. Appl. Electrochem. 47 (2011) 107–111.

[212] A. Blondel, B. Doudin, J.P. Ansermet, Comparative study of the magnetoresistance of electrodeposited Co/Cu multilayered nanowires made by single and dual bath techniques, J. Magn. Magn. Mater. 165 (1997) 34–37.

[213] G. Binasch, P. Grünberg, F. Saurenbach, W. Zinn, Enhanced magnetoresistance in layered magnetic structures with antiferromagnetic interlayer exchange, Phys. Rev. B 39 (1989) 4828–4830.

[214] R. Weil, The structures of electrodeposits and the properties that depend on them, Annu. Rev. Mater. Sci. 19 (1989) 165–182.

[215] D. Zalka, L. Péter, M. El-Tahawy, J. Gubicza, G. Molnár, I. Bakonyi, Structure and giant magnetoresistance of Co-Fe/Cu multilayer films electrodeposited from various bath formulations, J. Electrochem. Soc. 166 (2020) D923–D934.

[216] C. Rizal, Giant magnetoresistance and magnetic properties of ferromagnetic hybrid nanostructures, Thesis, University of British Columbia, 2012.

[217] A. Barthélémy, A. Fert, F. Petroff, Chapter 1 Giant magnetoresistance in magnetic multilayers, Handbook of Magnetic Materials, Elsevier, 1999, pp. 1–96.

[218] H.A.M. van den Berg, Physics of and methods for studying metallic multilayers with interlayer exchange coupling and GMR response. Magnetic Multilayers and Giant Magnetoresistance, Springer Berlin Heidelberg, 2000, pp. 179–262.

[219] R.M. White, Quantum Theory of Magnetism, Springer Series in Solid-State Sciences, Springer Berlin Heidelberg, 2007.

[220] M. Shima, L. Salamanca-Riba, T.P. Moffat, R.D. McMichael, Structural and magnetic properties of electrodeposited Co/Cu multilayers, J. Magn. Magn. Mater. 198-199 (1999) 52–54.

[221] H. Kuru, H. Kockar, M. Alper, Electrodeposited NiFeCu/Cu multilayers: Effect of Fe ion concentration on properties, J. Magn. Magn. Mater. 373 (2015) 135–139.

[222] A. Tekgül, M. Alper, H. Kockar, Simple electrodepositing of CoFe/Cu multilayers: Effect of ferromagnetic layer thicknesses, J. Magn. Magn. Mater. 421 (2017) 472–476.

[223] E. Gómez, A. Labarta, A. Llorente, E. Vallés, Characterisation of cobalt/copper multilayers obtained by electrodeposition, Surface and Coatings Technology 153 (2002) 261–266.

[224] F.J. Gómez-de la Cruz, Fernando Cruz-Peragón, J. Pedro, A vital stage in the large-scale production of biofuels from spent coffee grounds: the drying kinetics, Fuel Proc. Technol. 130 (2015).

[225] S.K. Ghosh, A.K. Grover, P. Chowdhury, S.K. Gupta, G. Ravikumar, D.K. Aswal, M. S. Kumar, R.O. Dusane, High magnetoresistance and low coercivity in electrodeposited Co/Cu granular multilayers, Appl. Phys. Lett. 89 (2006), 132507.

[226] V.M. Fedosyuk, O.I. Kasyutich, Hard magnetic Co/Cu superlattices, J. Magn. Magn. Mater. 125 (1993) 330–334.

[227] D.K. Pandya, P. Gupta, S.C. Kashyap, S. Chaudhary, Electrodeposition and characterization of Cu/Co multilayers: Effect of individual Co and Cu layers on GMR magnitude and behavior, Journal of Magnetism and Magnetic Materials 321 (2009) 974–978.

[228] A. Gündel, E. Chassaing, J.E. Schmidt, *In situ* magnetization measurements of Cu/Co multilayers during the process of electrodeposition,, J. Appl. Phys. 90 (2001) 5257–5260.

[229] G. Rivero, M. Multigner, E. Fraga, J. Alonso, J.L. Munoz, Control of magnetic anisotropy in electrodeposited CoP/Cu multilayers, IEEE Transactions on Magnetics 31 (1995) 4097–4099.

[230] B. Hamrakulov, I.S. Kim, M.G. Lee, B.H. Park, Electrodeposited Ni, Fe, Co and Cu single and multilayer nanowire arrays on anodic aluminum oxide template, Trans. Nonferr. Metals Soc. China 19 (2009) s83–s87.

[231] M. Almasi-Kashi, A. Ramazani, F. Kheyri, E. Jafari-Khamse, The effect of magnetic layer thickness on magnetic properties of Fe/Cu multilayer nanowires, Mater. Chem. Phys. 144 (2014) 230–234.

[232] A. Yamada, T. Houga, Y. Ueda, Magnetism and magnetoresistance of Co/Cu multilayer films produced by pulse control electrodeposition method, J. Magn. Magn. Mater. 239 (2002) 272–275.

[233] J. Zhang, M. Moldovan, D.P. Young, E.J. Podlaha, Electrochemical inspection of electrodeposited giant magnetoresistance CoNiCu/Cu multilayer films, J. Electrochem. Soc. 152 (2005) C626.

[234] F. Nasirpouri, P. Southern, M. Ghorbani, A. Iraji zad, W. Schwarzacher, GMR in multilayered nanowires electrodeposited in track-etched polyester and polycarbonate membranes, J. Magn. Magn. Mater. 308 (2007) 35–39.

[235] E.M. Palmero, C. Bran, R.P. del Real, C. Magen, M. Vazquez, Structural and magnetic characterization of FeCoCu/Cu multilayer nanowire arrays, IEEE Magn. Lett. 5 (2014) 1–4.

[236] H. Wang, B. Huang, H. Deng, H. Li, W. Zhang, S. Yao, Effect of sub-layer thickness on magnetic and giant magnetoresistance properties of Ni–Fe/Cu/Co/Cu multilayered nanowire arrays, Chin. J. Chem. Eng. 23 (2015) 1231–1235.

[237] K.H. Lee, S.W. Kang, G.H. Kim, W.Y. Jeung, Fabrication of multi-layered CoPtP alloy with high coercivity and squareness by electrochemical deposition, J. Magn. Magn. Mater. 272-276 (2004) E925–E926.

[238] C.H. Peng, T.Y. Wu, C.C. Hwang, A preliminary study on the synthesis and characterization of multilayered Ag/Co magnetic nanowires fabricated via the electrodeposition method, Sci. World J. 2013 (2013) 1–5.

[239] P. Pascariu, S.I. Tanase, D. Pinzaru, V. Georgescu, Microstructure, magnetic and magnetoresistance properties of electrodeposited [Co/Zn]50 multilayers, J. Superconduct. Novel Magn. 24 (2011) 1917–1923.

[240] P. Gupta, D.K. Pandya, S.C. Kashyap, S. Chaudhary, High giant magnetoresistance in electrodeposited Cu/Co nano-multilayers, Phys. Status Solidi (A) 204 (2007) 2453–2460.

[241] M. Haciismailoglu, M. Alper, H. Kockar, O. Karaagac, Electrodeposition and characterization of Co/Cu multilayers, Acta Phys. Polon. A 129 (2016) 773–775.

[242] A. Dogra, P. Chowdhury, S.K. Ghosh, S.K. Gupta, G. Ravikumar, Planar Hall effect in electrodeposited CoCu/Cu multilayer, Appl. Phys. A 111 (2013) 323–328.

[243] H. Kuru, H. Kockar, M. Alper, A study on total thickness dependency: microstructural, magnetoresistance and magnetic properties of electrochemically deposited permalloy based multilayers, J. Mater. Sci. Mater. Electron. 26 (2015) 5009–5013.

[244] L. Pérez, Ó. de Abril, M.C. Sánchez, C. Aroca, E. López, P. Sánchez, Electrodeposited amorphous CoP multilayers with high permeability, J. Magn. Magn. Mater. 215-216 (2000) 337–339.

[245] H. Zhou, G. Wei, M. Li, J. Wang, R. Xu, Y. Yu, H. Ge, H. Dettinger, $Fe_{50}Pt_{50}$/Fe_2Pt_{98} magnetic multilayers electrodeposited from ionic liquids, J. Electrochem. Soc. 160 (2013) D343–D348.

[246] H.R. Zhou, G.Y. Wei, J.W. Lou, Y. Cao, X.F. Meng, H.L. Ge, H. Dettinger, FePt magnetic multilayers electrodeposited from non-aqueous liquids, Surf. Eng. 29 (2013) 434–439.

[247] N. Rajasekaran, J. Mani, B.G. Tóth, G. Molnár, S. Mohan, L. Péter, I. Bakonyi, Giant magnetoresistance and structure of electrodeposited Co/Cu multilayers: The influence of layer thicknesses and Cu deposition potential, J. Electrochem. Soc. 162 (2015) D204–D212.

[248] K. Hong, J. Bae, W. Bang, J.-G. Kim, Effect of organic additives on magnetic properties of electroplated Cu/Co thin films, ECS Trans. ECS 2 (2007) 33–38.

[249] H. Chiriac, O.-G. Dragos, G. Stoian, M. Grigoras, N. Lupu, Contact and magnetoresistance measurement of a single NiFe/Cu multilayer nanowire within a template nanowire array, IEEE Trans. Magn. 50 (2014) 1–4.

[250] M. Panayotova, Deposition of Fe–C alloy on structural steel and cast iron for repair of worn machine parts, Surf. Coat. Technol. 124 (2000) 266–271.

[251] L. Kurmanaeva, J. McCrea, J. Jian, J. Fiebig, H. Wang, A.K. Mukherjee, E. J. Lavernia, Influence of layer thickness on mechanical properties of multilayered NiFe samples processed by electrodeposition, Mater. Des. 90 (2016) 389–395.

[252] J. Wang, Q. Zhou, S. Shao, A. Misra, Strength and plasticity of nanolaminated materials, Mater. Res. Lett. 5 (2016) 1–19.

[253] A. Misra, J.P. Hirth, R.G. Hoagland, Length-scale-dependent deformation mechanisms in incoherent metallic multilayered composites, Acta Mater. 53 (2005) 4817–4824.

[254] T. Hattori, Y. Kaneko, S. Hashimoto, Wear-induced microstructure in Ni/Cu nano-multilayers, J. Mater. Sci. 43 (2008) 3923–3930.

[255] C.A. Huang, C.Y. Chen, Hardness variation and annealing behavior of a Cr-Ni multilayer electroplated in a trivalent chromium-based bath, Surf. Coat. Technol. 203 (2009) 3320–3324.

[256] H.S. Hong, M.H. Seo, S. Lee, S.J. Hong, H.G. Suk, J.-H. Ahn, Fabrication and characterization of micro-sized copper bump of multi-layer PCB by pulse-reverse electroplating, Curr. Appl. Phys. 11 (2011) S289–S292.

[257] B. Bostani, N. Parvini Ahmadi, S. Yazdani, Manufacturing of functionally graded Ni–ZrO_2composite coating controlled by stirring rate of the electroplating bath, Surf. Eng. 32 (2016) 495–500.

[258] N. Rajasekaran, S. Mohan, Preparation, corrosion and structural properties of Cu–Ni multilayers from sulphate/citrate bath, Corros. Sci. 51 (2009) 2139–2143.

[259] S. Mohajeri, A. Dolati, M. Ghorbani, The influence of pulse plating parameters on the electrocodeposition of Ni-TiO_2 nanocomposite single layer and multilayer structures on copper substrates, Surf. Coat. Technol. 262 (2015) 173–183.

[260] S.R. Cross, C.A. Schuh, Ternary alloying additions and multilayering as strategies to enhance the galvanic protection ability of Al-Zn coatings electrodeposited from ionic liquid solution, Electrochim. Acta 211 (2016) 860–870.

[261] M. Rahsepar, M.E. Bahrololoom, Corrosion study of Ni/Zn compositionally modulated multilayer coatings using electrochemical impedance spectroscopy, Corros. Sci. 51 (2009) 2537–2543.

[262] Y. Ullal, A. Chitharanjan Hegde, Corrosion protection of electrodeposited multilayer nanocomposite Zn-Ni-SiO_2 coatings, Surf. Eng. Appl. Electrochem. 49 (2013) 161–167.

[263] R.S. Bhat, A.C. Hegde, Electrodeposition of cyclic multilayer Zn-Co films using square current pulses and investigaions on their corrosion behaviors, J. Miner. Mater. Charact. Eng. 11 (2012) 896–903.

[264] I. Ivanov, I. Kirilova, Corrosion resistance of compositionally modulated multilayered Zn–Ni alloys deposited from a single bath, J. Appl. Electrochem. J. Appl. Electrochem. 33 (2003) 239–244.

[265] J.L. Zhang, C.D. Gu, S. Fashu, Y.Y. Tong, M.L. Huang, X.L. Wang, J.P. Tu, Enhanced corrosion resistance of Co-Sn alloy coating with a self-organized layered structure electrodeposited from deep eutectic solvent, J. Electrochem. Soc. 162 (2014) D1–D8.

[266] J.Y. Fei, G.D. Wilcox, Electrodeposition of zinc–nickel compositionally modulated multilayer coatings and their corrosion behaviours, Surf. Coat. Technol. 200 (2006) 3533–3539.
[267] B. Bahadormanesh, M. Ghorbani, Ni-P/Zn-Ni compositionally modulated multilayer coatings – part 2: corrosion and protection mechanisms, Appl. Surf. Sci. 442 (2018) 313–321.
[268] J.Y. Fei, G.Z. Liang, W.L. Xin, W.K. Wang, Surface modification with zinc and Zn-Ni alloy compositionally modulated multilayer coatings, J. Iron Steel Res. Int. 13 (2006) 61–67.
[269] D. Blejan, L.M. Muresan, Corrosion behavior of Zn-Ni-Al_2O_3 nanocomposite coatings obtained by electrodeposition from alkaline electrolytes, Mater. Corros. 64 (2012) 433–438.
[270] M. Shourgeshty, M. Aliofkhazraei, A. Karimzadeh, R. Poursalehi, Corrosion and wear properties of Zn–Ni and Zn–Ni–Al_2O_3 multilayer electrodeposited coatings, Materials Research Express 4 (2017), 096406.
[271] N.P. Wasekar, S. Gowthami, A. Jyothirmayi, J. Joardar, G. Sundararajan, Corrosion behaviour of compositionally modulated nanocrystalline Ni–W coatings, Surface Engineering 36 (2019) 952–959.
[272] A.R. Jones, J. Hamann, A.C. Lund, C. Schuh, Nanocrystalline Ni-W alloy coating for engineering applications, Plating and Surface Finishing 97 (2010) 52–60.
[273] M.H. Allahyarzadeh, M. Aliofkhazraei, A.S. Rouhaghdam, Electrodeposition on superalloy substrates: A review, Surface Review and Letters 23 (2016), 1630001.
[274] T. Hoornaert, Z. Hua, J. Zhang, Hard wear-resistant coatings: A review, Advanced tribology, Springer, 2009, pp. 774–779.
[275] H.E. Rebenne, D.G. Bhat, Review of CVD TiN coatings for wear-resistant applications: deposition processes, properties and performance, Surface and Coatings Technology 63 (1994) 1–13.
[276] A. Sabour Rouhaghadam, M. Azadi, A review on titanium nitride and titanium carbide single and multilayer coatings deposited by plasma assisted chemical vapor deposition, International Journal of Engineering 29 (2016) 677–687.
[277] S. Zhang, D. Sun, Y. Fu, H. Du, Toughening of hard nanostructural thin films: A critical review, Surface and Coatings Technology 198 (2005) 2–8.